TECHNICAL REPORT STANDARD TITLE PAGE

1. Report No.	2. Government Accession No.	3. Recipient's Catalog No.
FHWA/TX-83/25 + 236-2F		

4. Title and Subtitle	5. Report Date
Cantilever Retaining Wall Design	May 1983
	6. Performing Organization Code

7. Author(s)	8. Performing Organization Report No.
Robert F. Bruner, Harry M. Coyle, and Richard E. Bartoskewitz	Research Report 236-2F

9. Performing Organization Name and Address	10. Work Unit No.
Texas Transportation Institute The Texas A&M University System College Station, Texas 77840	11. Contract or Grant No. Study No. 2-5-78-236
	13. Type of Report and Period Covered
12. Sponsoring Agency Name and Address Texas State Department of Highways and Public Transportation; Transportation Planning Division P. O. Box 5051 Austin, Texas 78763	Interim - September 1977 May 1983
	14. Sponsoring Agency Code

15. Supplementary Notes
Research performed in cooperation with DOT. FHWA.
Research Study Title: Determination of Earth Pressures for Use in Cantilever Retaining Wall Design.

16. Abstract

Current retaining wall design procedures are summarized with emphasis on the prediction of lateral earth pressures using the Coulomb and Rankine earth pressure theories, and the equivalent fluid pressure method. Results from previous large scale retaining wall tests and field studies are presented. Different design aspects are introduced as background for a recent field performance study.

Instrumentation for measuring earth pressures on bearing surfaces and movement of a test wall constructed on a Texas State Department of Highways and Public Transportation (TSDHPT) project is described. Measured pressures and movements along with results of geotechnical tests of the foundation and backfill soils are presented in detail.

The test wall design based on the District 12 TSDHPT design standard is outlined and compared with results from the field performance study. A proposed new design procedure is developed based on modification of current design procedures. Significant modifications were made in the areas of the use of cohesive soil in the backfill, the computation of lateral earth pressures, and the computation of stability against overturning.

17. Key Words	18. Distribution Statement
Cantilever Retaining Wall, Lateral Earth Pressure, Deflection, Rotation, New Design Procedure.	No restrictions. This document is available to the public through the National Technical Information Service, 5285 Port Royal Road, Springfield, Virginia 22161.

19. Security Classif. (of this report)	20. Security Classif. (of this page)	21. No. of Pages	22. Price
Unclassified	Unclassified	192	

Form DOT F 1700.7 (8-69)

CANTILEVER RETAINING WALL DESIGN

by

Robert F. Bruner
Research Assistant

Harry M. Coyle
Research Engineer

and

Richard E. Bartoskewitz
Engineering Research Associate

Research Report No. 236-2F

Determination of Earth Pressures for Use
in Cantilever Retaining Wall Design
Research Study Number 2-5-78-236

Sponsored by
State Department of Highways and Public Transportation
in cooperation with the
U. S. Department of Transportation
Federal Highway Administration

May 1983

TEXAS TRANSPORTATION INSTITUTE
The Texas A&M University System
College Station, Texas

Disclaimer

The contents of this report reflect the views of the authors who are responsible for the facts and accuracy of the data presented herein. The contents do not necessarily reflect the views or policies of the Federal Highway Administration. This report does not constitute a standard, specification or regulation.

There was no invention or discovery conceived or first actually reduced to practice in the course of or under this contract, including any art, method, process, machine, manufacture, design or composition of matter, or any new and useful improvement thereof, or any variety of plant which is or may be patentable under the patent laws of the United States of America or any foreign country.

ABSTRACT

Current retaining wall design procedures are summarized with emphasis on the prediction of lateral earth pressures using the Coulomb and Rankine earth pressure theories, and the equivalent fluid pressure method. Results from previous large scale retaining wall tests and field studies are presented. Different design aspects are introduced as background for a recent field performance study.

Instrumentation for measuring earth pressures on bearing surfaces and movement of a test wall constructed on a Texas State Department of Highways and Public Transportation (TSDHPT) project is described. Measured pressures and movements along with results of geotechnical tests of the foundation and backfill soils are presented in detail.

The test wall design based on the District 12 TSDHPT design standard is outlined and compared with results from the field performance study. A proposed new design procedure is developed based on modification of current design procedures. Significant modifications were made in the areas of the use of cohesive soil in the backfill, the computation of lateral earth pressures, and the computation of stability against overturning.

KEY WORDS: Cantilever Retaining Wall, Lateral Earth Pressure, Deflection, Rotation, New Design Procedure

SUMMARY

The information presented in this report was obtained during the last three years of a five year study on "Determination of Earth Pressures for Use in Cantilever Retaining Wall Design". The objective of this research was to conduct a field performance study on a full scale cantilever retaining wall in order to verify or modifyu current design procedures. This objective has been accomplished and the proposed modifications in design procedure are based on measured earth pressures, measured wall movements, and measured geotechnical properties of the soils adjacent to the wall.

The measured earth pressures on the heel (back) side of the wall were greater than those predicted by current design procedures. A proposed uniform pressure of 2 psi and an earth pressure coefficient of unity are indicated for use in the proposed design modifications. The measured earth pressure on the toe (front) was 3.5 times greater than the pressure measured on the heel (back) at the same depth. Also, significant earth pressure was measured on the front of the key. These pressures contribute to the stability of the wall against sliding and overturning. The measured pressures along the base of the footing were nearly uniform because of foundation soil resistance which contributes to stability against overturning. This contribution is included in the proposed design modifications.

Total horizontal movement measurements indicated that most of the movement occurred during the construction backfilling process. Vertical movement and tilt measurements were relatively small because

of the stiff clay foundation soil. The undrained shear strength is recommended in the modified design procedure because it is the appropriate strength parameter during construction.

The proposed modification in design procedure should be verified by additional field performance studies. These studies should include walls with different proportions that are founded on and backfilled with different soil types. This report contains recommendations for instrumentation on future field studies.

IMPLEMENTATION STATEMENT

The proposed modifications in design procedures for cantilever retaining walls which are presented in this report can be implemented by the sponsoring agencies. However, the use of the proposed design modifications should be limited to applications where the soil conditions are essentially the same as those surrounding the wall tested in this study. Use of the design modifications in different soil conditions should be verified by additional field performance studies. The addition of a key on the base of a footing founded on clay soils could result in the elimination of the need for drilled piers or H-piles under the footing, thereby reducing the overall cost of a cantilever retaining wall.

TABLE OF CONTENTS

TABLE OF CONTENTS (Continued)

TABLE OF CONTENTS (Continued)

LIST OF TABLES

LIST OF FIGURES

LIST OF FIGURES (Continued)

LIST OF FIGURES (Continued)

INTRODUCTION

Problem Statement

The Texas State Department of Highways and Public Transportation (TSDHPT) is responsible for the acquisition of right of way, design, construction inspection and maintenance of transportation facilities throughout the state. Many high volume traffic routes pass through urbanized areas which require grade separations at street or highway intersections. This creates the problem of providing grade separations within a minimum amount of right of way, and the problem is especially prevalent in urban areas where land costs are very high. This problem can be solved by utilizing a retaining wall, which is a structure used to maintain a difference in elevation between ground surfaces when space limitations prevent the use of a natural slope. Retaining walls have been constructed successfully on TSDHPT projects for many years. However, there is some concern among TSDHPT engineers that these walls have been overdesigned. The future need for additional retaining walls has led to the proposal that the current design procedures be verified or that an improved design procedure be developed.

Terminology

The terminology associated with a cantilever wall cross section is given in Fig. 1. The stem acts structurally as a cantilever beam which must resist the lateral thrust caused by the soil mass against the wall.

Numbers in parentheses refer to the references in Appendix I.

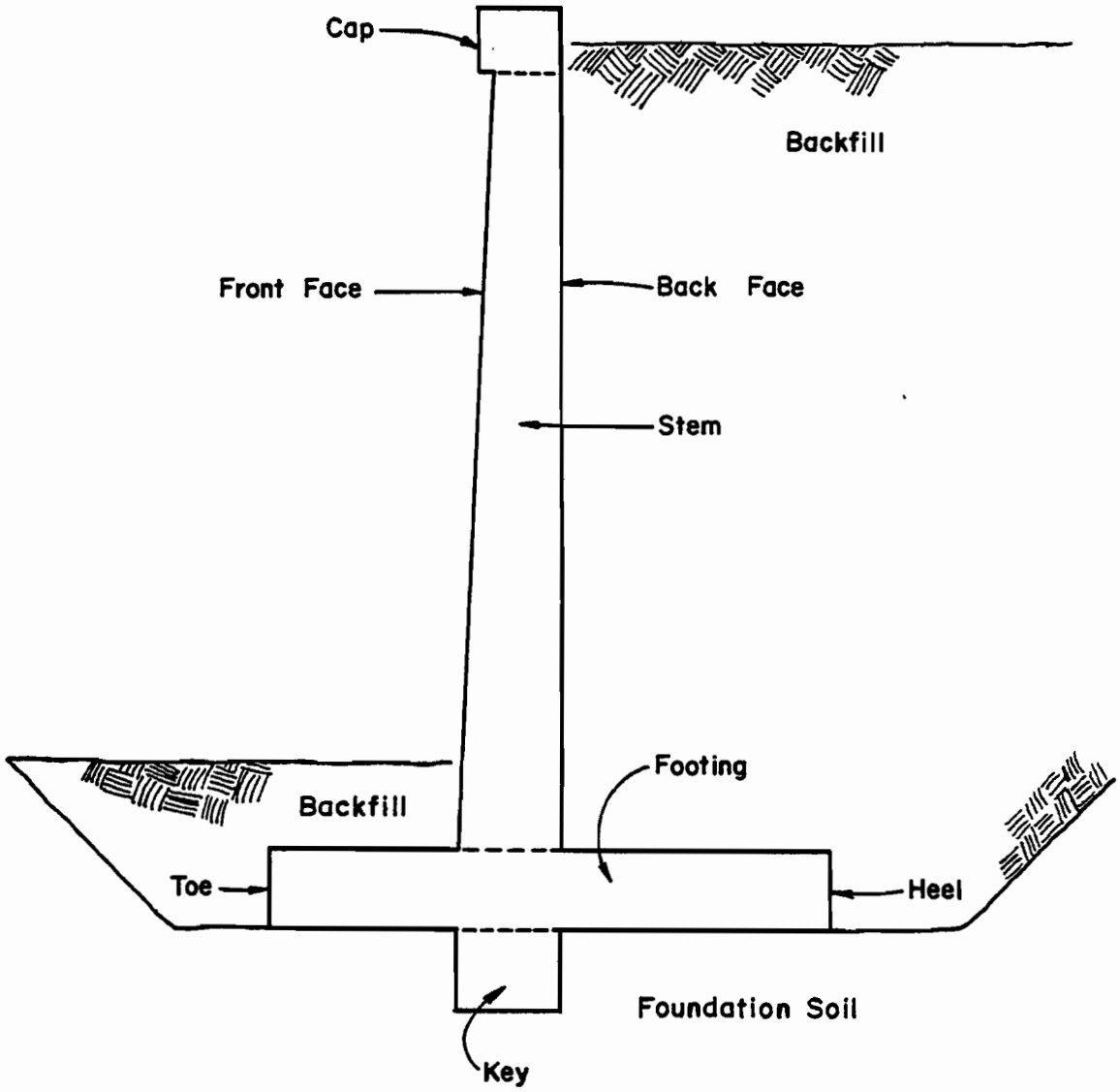

FIG. 1 - Cantilever Retaining Wall Terminology

The front face is the side of the stem which is exposed for much of the wall height and the back face is the side of the stem which is adjacent to the backfill for most of the wall height. The cap is an optional component which is often included if a guard rail or barrier fence is attached to the top of the stem. The footing is the structural component that must transmit vertical forces to the undisturbed soil. Consequently, the footing is designed using the same criteria as those used for shallow foundations. Backfill is the disturbed material used to bring the ground surfaces up to design elevations. A key is an optional component that may be included to resist lateral thrust and movement. Keys may be located at different positions along the base of the footing. The heel is the face of the footing on the back side of the wall, and the toe is the footing face on the front side of the wall. Those portions of the footing on the front and back sides of the wall are termed the toe projection and heel projection respectively.

Basic Design Procedures

Cantilever retaining walls are currently designed by a process of trial and correction of section dimensions. Earth pressures acting on the trial section are computed based on earth pressure theories, the assumed wall movement and the geotechnical properties of the foundation soil and backfill. The section dimensions are revised until the wall is stable against sliding, bearing failure or excessive settlement and overturning. Then computations for areas of steel, depth of sections, bond stresses and resisting moments typical of reinforced concrete design are performed, but are not a part of this study.

Objective of the Study

The objective of this research is to conduct a field performance study on a full scale cantilever retaining wall in order to verify or modify current design procedures and to propose an improved design procedure. The design procedures to be proposed are based on measured earth pressures, measured wall movements and the geotechnical properties of the soil adjacent to the wall. The basic means to achieve this objective are:

1. Review current design procedures to use as a format for the proposed design procedure.
2. Review previous research to plan the field performance study procedures and select instrumentation methods.
3. Install instrumentation to measure earth pressures on the bearing surfaces of the test wall for the duration of the study to obtain the critical earth pressure distributions to be used in the proposed design procedure.
4. Install instrumentation to measure horizontal and vertical displacement and tilt of the wall for the duration of the study to obtain the response to earth pressures.
5. Obtain soil samples of the foundation soil and backfill to determine the geotechnical properties and supplement these results with reports of soil exploration at the site and soil test results by the project inspector.
6. Compare the test wall design procedures with corresponding study measurements.

CURRENT RETAINING WALL DESIGN PROCEDURES

Wall Proportions

Each project will impose certain requirements on the wall proportions. The height of the wall is a function of the required elevation difference on each side of the wall and the depth of cover on the toe side of the wall. The footing width is a function of wall height and stability requirements established in the design procedures. A cantilever wall is most often used and is the type of cross section under consideration in this study. Trial proportions are given in many references (1, 11).

Geotechnical Properties

The geotechnical properties of the foundation soil and backfill should be measured in order to obtain the most efficient design. The shear strength and compressibility of the foundation soil are needed to ensure that bearing failure or excessive settlement does not occur. Lateral earth pressures are a function of the unit weight and shear strength of the backfill. The location of the ground water table is important as porewater pressure affects each of the properties mentioned above. The permeability of the backfill is also a consideration.

Gravity Forces

The gravity forces which contribute to the earth pressures are the weight of the structure and the portion of the backfill included in the free body diagram. Typical free body diagrams are given later. The weight of any structure which falls within the free body diagram must also be included. Many designers include live loads. In current

design procedures, liveloads are represented by an additional uniform depth of backfill placed on the heel side of the wall (18, 19). This hypothetical backfill is described as an equivalent surcharge.

Lateral Earth Pressures

The lateral earth pressures which develop on the vertical bearing surfaces of the wall must be predicted. These predictions of lateral earth pressures are generally based on limiting equilibrium mechanics and the assumptions that the active state of stress develops in the soil on the heel side of the wall and the passive state of stress develops on the toe side of the wall. The concept associated with limit or plastic equilibrium is that sufficient wall movement occurs so that the full shearing strength of the backfill soil is developed. The active state of stress corresponds to the minimum lateral pressure that can develop, and the passive state of stress corresponds to the maximum lateral pressure that can develop (8, 11). The at rest state of stress implies no wall movement and elastic equilibrium conditions.

The lateral earth pressure predictions are based on the geotechnical properties of the soil and the original classical earth pressure theories of Coulomb in 1776 (1,8) or Rankine in 1857 (1,8). Designers currently apply these theories either directly by analytical solutions or indirectly through graphical and semiempirical methods.

Coulomb's Theory.- Coulomb's theory is an attempt to mathematically interpret the force system acting upon a retaining structure. There are two basic parts to this theory:

1. Obtaining the magnitude of the lateral force acting upon the retaining structure, and

2. Describing the lateral pressure distribution in order to define the point of application of the lateral force.

Coulomb observed that a wedge of soil formed behind the retaining structure when the lateral force became a minimum. He made these observations on walls with a planar back face. These conditions infer that the active state of stress develops behind the wall and the soil within the failure wedge is in a state of plastic equilibrium. The failure wedge is bounded by the back of the wall and a rupture surface through the backfill as shown in Fig. 2. To obtain the magnitude of the lateral force, Coulomb assumed (1):

1. The soil is homogeneous and isotropic.
2. The rupture surface is a plane.
3. The shear resistance is uniformly distributed along the rupture surface.
4. The failure wedge acts as a rigid body.
5. Friction is developed between the wall and the failure wedge.
6. Plane strain applies.

The magnitude of the minimum force against the wall is obtained by considering equilibrium of the failure wedge in light of the assumptions above. The force system is shown in Fig. 3. The weight of the soil within the failure wedge is W_w. P_a is the resultant of the pressures along the structure and acts at the wall friction angle, δ, from the normal. R is the resultant of the normal and shear stresses along the rupture surface and acts at the angle of shear resistance, ϕ, from the normal.

The point of application of P_a is obtained by considering that

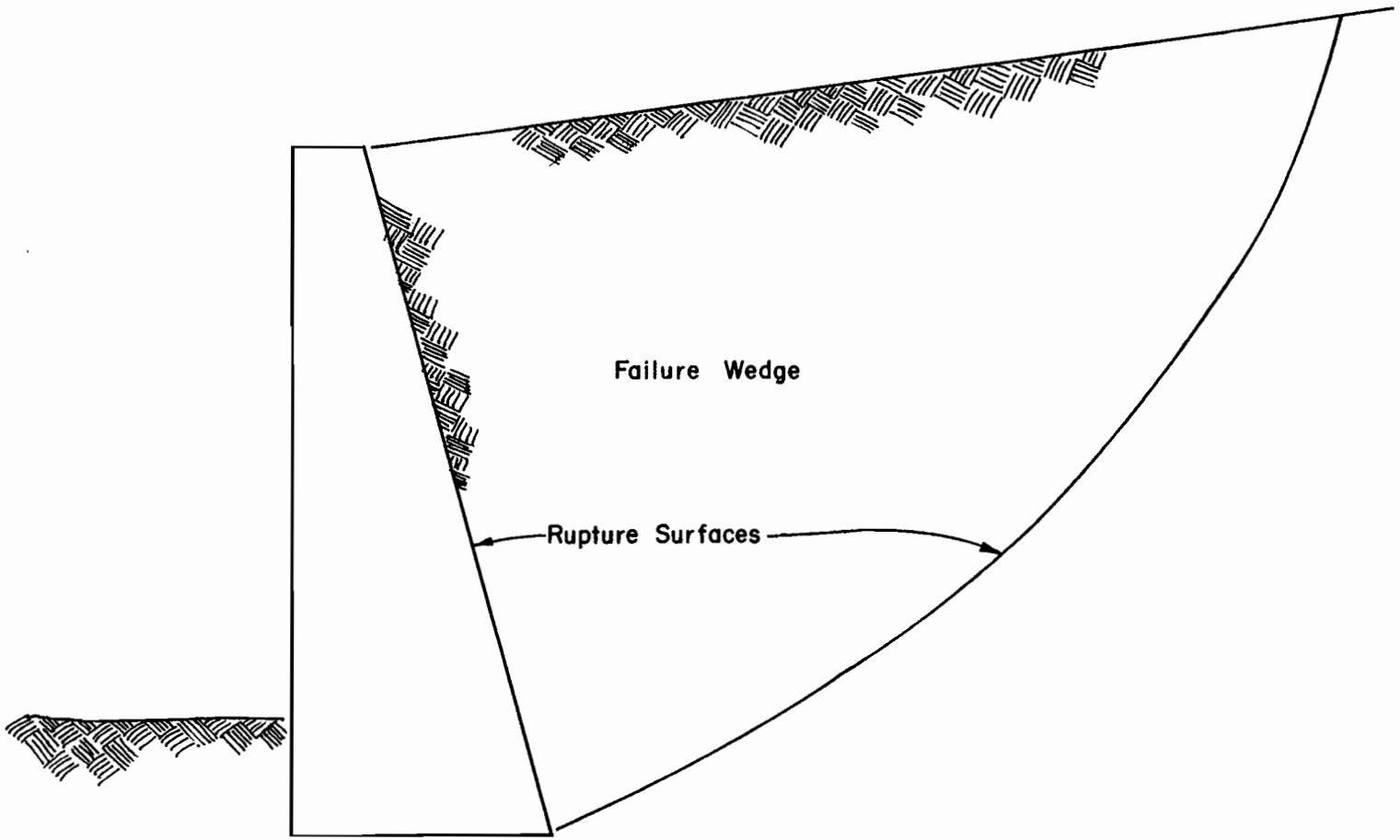

FIG. 2 - Failure Wedge - Coulomb Conditions

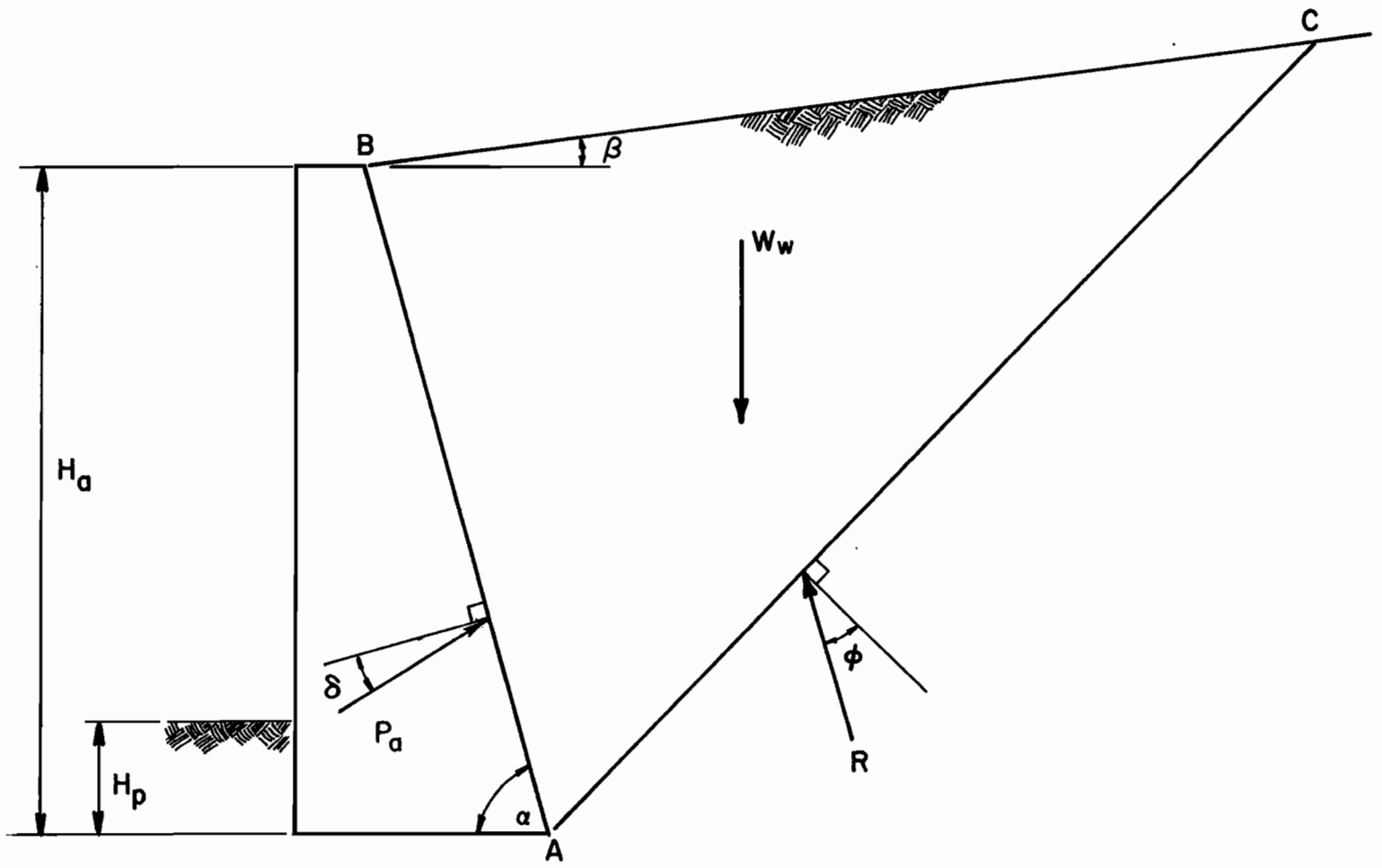

FIG. 3 - Assumed Failure Conditions - Coulomb

the force acts through the centroid of the earth pressure distribution along the back face of the retaining structure. For this part of his theory, Coulomb assumed a distribution that increases linearly with depth, as a hydrostatic pressure. No attempt was made to justify this assumption (22). This solution places the point of application of P_a at one-third of the wall height above the base of the structure.

The hydrostatic pressure distribution and the development of trigonometry simplified the calculation of P_a to

$$P_a = \frac{K_a \gamma H_a^2}{2} \quad \ldots\ldots\ldots\ldots\ldots\ldots\ldots\ldots\ldots\ldots\ldots\ldots \quad (1)$$

in which γ = the unit weight of the backfill and H_a = the depth of backfill on the heel side of the wall. K_a is the coefficient of active earth pressure and is defined, in terms of Coulomb's conditions as

$$K_a = \frac{\sin^2 (\alpha + \phi)}{\sin^2 \alpha \sin (\alpha - \delta) \left(1 + \sqrt{\frac{\sin (\phi + \delta) \sin (\phi - \beta)}{\sin (\alpha - \delta) \sin (\alpha + \beta)}} \right)^2} \quad \ldots\ldots\ldots \quad (2)$$

in which α, β, δ and ϕ are angles as shown in Fig. 3. The derivation of these equations can be found in many soil mechanics texts (1).

Passive earth pressures act on the front of the retaining structure. By analogy, the resultant force of the passive earth pressure, P_p, is defined by the equation

$$P_p = \frac{K_p \gamma H_p^2}{2} \quad \ldots\ldots\ldots\ldots\ldots\ldots\ldots\ldots\ldots\ldots\ldots\ldots \quad (3)$$

in which H_p = the depth of backfill in front of the wall. K_p is the coefficient of passive earth pressure and is defined, in terms of Coulomb's conditions, as

$$K_p = \frac{\sin^2 (\alpha-\phi)}{\sin^2 \alpha \sin (\alpha+\delta) \left(1 - \sqrt{\frac{\sin (\phi+\delta) \sin (\phi+\beta)}{\sin (\alpha+\delta) \sin (\alpha+\beta)}}\right)^2} \quad \ldots\ldots\ldots (4)$$

The main deficiencies in Coulomb's basic assumptions are those involving the ideal soil and plane rupture surface. Real soils are neither homogeneous nor isotropic. A plane rupture surface was assumed to simplify computations. This is considered to have a minor effect for the active case but can lead to large errors for the passive case. Cantilever retaining walls do not have the planar back face which is a basic condition in the derivation of Coulomb's theory.

Rankine's Theory.- Rankine considered an infinitely long and deep cohesionless soil deposit with no external forces and examined the effects of laterally expanding or compressing the soil mass. This condition implies that the change from an at rest state of stress to the active passive state of stress is impending (22). In applying Rankine's theory to retaining walls, both rupture surfaces must occur within the soil (8,19). This condition requires that neither rupture surface intersect the back face of the retaining wall; therefore, no sliding occurs betweeen the wall and the soil. This is illustrated in Fig. 4. Soil wedge ABF would remain in position and remain in an elastic state of stress. The failure wedge would slip along the rupture surface, or shear plane, AF, not along the back face of the

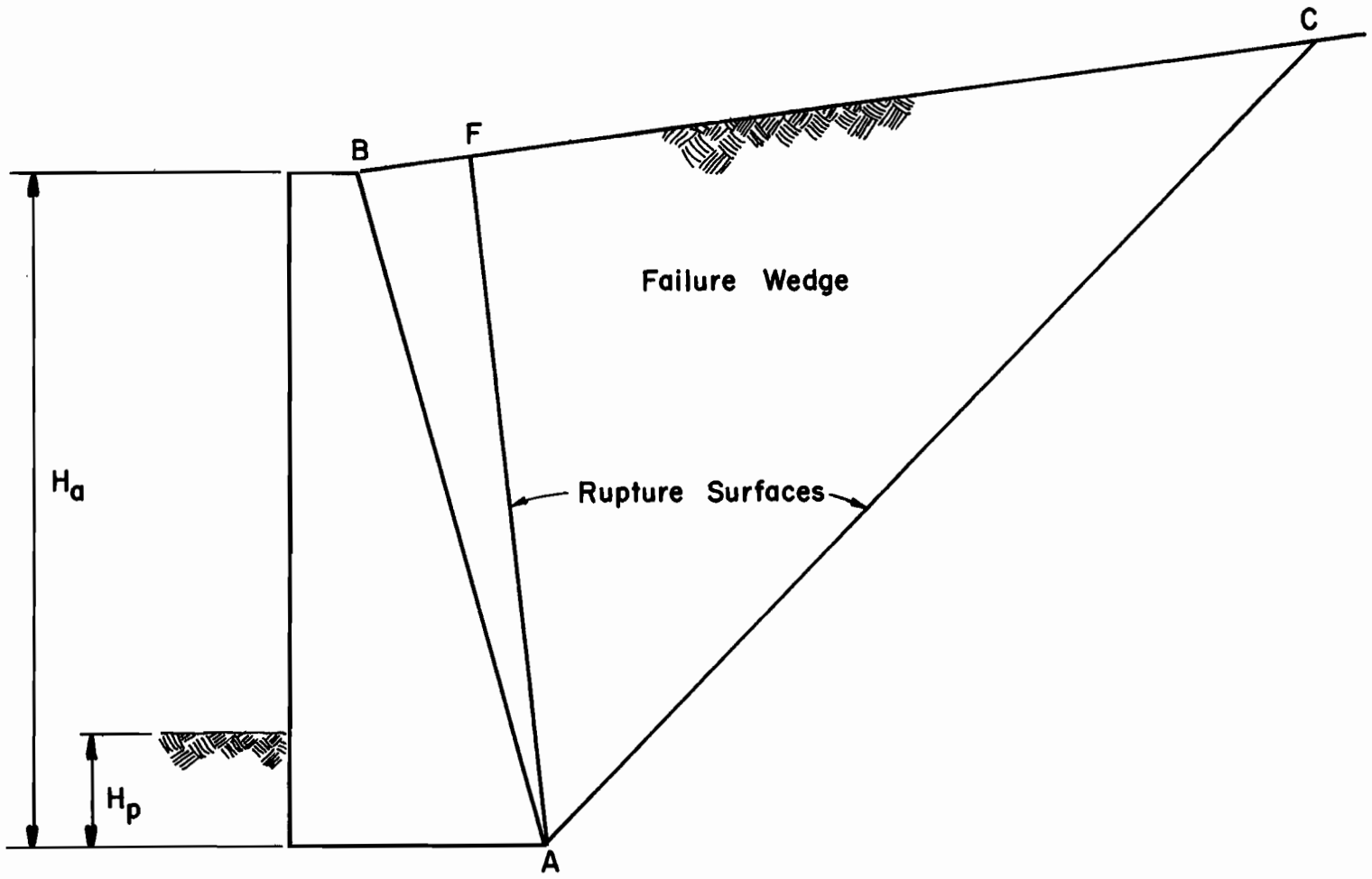

FIG. 4 - Assumed Failure Wedge - Rankine

wall. This condition is often incorrectly treated as a requirement that the back face of the wall be frictionless for Rankine's theory to apply.

Rankine's active state of stress occurs when the soil within the failure wedge is in a state of plastic equilibrium and the lateral earth pressure developed is a minimum. Since no rupture surface occurs along the retaining wall, the lateral force is determined on a vertical plane which passes through point A on the failure wedge as shown in Fig. 5. W_w is the weight of the soil bounded by the vertical plane and the rupture surface. R is the resultant of the normal and shear stresses along the rupture surface and it deviates from the normal to the rupture surface by the angle of shear resistance of the soil, ϕ. P_a is the resultant of the active pressures along the vertical plane and it deviates from the horizontal by the angle of the ground surface slope, β.

P_a acting parallel with the ground slope, is consistent with Rankine's assumed ideal soil properties. A hydrostatic pressure distribution is assumed. This places the point of application of P_a and R at the lower one-third points of the vertical plane and the rupture surface as illustrated in Fig. 5. The lines of action of these forces intersect at the line of action of W_w as required for equilibrium (8). The resultant force of the lateral earth pressure is computed using Eq. 1, except the coefficient of active earth pressure in terms of Rankine's conditions is used which is

$$K_a = \cos \frac{\cos \beta - \sqrt{\cos^2 \beta - \cos^2 \phi}}{\cos \beta + \sqrt{\cos^2 \beta - \cos^2 \phi}} \qquad (5)$$

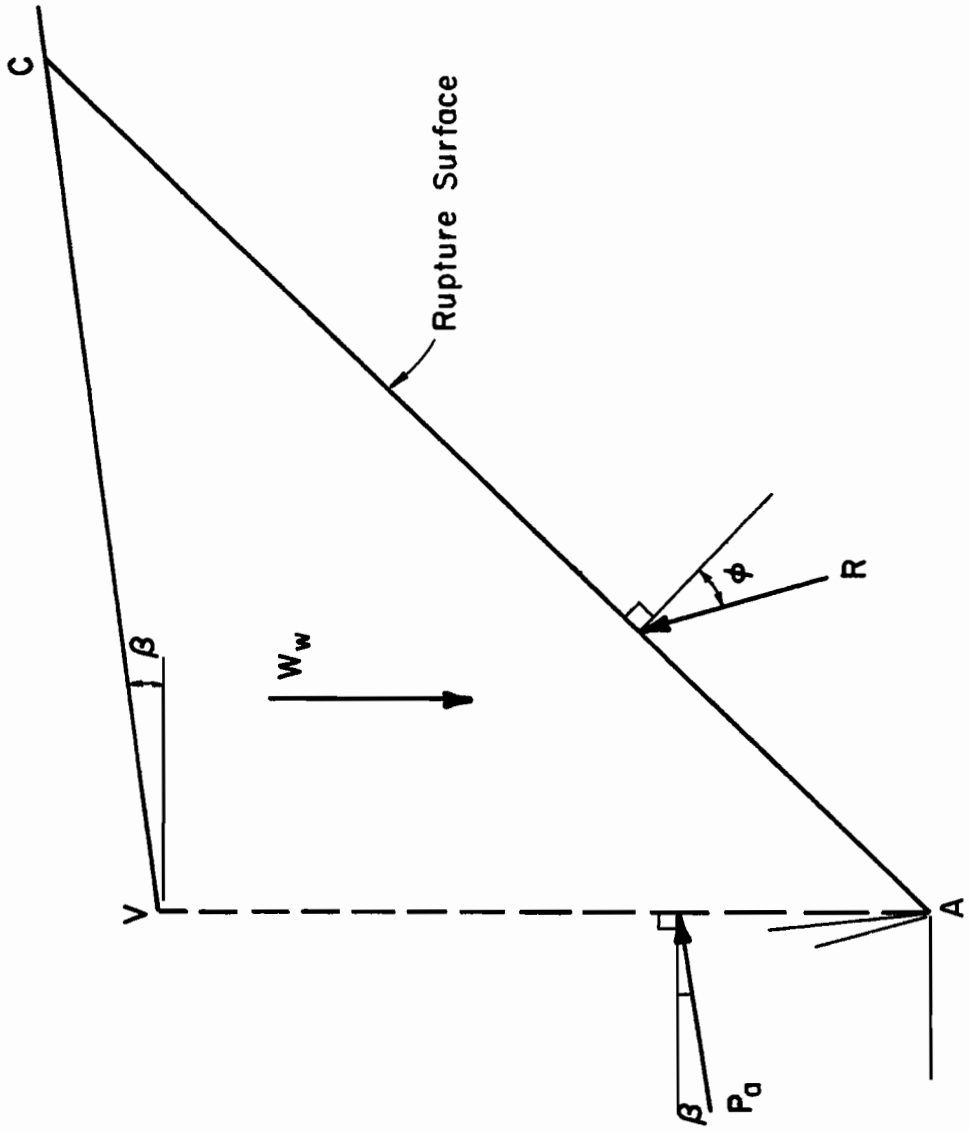

FIG. 5 - Assumed Failure Conditions - Rankine

The lateral force, P, acting against the back face of the retaining wall is the resultant of P_a and the weight of the soil, W_I, between the vertical plane and the back face of the retaining wall. P deviates from the normal to the back of the wall by the angle ψ as shown in Fig. 6. For Rankine's theory to apply the angle ψ must be less than or equal to the friction angle between the wall and the soil. The resultant of passive pressures, P_p, can be computed by Eq. 3 except the coefficient of passive earth pressure in terms of Rankine's theory is used which is

$$K_p = \cos \beta \frac{\cos \beta + \sqrt{\cos^2 \beta - \cos^2 \phi}}{\cos \beta - \sqrt{\cos^2 \beta - \cos^2 \phi}} \quad \ldots\ldots\ldots\ldots\ldots \quad (6)$$

Note that the earth pressure coefficients based on Rankine's theory are independent of wall friction.

The main deficiency in Rankine's theory concerns the ideal soil which was assumed and is inconsistent with real soil deposits. The planar rupture surfaces are assumed to simplify computations. The derivation of Rankine's earth pressure coefficients is found in most soil mechanics texts (1).

Equivalent Fluid Method.- Coulomb and Rankine's theories have been used as a basis for determining lateral earth pressures empirically. The hydrostatic earth pressure distribution assumed in each theory is used in the equivalent fluid method. The backfill is

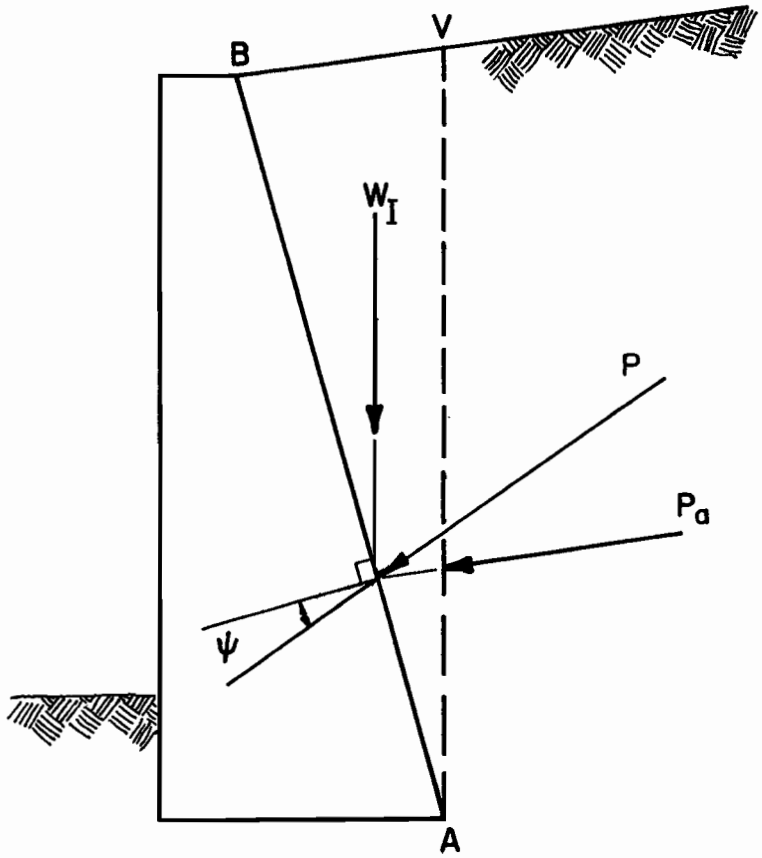

FIG. 6 - Force on Back of Wall - Rankine

assigned a unit weight of an equivalent fluid, γ_e, depending upon the soil type. The magnitude of the lateral force on the heel side of the wall is

$$P_h = \frac{\gamma_e H^2}{2} \quad \ldots\ldots\ldots\ldots\ldots\ldots\ldots\ldots\ldots\ldots \quad (7)$$

in which H = the depth of backfill above the base of the heel. Values of γ_e range between 30 to 120 pcf (4.7 to 18.9 kN/m^3) for backfills placed horizontally (23). The point of application of P_h is at the lower third point of the section considered. The section used for cantilever retaining walls is typically a vertical plane which passes through the heel of the footing. H is the vertical distance from the bottom of the heel to the ground surface. The line of action of P_h should be horizontal, but agrees better with theory if taken to be parallel with the ground slope (8). The resultant force on the back of the retaining wall is obtained as the vector sum of the weight of the soil between the back of the wall and the vertical plane through the heel and P_h.

The use of the equivalent fluid method is consistent with the Rankine theory when the ground slope is horizontal. The equivalent fluid method should not be used for sloping backfills as a fluid would have a level surface. This discrepancy is partially offset by using a γ_e value which is larger than would be used for a level ground surface (8,23).

The values of γ_e discussed above apply to the active state of stress. If the resultant of the passive pressure on the toe side of

the wall is desired, the value of γ_e should be increased, but no accepted method has been published. Also, most designers conservatively omit lateral support on the toe side of the wall.

Footing Pressure

The lateral forces computed using the methods described previously cause eccentric loading on the spread footing. The pressure distribution along the base of the footing is commonly computed using the formula for flexure and direct stress in the form

$$q = \frac{V}{B}\left(1 \pm \frac{6e}{B}\right) \quad \ldots\ldots\ldots\ldots\ldots\ldots\ldots\ldots\ldots\ldots\ldots\ldots \quad (8)$$

in which V = the sum of the gravity forces above the footing, B = the footing width and e = the eccentricity as illustrated in Fig. 7. The solution of Eq. 8 yields the maximum and minimum footing pressures at the toe and heel of the footing respectively. The distribution of pressure is assumed to be linear as shown. The area of the pressure diagram should equal the vertical load. The centroid of the area is on the line of action of the vertical load. The footing is sized to ensure that e is less than or equal to B/6 which results in the vertical force being applied within the middle third of the footing. This assures a compressive contact pressure throughout the footing.

Stability

At this point in the design the engineer will have established: the dimensions of the trial section, the geotechnical properties of the soil and the earth pressures on the bearing surfaces of the retaining wall. The next step is to evaluate the stability of the design against

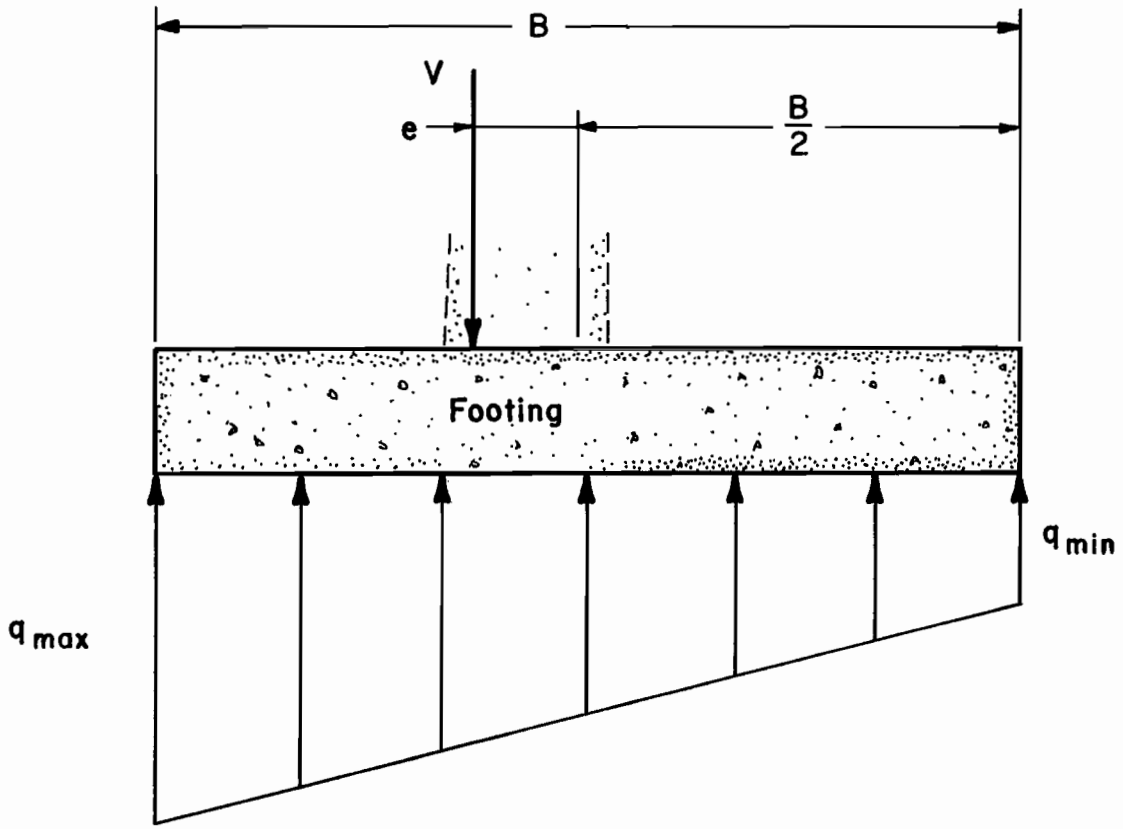

FIG. 7 - Assumed Pressure Distribution on Footing Base

sliding, bearing and settlement failure, and overturning.

Sliding.- The lateral pressures tend to push the retaining wall away from the higher backfill. A sliding failure can occur along the contact surface of the bottom of the footing and the foundation soil, or by shear along a surface through the soil beneath the footing. The factor of safety against sliding is defined as the ratio of the forces which resist sliding to driving forces. The contribution of the resultant force that would develop from the passive pressure on the front side of the wall is often omitted, because the backfill may be placed behind the wall before the fill is placed in front of the wall. Also, passive pressures may not fully develop, especially if the fill is clay (18). The resisting force is a function of the shear strength of the foundation soil. If the resistance to sliding is not sufficient to offset the driving forces, the footing size may be increased, or a key is added to the footing. This may increase the length of the shear surface and passive resistance and therefore, the magnitude of the resisting force. There are several potential shapes the shear surface may follow, which are affected by the location and length of the key as illustrated in Fig. 8 (13). Deep seated failure surfaces may occur if the footing is founded on a soft soil or a firm soil which overlies a soft stratum. This problem is best solved using techniques based on slope stability analysis but is not a part of this study.

Bearing and Settlement.- The footing should be sized to ensure that the maximum contact pressure does not exceed the bearing capacity of the soil. The bearing capacity of the foundation soil is determined using the same criteria as for spread footings. A settlement analysis

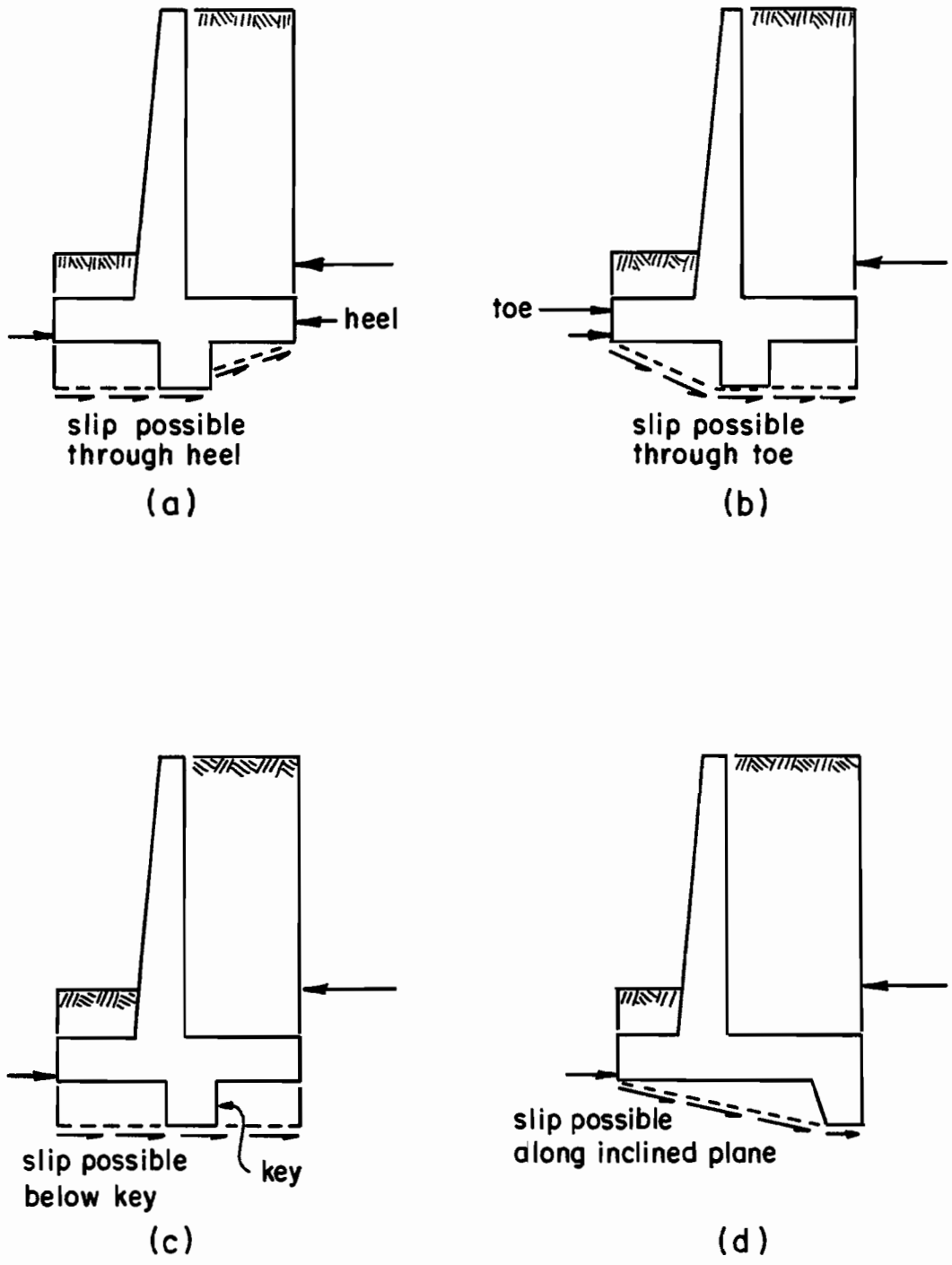

FIG. 8 - Possible Slip Surfaces Beneath Footing

is required if the applied pressures exceed the preconsolidation pressure of the foundation soil. The analysis is based on the computed pressure distribution along the bottom of the footing. Also, excessive differential settlement will contribute to the instability of the wall. Walls that are founded on soft soils may settle towards the backfill and significantly increase the earth pressures on the back face of the wall (23). If these settlement problems cannot be overcome by adjusting the size of the footing, pile supports may be necessary.

Overturning.- Computations for the stability against overturning are usually accomplished by comparing moments of the forces which tend to overturn the wall and moments of the forces which resist overturning (1,10,19,26). The factor of safety against overturning is the ratio of the moments which resist overturning to the moments which cause overturning. A considerable range in values for the factor of safety will result, depending on the interpretation of the effect of each moment. There is no generally accepted procedure for computing the factor of safety (8). An alternate method of evaluation is to consider that a wall is safe against overturning if the resultant pressure on the foundation passes through the middle third of the footing if it is founded on soil, or the middle fourth of the footing if it is founded on rock (11,23). The size of the footing may need adjustment to ensure stability against overturning.

Structural Design

The structural components of the retaining wall are treated as separate cantilever beams with each component loaded with the appropriate earth pressures acting on the bearing surfaces. Some adjustment

of wall dimensions may be necessary to develop the bending moments and shear stresses necessary to resist the applied pressures.

Drainage

It should be emphasized that the Coulomb and Rankine lateral earth pressure computation procedures described previously are in terms of effective stress. It is desirable to prevent water retention behind the retaining wall; otherwise, the retaining wall must be designed to withstand the porewater pressures developed in addition to earth pressures. This is accomplished by providing adequate surface drainage and by using a free draining backfill material with direct outlets such as weep holes or a collection system such as pipe drains. Filters may be necessary to prevent the drainage system from becoming clogged with fine soil particles.

Construction

Upon revising the initial wall proportions to meet the conditions described above, the retaining wall should perform satisfactorily if the field conditions do in fact match those assumed in the design procedure. Special consideration should be given to verifying these assumptions during the construction of the wall. The design engineer should be apprised of any field changes that occur. Additional conservatism in design is warranted if close field monitoring is not expected. Most design procedures are based on cohesionless backfills, as the classical theories apply directly to this type of backfill. Also, cohesionless soils provide the high permeability required for drainage to prevent porewater pressures from acting on the walls. Much less is known or understood about the performance of retaining walls

which support cohesive soils.

REVIEW OF PREVIOUS RESEARCH

Large Scale Retaining Wall Tests

Laboratory Conditions.- Terzaghi made significant contributions to the understanding of earth pressures in 1920 (20), 1934 (21), and 1936 (22). This study of the classical earth pressure theories was initiated because many engineers and contractors claimed that the earth pressures determined theoretically had no resemblance to observed earth pressures during subway construction.

Terzaghi concludes that the use of Rankine's theory should be discontinued because the assumptions are not compatible with the stress-strain relationships observed in soils (22). Based on tests, Terzaghi concludes that Coulomb's earth pressure theory is valid if sufficient wall movement occurs. It is observed from tests that the magnitude of lateral earth pressure proposed by Coulomb is developed, and that a hydrostatic pressure distribution does occur. However, the hydrostatic pressure distribution requires about ten times more movement than that required to develop the active lateral force (22).

Tests were performed by backfilling large scale test walls and then moving the walls away from the backfill. In one test, the wall was rotated about its base, while in another test, the wall was moved laterally away from the backfill. When the backfill was a dense sand, the active force was developed when the wall movement was 0.0005H at the midpoint of the wall and an approximate hydrostatic pressure distribution developed when the top of the wall had moved 0.005H, at which

time "a visible and audible slip" occurred. For loose sands, the active earth force required much more average movement than 0.005H and the pressure distribution became hydrostatic with essentially no movement.

In summary, Terzaghi's conclusions are:

1. Rankine's earth pressure theory is not valid.
2. Coulomb's theory for the magnitude of lateral force is generally correct because movements to develop the active state can occur for most types of retaining structures.
3. Coulomb's assumption of a hydrostatic pressure distribution is valid when every point on the wall moves 0.005H. This is generally true for retaining walls but is seldom true for braced or rigid structures. Also, the pressure distribution is approximately trapezoidal for wall movements less than 0.005H due to arching.

Most design standards and texts in use today include one or both of the classical theories for earth pressure computations, and specify a minimum movement requirement for the active state of stress to develop. The movement specification in most published tables lies between the values Terzaghi reported necessary to develop the active state of stress and those necessary to produce the hydrostatic pressure distribution.

Effect of Compaction.- Constructing the backfill in lifts with relatively heavy compactive effort is a recent innovation with respect to the development of the classical earth pressure theories used in retaining wall design. The development of lateral stresses due to

compaction has been researched and reported by Sowers et al. in 1957 (17), Broms in 1971 (2), Carder et al in 1977 (3), and Ingold in 1979 (9). Results show earth pressures against the stem of retaining walls to be different in magnitude and distribution than those predicted using the classical earth pressure theories. In Ingold's test, compaction caused the stem to crack. Broms and Ingold proposed new earth pressure theories which predict the magnitude of the lateral pressures on the stem as a function of compaction and soil properties. An approximately uniform pressure distribution due to compaction was theorized based on the analysis of these studies.

Field Performance Studies.- The West Riding County Council in Yorkshire, England is responsible for the maintenance of 1600 bridges that were built before the 1930's. Some of the retaining structures for these bridges have recently failed and many others show excessive bulging and cracking in the middle of the walls. Simple deterioration and classical lateral earth pressure theories do not explain the distress and failures observed (16).

These failures led to the instrumentation, by Sims and others (15,16), of a large retaining wall constructed between 1966 and 1968 on the M1 Motorway in Rotterdam, England. This wall was designed using Coulomb's lateral earth pressure theory. Vibrating wire pressure cells were installed in the backfill to measure horizontal and vertical earth pressures. Strain gauges were installed in the front face and back face of the reinforced concrete stem of the retaining wall. No pressure readings were made until the backfilling had been completed to the top

of the wall.

The first pressure readings were significantly different from those computed by the Coulomb theory. The earth pressures increased with time, particularly after the motorway was opened to traffic. Pressures increased more at the midheight of the wall for about the first five years after the completion of construction. In all cases, the lateral pressures were greater than predicted by the Coulomb theory.

The significant differences between the theoretical earth pressures and pressure distribution and measured earth pressure and pressure distributions require explanation. This is provided by the researchers as follows:

1. Present construction methods are different from those used when the theory was developed.
2. The overdesign of the stem due to excessive factors of safety for stability contribute to the differences between measured and predicted pressures and pressure distribution.
3. Traffic loads appear to have a significant effect on the earth pressures acting on the wall.

Terzaghi evaluated the Coulomb theory using procedures inherent with Coulomb's assumptions and basically practiced in construction before the 1930's. At that time, walls were propped or braced during backfilling. Compaction was minimal, essentially accomplished by the construction equipment used to dump the backfill in place. Upon completion, the props were removed, thereby allowing the necessary movement

to develop the Coulomb active earth pressure and hydrostatic pressure distribution. The walls were relatively flexible gravity walls composed of rock stacked vertically with smaller rocks on the back face and larger rocks on the front face.

Propping retaining walls during backfilling is no longer practiced. Backfill is now placed in lifts and each lift is compacted. Reinforced concrete walls built today generally are more rigid than typical walls built in the past. The high safety factors against sliding, the large footings and the rigidity of reinforced concrete used in present designs are significantly different than walls and conditions which Coulomb considered in the development of his theory. These factors tend to keep the wall movements below those required to develop the Coulomb active state of stress during the construction process, although there is a possibility for sufficient movement to occur after construction. Even so, design procedures should be based on the maximum earth pressures the retaining structures must support. Evidence indicates that earth pressures developed during construction are greater than earth pressures obtained from Coulomb's theory.

Wright et al. (25), in 1975, reported on field performance measurements of earth pressures and wall movements on the stem of a precast panel retaining wall (12), and a cantilever retaining wall (5) which was supported on H piling. It was concluded that the classical earth pressure predictions were satisfactory for the upper portion of the stem, but at rest lateral pressures are more appropriate for the lower portion of the stem.

In 1978, a bridge abutment near Toronto, Canada was instrumented to measure earth pressure and movements. It was observed that the lateral earth pressures were approximately parabolic on the lower three-fourths of the wall and decreased linearly on the upper one-fourth. A linear pressure distribution was recommended for design, using the at rest triangular distribution, even though the movements were sufficient for active pressures to develop according to published criteria. Footing contact pressures were also measured. Nonsymmetrical contact pressures were observed which could not be explained by theory, including finite element analysis.

The results of these research efforts clearly point to the need for additional field performance tests on retaining walls to determine earth pressures on retaining walls, the pressure distributions, and associated wall movements. These parameters are common to design procedures that have been in use for decades and are the logical starting points for design modification recommendations.

Unstudied Design Aspects of Cantilever Retaining Walls

The small amount of published literature on cantilever retaining wall performance tests reveals that several aspects have not been satisfactorily studied. The bearing pressures on spread footings of these retaining walls have not been measured. Most typical designs include keys, but no field measurements have been made to evaluate their effectiveness. In fact, so little is known about the contribution of keys that many designers conservatively neglect certain contributions of keys in design. Some of the uncertainties in evaluating

pressures on the front of a cantilever wall can be clarified with field measurements. No published literature can be found on field measurements of lateral pressures produced by cohesive backfills. Backfilling with clay is undesirable, but is often an alternative a designer must consider because the use of a cohesionless backfill may be economically prohibitive if this material is unavailable locally. An empirical design procedure based on field performance studies of retaining walls backfilled with cohesive soils would help fill a significant void in the state of the art of retaining wall design.

Background on Present Research Program

Planning and Preparation.- A five-year research study was begun in 1977 at Texas A&M University to measure earth pressures acting on the bearing surfaces of cantilever retaining walls founded on spread footings and to measure the movement of the walls due to the applied earth pressures. Initially the study was devoted to a literature survey, preparations for field tests and site selections (13).

The literature survey established the state of the art for cantilever retaining wall design and field performance studies. This information influenced the procedures and instrumentation used to achieve the objective of this study.

Earth pressure cells were selected based on reliability, simplicity, accuracy and satisfactory performance in other studies (5,6,12). A method for installing the earth pressure cells was developed (13) and a plan for locating the earth pressure cells was established. A wall movement measurement system was developed based on procedures found to be effective on similar studies (6,12). A soils investigation program

was established and data collection procedures were finalized.

Potential sites were reviewed and the criteria for test wall selection were as follows:

1. The cantilever retaining walls were to have a conventional cross section and be constructed of reinforced concrete.
2. The walls were to be supported on a spread footing with a protruding key.
3. The cantilever walls were to be constructed on TSDHPT projects.
4. The walls were to be located as near Texas A&M University as possible to ensure adequate monitoring.

Although these selection criteria had the practical advantages of minimizing the cost of the study and obtaining measurements from actual field conditions, the major disadvantage was that construction progress was entirely controlled by the contractor. Therefore, the progress of the study was totally dependent upon the progress made by the contractor.

First Test Wall.- The first wall selected for instrumentation was at the intersection of Interstate Highway 10 and Federal Road in Houston, Texas. Instrumentation of the wall was accomplished, to provide for measurements of:

1. Earth pressures on the footing, key and stem,
2. Tilt of the stem, and
3. Horizontal displacement of the stem.

Geotechnical properties of the in place soils were obtained from the TSDHPT. An additional test boring was made to provide soil samples

for testing at the Texas A&M Geotechnical Laboratory. These test results were supplemented by field tests performed by project inspectors.

Measurements of earth pressures, wall tilt and horizontal displacement were made as the construction procedures allowed and the backfilling operations progressed. The backfilling operations were essentially completed during the summer of 1980 and the analysis of these measurements were reported by Schulze (14). Shortly after this report was completed, the instrumentation at this site was destroyed by construction equipment working adjacent to the test wall. No additional useful information was obtained since TTI Report 236-1 was published; therefore, the field performance study of this wall is not included herein.

TEST WALL

Test Site

The test site selected for this phase of the study is located at the southwest intersection of State Highway 288 and South MacGregor Avenue in the south central area of Houston, Texas. MacGregor Avenue crosses over State Highway 288 at this intersection. Each is a multi-lane roadway. MacGregor Avenue is open to traffic, and Brays Bayou runs through the large median area which separates westbound North MacGregor Avenue and the eastbound South MacGregor Avenue. State Highway 288 is still under construction at this time (1983).

Test Wall Description

Panel 5 of wall LB was instrumented for this study. Panel 5 is an interior panel which was selected to negate end effects. Wall LB is a continuation of the retaining wall which supports the embankment of South MacGregor Aveune. A portion of the plan and elevation views are shown in Fig. 9. The entire length of the wall is 382.5 ft (116.6 m) consisting of twelve 30 ft (9.14 m) panels and one 22.5 ft (6.86 m) panel. Wall LB supports the Left Frontage Street Ramp which provides access to the southbound lanes of State Highway 288 from South MacGregor Avenue and the frontage road. The retaining wall is also used to provide space within the right of way for the Left Access Street as shown in Fig. 10.

Wall LB is a cantilever retaining wall which is supported by a spread footing with a key protruding from the base of the footing. The key is located directly below the stem. The stem is 14 ft (4.27 m)

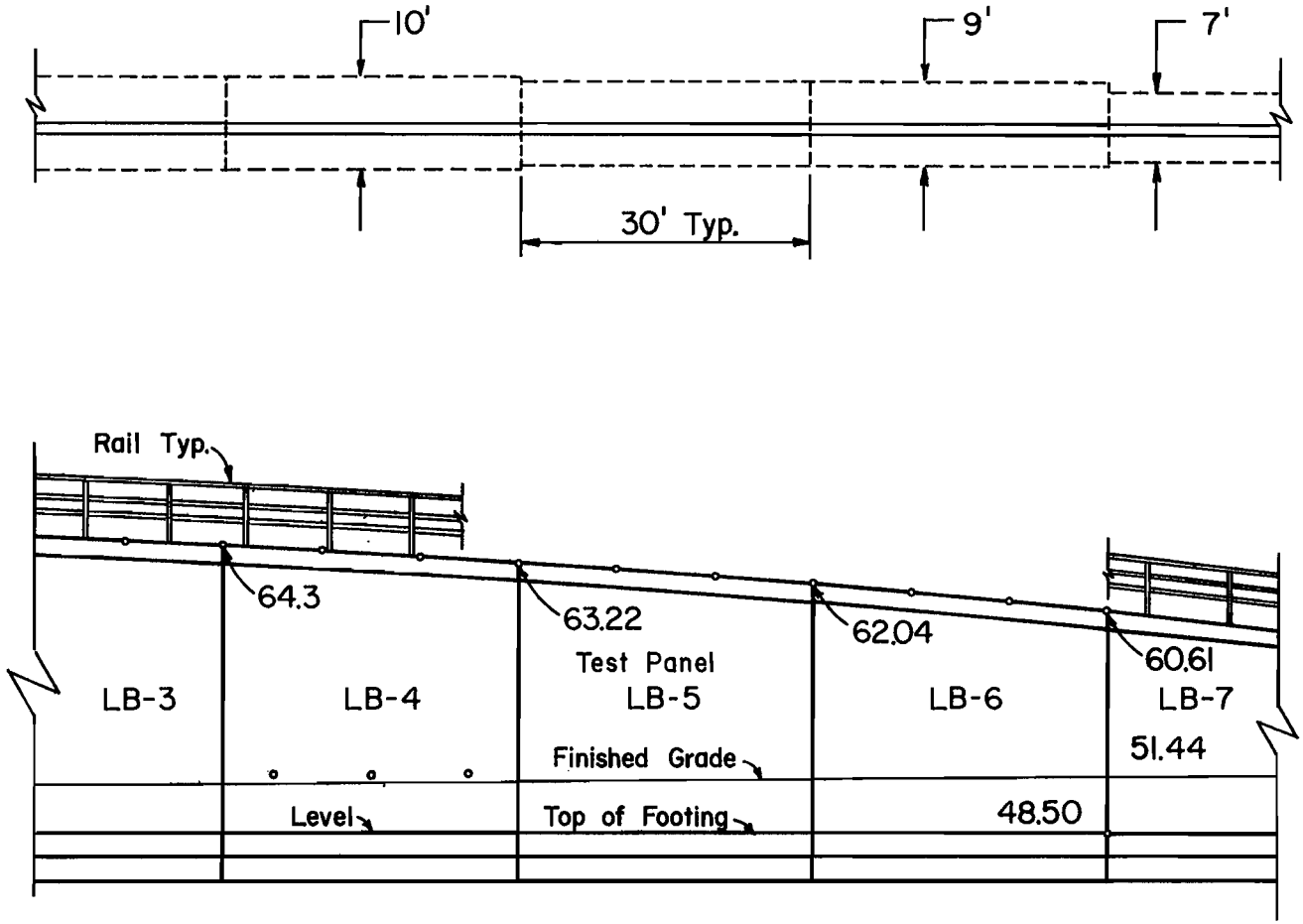

FIG. 9 - Test Wall Plan-Profile
(1 ft = 0.305 m)

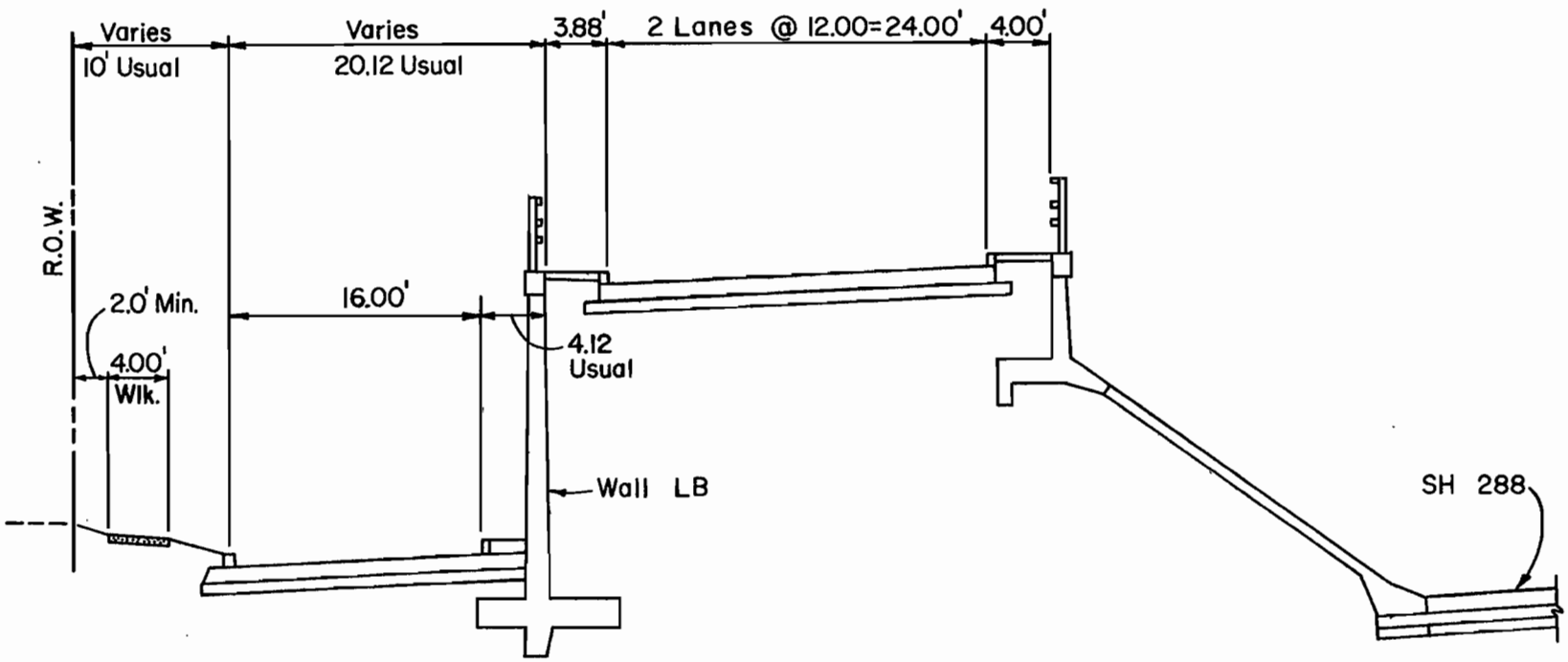

FIG. 10 - Typical Section at Test Panel
(1 ft = 0.305 m)

high at the center of panel 5. The footing is 9 ft (2.74 m) wide and 1.25 ft (0.38 m) thick, poured on a cement stabilized sand 8 in. (20 cm) deep. Drainage is provided by weep holes every 10 ft (3.05 m) with fiber and wire mesh filters inset into the back face of the stem. The dimensions at the center of panel 5 are given in Fig. 11. There are construction joints between the footing and the stem, and between the stem and the cap.

Instrumentation

The objective of the instrumentation was to measure the magnitude and distribution of the earth pressure, and the magnitude and direction of wall movement. These measurements were considered essential in order to evaluate current design procedures. Earth pressure cells were installed in the back face of the stem and in the footing. Measurement points were attached to the front face of the stem and reference points were set in the ground near the right of way line in order to measure wall movement. Installation of instrumentation was controlled by construction progress and procedures.

Earth Pressure.- Terra Tec pneumatic total pressure cells were selected to instrument the test wall. These are composed of a fluid filled loading plate, a bellows and valve mechanism, and a lead containing a pressure line and return line. A cross section of a Terra Tec pressure cell is shown in Fig. 12. The loading plate has two active faces which are 6 in. by 6 in. (152 mm by 152 mm) thin stainless steel sheets welded together along the stiff rim.

Loading the active faces causes the fluid pressure within the loading plate and the bellows mechanism to increase. The pressure on

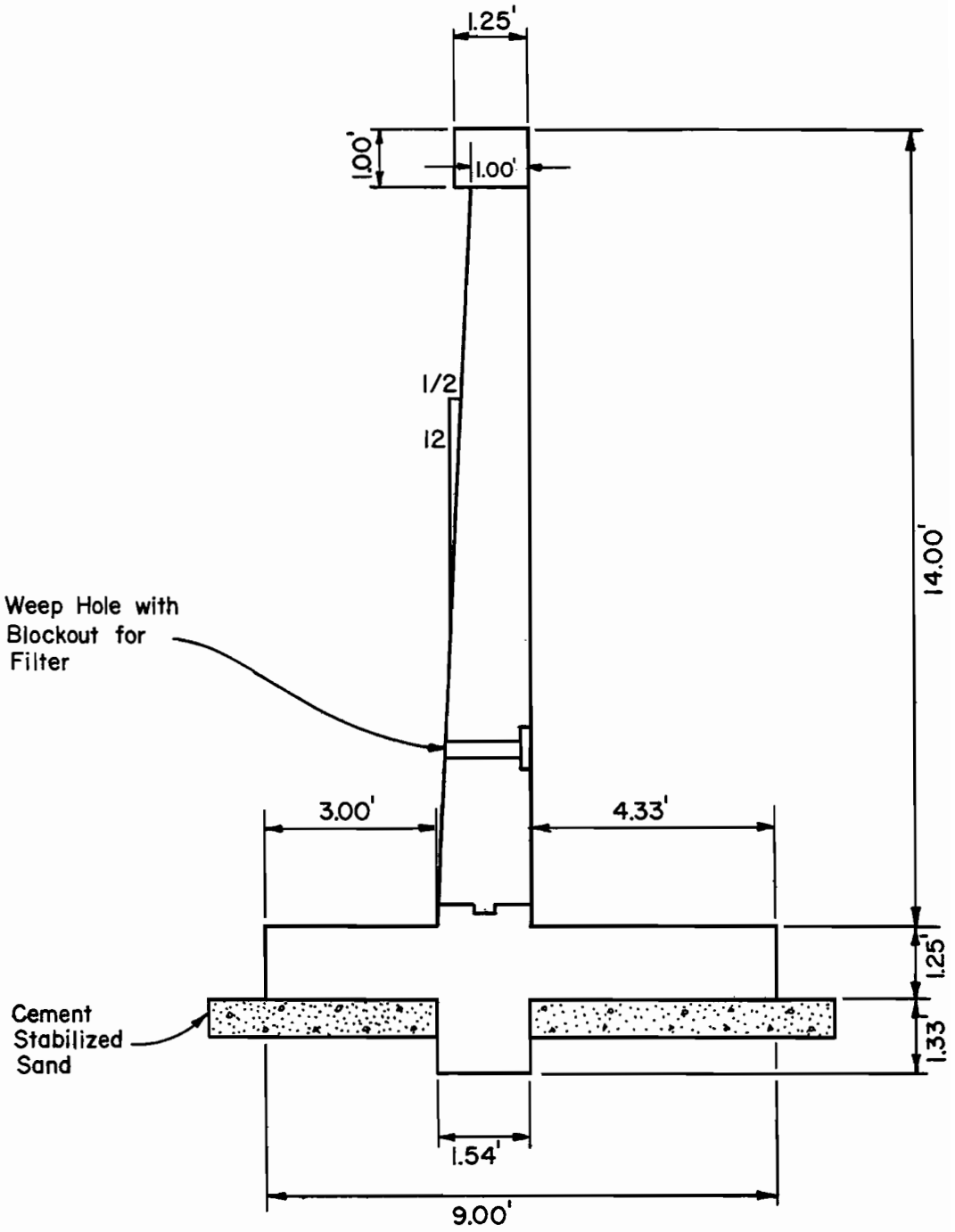

FIG. 11 - Test Wall Cross Section
(1 ft = 0.305 m)

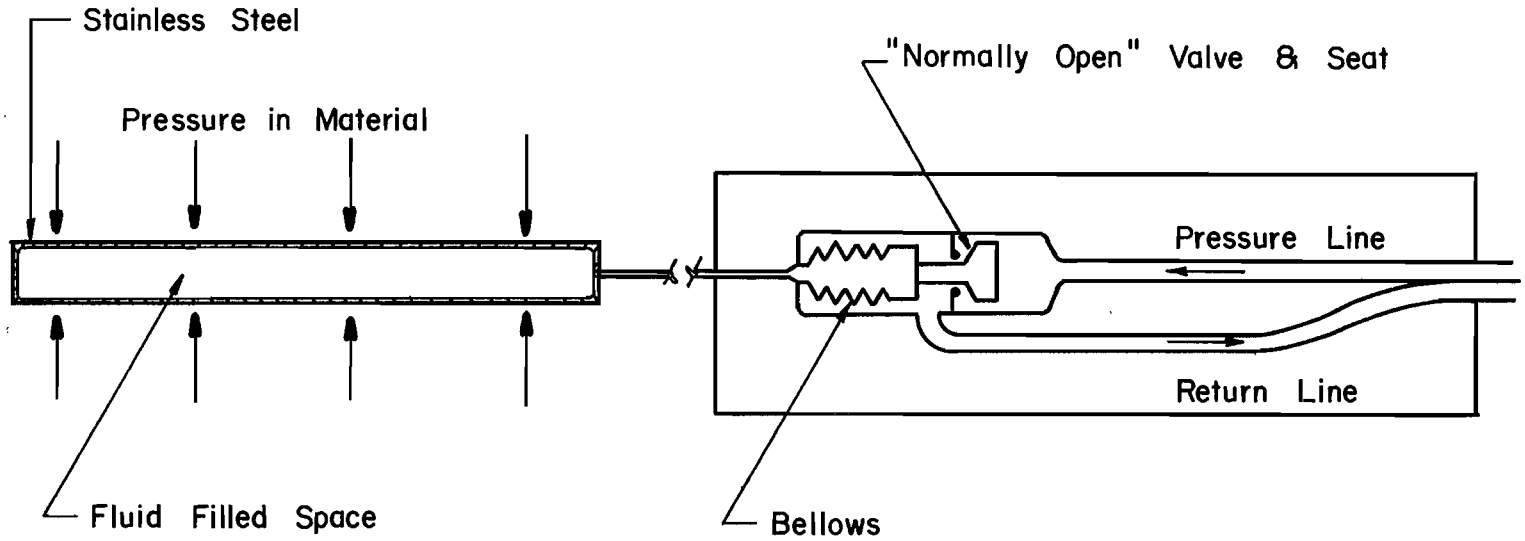

FIG. 12 - Terra Tec Pressure Cell Cross Section

the active faces of the cell is measured by a readout unit which supplies nitrogen gas through the pressure line in the lead. When the supply pressure matches the fluid pressure, the bellows contracts and closes the piston valve. The readout unit monitors the return line pressure which remains constant when the valve closes. Each cell has a unique factory preload pressure, i.e., the cell reading is not zero when no load is applied.

The manufacturer's specifications rate the cells at 250 psi (1720 kPa) capacity with an accuracy of 0.1%. Each cell was tested by the manufacturer for proper function and a built-in preload pressure was established. The results of these tests were supplied by the manufacturer. Most of the cells were also tested at the Texas Transportation Institute (TTI) calibration laboratory to verify linearity and repeatability prior to installation at the site. Cells which failed these tests were returned to the manufacturer for repair and/or adjustment.

The cantilever retaining wall was instrumented with 14 pressure cells, six in the back face of the stem and eight in the footing, at the locations shown in Fig. 13. The cells were identified by the manufacturer's serial numbers. The pressure cells were cast in place since this is considered the best method of installation to prevent damage to the cells during construction (13).

The pressure cells in the footing were placed in the middle of the footing on a line perpendicular to the longitudinal axis, after the reinforcing steel was in place. The five cells along the base of the footing were pinned directly against the cement stabilized sand. The cell installed in the key was pinned against the cement stabilized sand

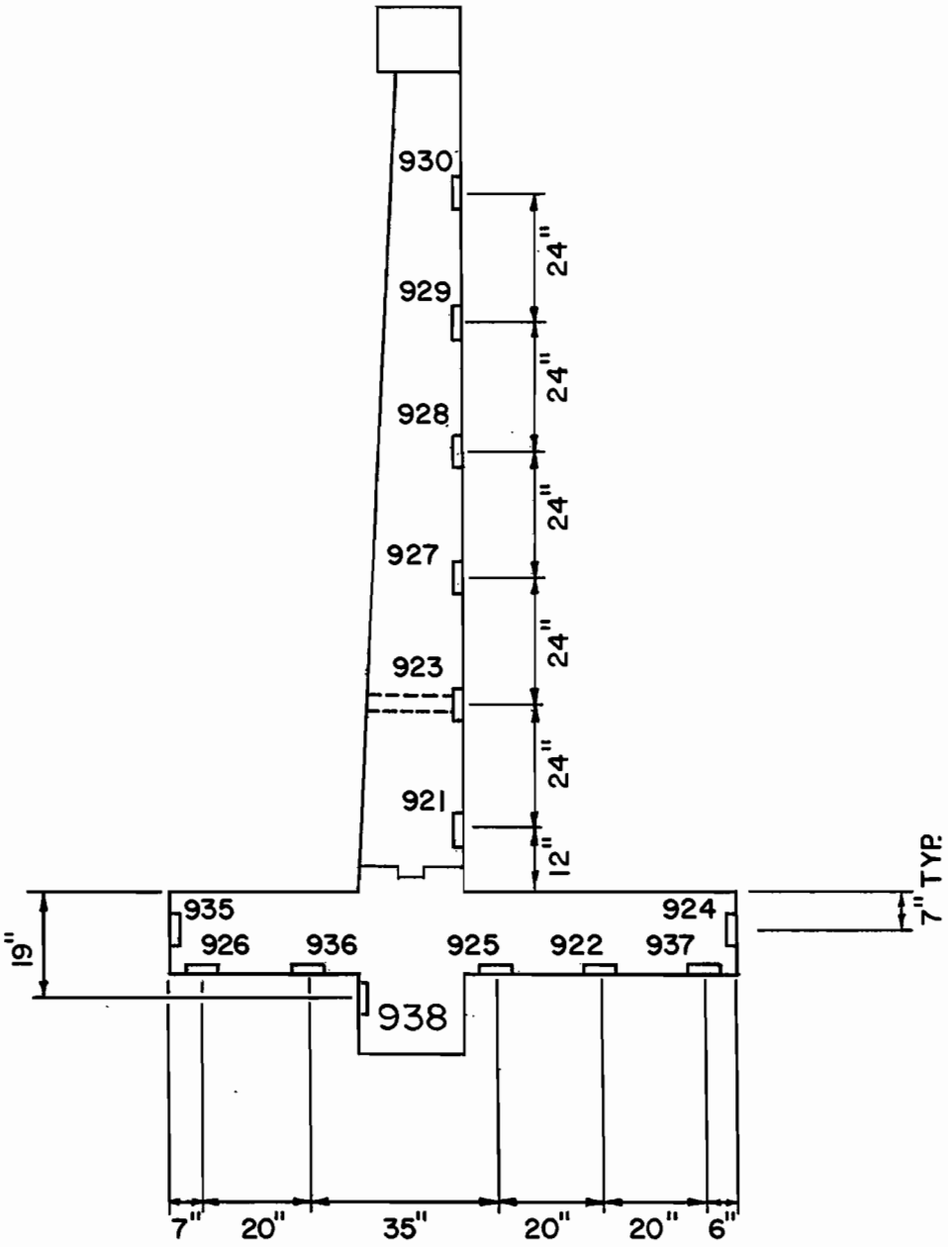

FIG. 13 - Location of Pressure Cells
(1 in. = 25.4 mm)

on the front side. Cells 924 and 935 were wired to the forms of the heel and toe respectively. For protection, the pressure cell leads were routed through a PVC pipe conduit as shown in Fig. 14. The PVC conduit was located several feet from the axis of instrumentation. The footing was instrumented and the concrete was placed in November of 1979.

Pressure cells were wired to the back face stem form on a vertical line 1 ft (0.305 m) off of the center of the panel to avoid a form splice. This installation was done in January of 1980. The leads were wired to tensile reinforcing steel for protection and routed through the PVC pipe conduit. The remaining reinforcing steel and front face form was put in place and the stem concrete was poured in June of 1980. A metal box was attached to the front face of the stem to house the pressure cell lead terminals. The PVC conduit was extended from the top of the footing into the metal box. Thermocouples, for temperature measurements, were not installed during the construction of the retaining wall because prior research experience indicated that temperature-induced pressure variance would be negligible (5,6,12).

Several sets of pressure readings were made between November, 1979 and July, 1980. A significant change in pressure reading was observed for each cell although it was expected that each cell would have a constant reading approximately equal to its factory preload value, especially those cells exposed to the atmosphere. The variation in reading was systematic since each cell reading changed in approximately equal increments when different sets of readings were compared. The magnitude of the readings increased from the winter through summer months. The variation in pressure readings on the stem and footing

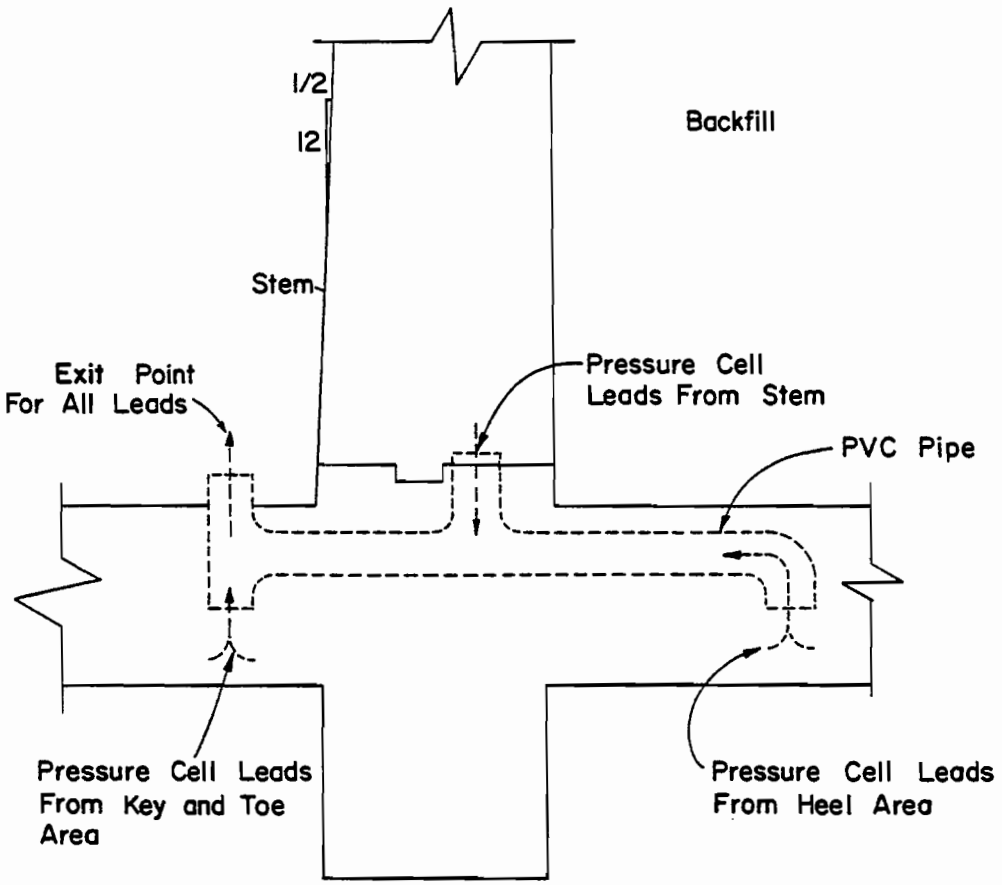

FIG. 14 - Pressure Cell Lead Conduit

faces could not be attributed to seasonal earth pressure changes because no backfill had been placed against them.

Thermocouples were installed in August of 1980 to evaluate the effect of temperature on the pressure readings. No backfill had been placed behind the wall at this time, so thermocouples T, M, B, BF and FW as shown in Fig. 15 , were installed. The toe of the footing was covered with soil and thermocouple FF was installed in June of 1981 by digging down to the toe of the footing, setting the thermocouple, and replacing the soil. The thermocouple wires were routed through a PVC conduit which ran through a weep hole and the conduit was attached to the PVC riser from the top of the footing to the metal box.

Wall Movement.- Provision was made to measure horizontal and vertical displacement, and wall tilt. The wall movement measurement systems are shown in Fig. 16. The horizontal displacement was measured directly with a steel tape. A rigid hook was securely embedded in the front face of the stem. A reinforced concrete pier, to serve as a reference point, was set near the right of way line with the top approximately flush with the ground surface to minimize disturbance by construction operations. The concrete pier was set in November of 1980 after the right of way line was cleared of excavation spoil. A 12 in. (305 mm) bolt was cast in the top of the concrete pier. The top of the bolt and the hook shaft were set at the same elevation in order to obtain horizontal distances directly. A cross was cut in the bolt head to obtain a specific measurement point. A steel tape was stretched between the hook and the cross in the bolt head using a measured tension of 10 pounds (44.5 N) for all observations and a tape thermometer was

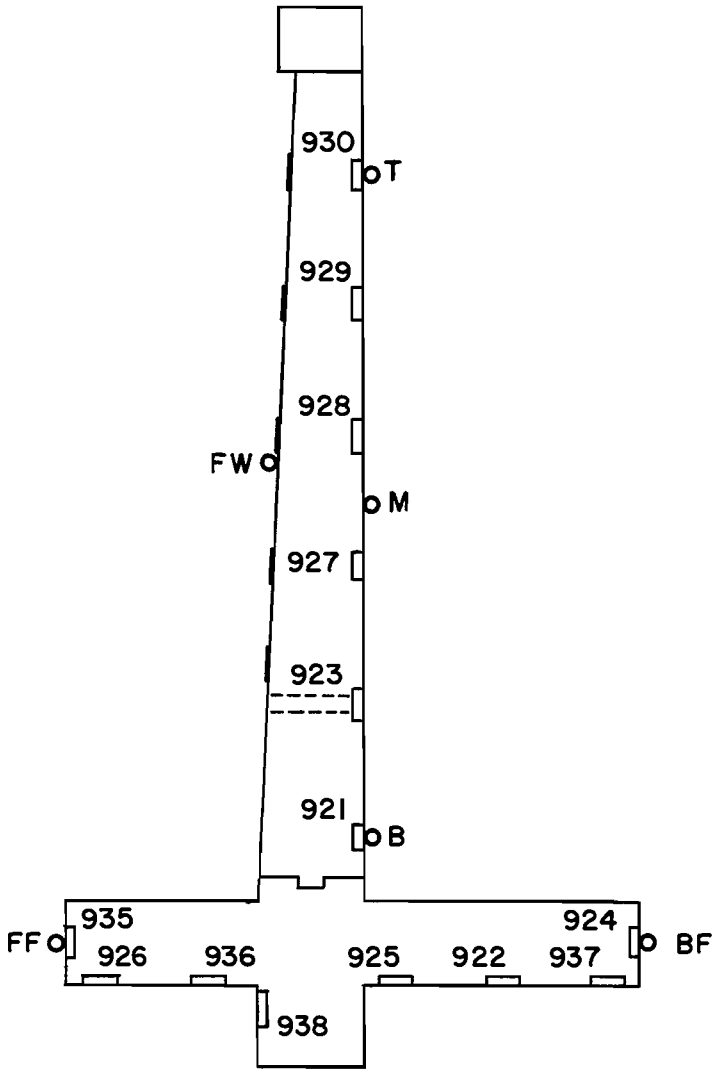

FIG. 15 - Location of Thermocouples

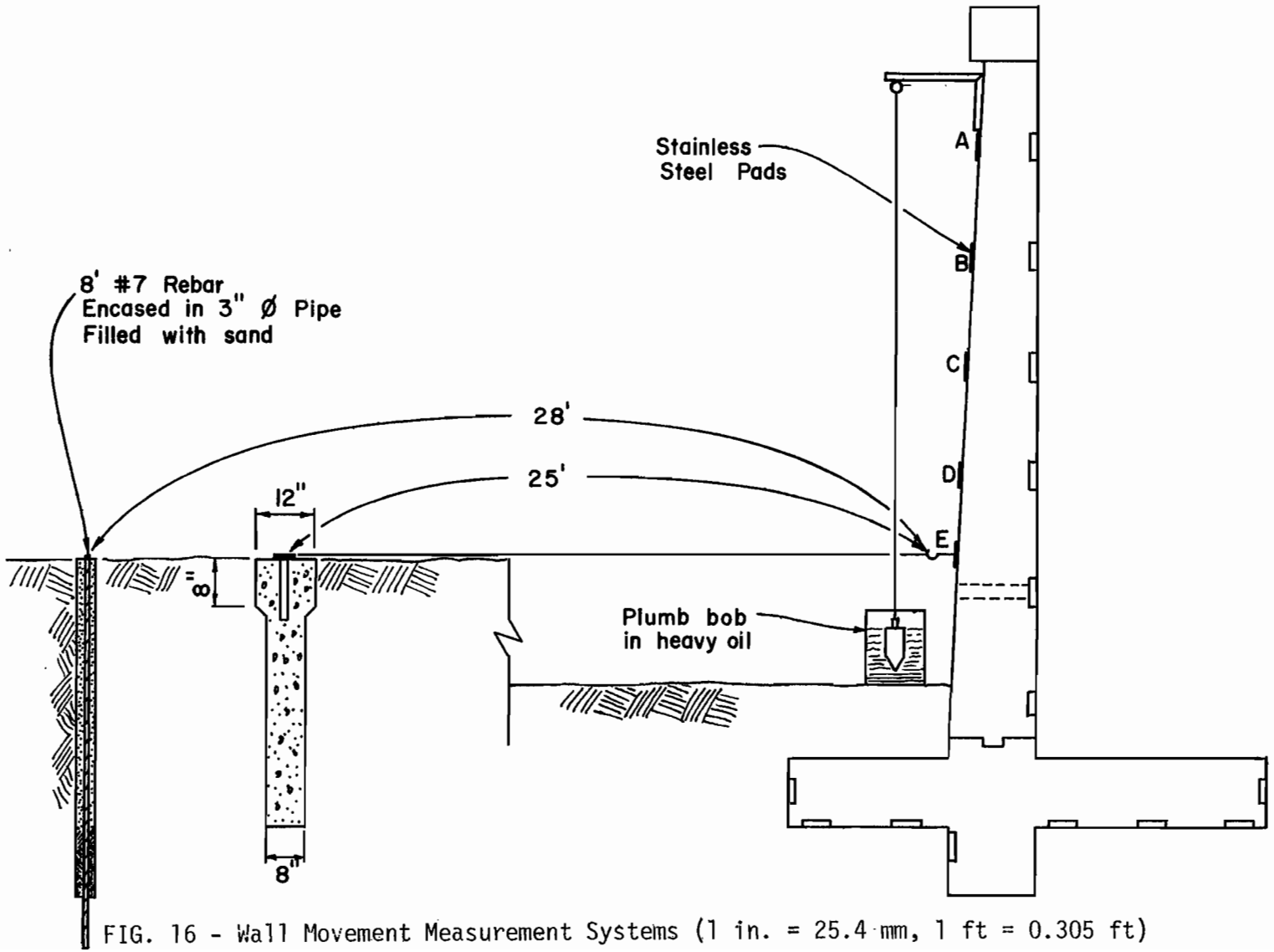

FIG. 16 - Wall Movement Measurement Systems (1 in. = 25.4 mm, 1 ft = 0.305 ft)

used to establish the tape temperature for all observations. The measured distances were adjusted for thermal-induced changes in the tape length. An additional reference point was set in June of 1981 to serve as a back-up for the concrete pier, and to serve as a means to verify displacement measurements. The back-up reference point was a groove cut in the top of a steel reinforcing rod. The installation method is illustrated in Fig. 16.

The vertical displacement of the wall was obtained by differential leveling using an automatic level and Philadelphia rod. Rod readings were taken on the hook shaft, bolt head, and later on the top of the reinforcing rod. The bottom of the concrete pier was set at the same elevation as the base of the retaining wall footing to help cancel the effects of local heave or subsidence.

Wall tilt was measured using two independent methods. Both methods utilized five stainless steel pads, A through E, which are shown in Fig. 16. The pad faces were machined smooth after a point marking their centers was established. Pads A through D were attached on 2 ft (0.610 m) centers, opposite the stem pressure cells on the back face. Pad E was set 1.427 ft (0.435 m) below Pad D to avoid covering the weep hole. Pad E was set adjacent to the hook used for horizontal and vertical movement measurements. Stainless steel pads were used because they are noncorrosive and the coefficient of thermal expansion for steel and concrete are almost identical.

One method of measuring tilt was to place an inclinometer on each pad and read the observed angles. The magnitude and direction of the tilt was obtained by comparing subsequent readings with those initially

taken.

A second method for measuring tilt involved measuring the horizontal distance from a vertical line to the punch mark on each stainless steel pad. A rigid bracket was attached to the front face of the stem near the top of the wall. From the bracket a 12 pound (54 N) plumb bob was suspended by a piano wire into a bucket of oil. The horizontal distance between the piano wire and punch mark on each pad was measured with a steel scale with a level vial attached. Wall tilt was computed using the observed change in horizontal distance at each pad and the vertical distance from the bracket to each pad. The horizontal movement at each pad was computed from the plumb line readings.

Soil Conditions

Profile.- The instrumented retaining wall was founded on a stiff, fissured and extremely heterogeneous preconsolidated clay. Pockets and lenses of fine sand and silt were randomly dispersed throughout the clay. Fine sand and silt were often found in the fissure cracks.

The retaining wall was backfilled intermittently over a 15 month period. The clay excavation spoil was dozed onto the footing on the front side of the wall. Select backfill, a bank run sand, was used to fill the excavation to natural grade on the back side of the wall. The native clay was used as backfill for the remaining 9 ft (2.74 m). A vertical sand blanket, about 2.5 ft (0.75 m) wide, was placed against the back of the stem, separating the wall and the clay. A representative profile of the backfill in July, 1982 is shown in Fig. 17. The profile shown represents a field change agreed upon between the TSDHPT field representative and the contractor. Originally, select backfill

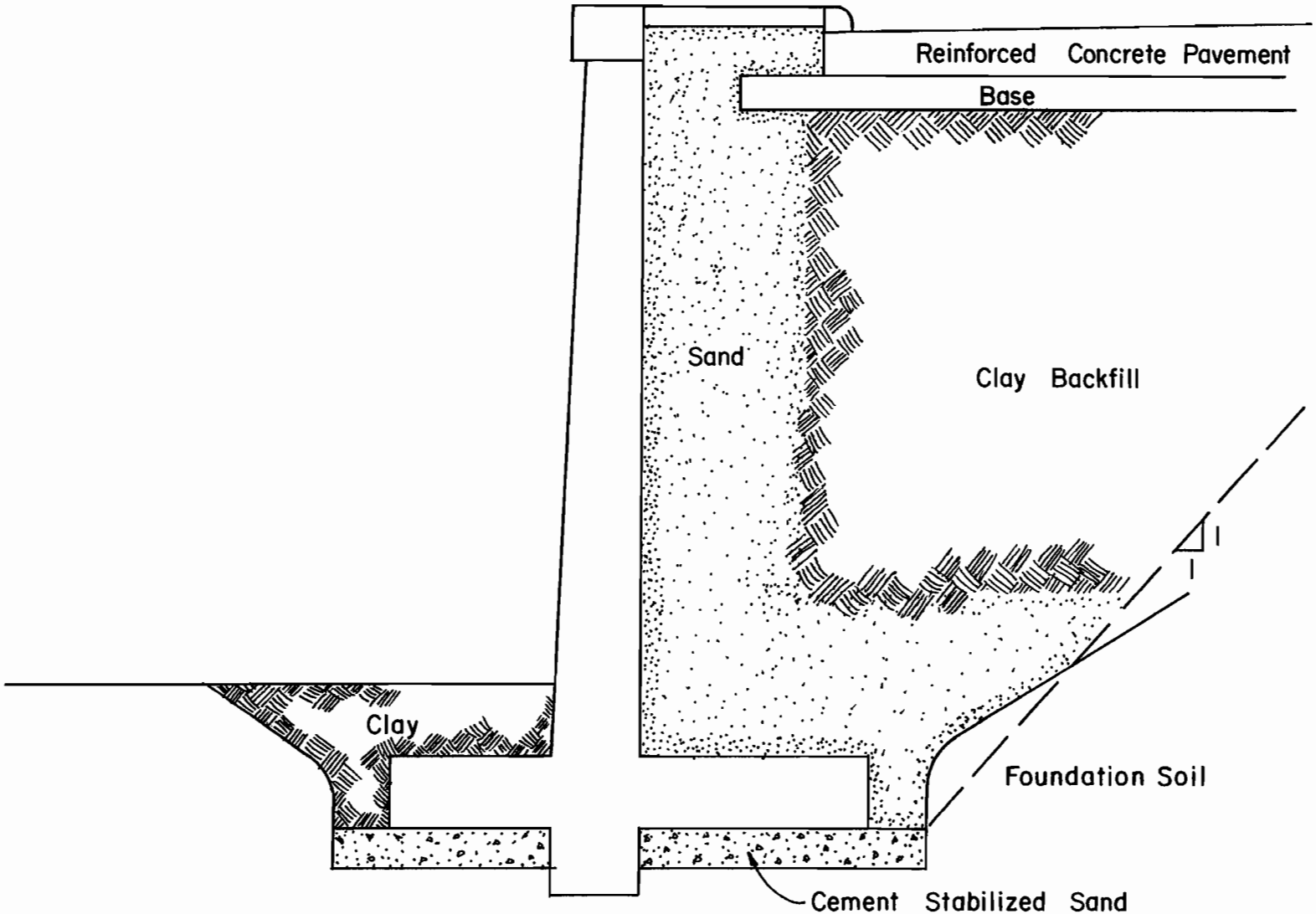

FIG. 17 - As-Built Profile

was to have extended to the dashed line shown in Fig. 17.

Soil Borings.- Soil borings were made in June of 1980 and August of 1981 to obtain core samples for testing at the Texas A&M University Geotechnical Laboratory. The soil boring performed in June 1980 was located 18 ft (5.49 m) from the test panel stem on the back side of the wall. The ground surface was at natural grade at that time. The soil boring performed in August 1981 was located 10 ft (3.05 m) from the test panel stem on the back side of the wall. The majority of the backfill had been placed at that time. Soil tests were performed to obtain the following soil properties: specific gravity of solids, unit weight, water content, Atterberg limits and shear strength.

Laboratory tests.- The specific gravity of solids of the clay was found to average 2.72. A summary of representative laboratory test results is given in Fig. 18 along with the soil description and location of the retaining wall with respect to the clay backfill and foundation soil. The Unified Soil Classification symbols are indicated, and the total unit weight and natural water content are tabulated. The undrained shear strength was obtained by unconfined compression tests on the foundation clay, and unconsolidated undrained direct shear tests on the clay backfill. Consolidated drained direct shear tests were also performed on clay backfill samples. Drained shear strength was deemed appropriate due to the length of time used in completing the backfill operations. The Coulomb failure envelope obtained from the drained direct shear tests is shown in Fig. 19. The curved portion of the failure envelope represents normal stresses below the preconsolidation pressure of the clay and the linear portion of the failure

SOIL DESCRIPTION	Depth, ft	Unified Soil Classification	Unit Weight, pcf	Water Content	Liquid Limit	Plastic Limit	Shrinkage Limit	Plasticity Index	Undrained Shear Strength, psi
BACKFILL:	1								
	2		131	20					
Clay, slightly silty; multi-colored, brown, gray; stiff, moist	3	CH	128	23/27	69	19	9	50	13/13 21
	4								
	5		127	26					
	6	CH	123	25	63	17	9	46	
	7		129	21					
*	8								
	9	CH		26	67	18	11	49	
	10								
	11								
*	12	CH		29	63	15	9	48	
	13								
	14	CH	122	28	76	23	11	53	23
*	15								
	16								
FOUNDATION SOIL	17								
	18								
Clay, slightly silty & sandy; multi-colored, gray, brown, stiff, moist, some calcareous nodulus	19	CH	125	24	63	20	10	43	25
	20								
	21								
	22								
	23								
	24	CH	126	22	60	18	10	42	22
	25								
**	26								
**	27								
Clay, sandy, light tan, gray very stiff	28								
	29	CL	124	14	37	14	13	26	39

*Thin sand seam ** Becomes sandy

FIG. 18 - Laboratory Log of Soil Borings
(1 ft = 0.305m, 1 pcf = 0.157 kN/m^3, 1 psi = 6.89 kPa)

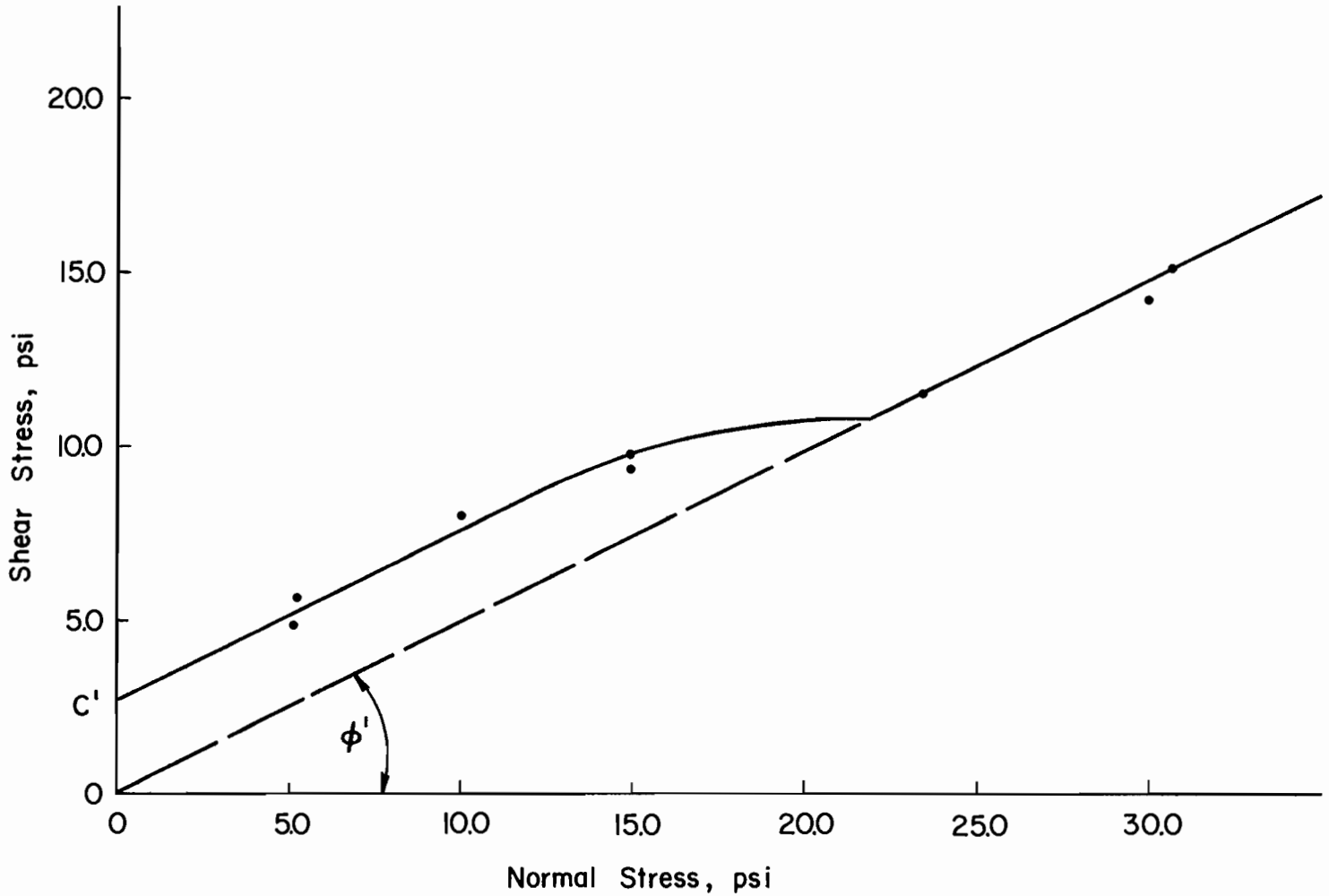

FIG. 19 - Failure Envelope for Drained Shear - Backfill
(1 psi = 6.89 kPa)

envelope represents normal stresses above the preconsolidation pressure. The effective angle of shearing resistance is 25° for normal stresses greater than the preconsolidation pressure. The stress-strain characteristics of the clay backfill are presented in Fig. 20, which shows shear stress versus displacement from direct shear tests for normal stresses of 5, 15 and 30 psi (34, 103 and 207 kPa). Displacement is used on the abscissa of the graph because the samples were sheared on a circular cross section with a 2.50 in. (6.35 cm) diameter. The clay is relatively brittle and small displacements caused failure. Note that the peak shearing stresses occur at strains on the order of one percent if the diameter is taken as the original length in the standard definition of strain. Fig. 21 illustrates the vertical displacement the test samples underwent during slow shear for the same tests given in Fig. 20. Note that the tests with normal stresses below the 20 psi (138 kPa) dilated during shear and the test with the normal stress above 20 psi (138 kPa) consolidated during shear.

Soil exploration reports were obtained from the TSDHPT to supplement the information gained from the soil borings and laboratory tests. These reports show that the very stiff sandy clay stratum, (see Fig. 18), is 15 ft (4.57 m) thick and overlies a 44 ft (13.4 m) stratum of dense to very dense silty sand. The ground water table is at least 12 ft (3.7 m) below the base of the retaining wall footing.

The sand blanket (see Fig. 17), serves primarily as a drain to prevent porewater pressures from acting on the wall. The sand was classified as uniform, fine, silty sand, SP-SM. Field density tests performed by the TSDHPT inspector indicated that the sand blanket was

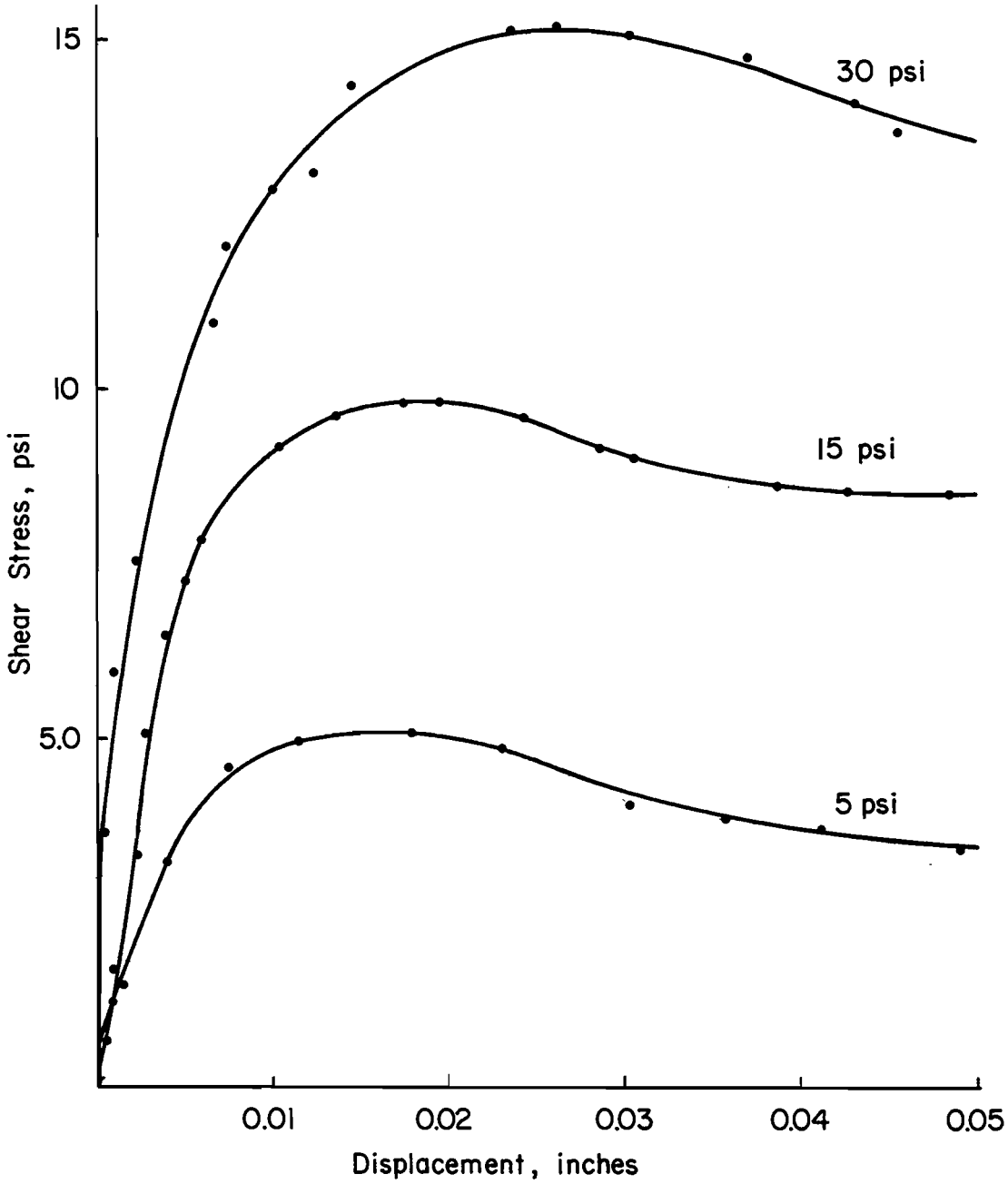

FIG. 20 - Shear Stress versus Displacement - Backfill
(1 psi = 6.89 kPa, 1 in. = 25.4 mm)

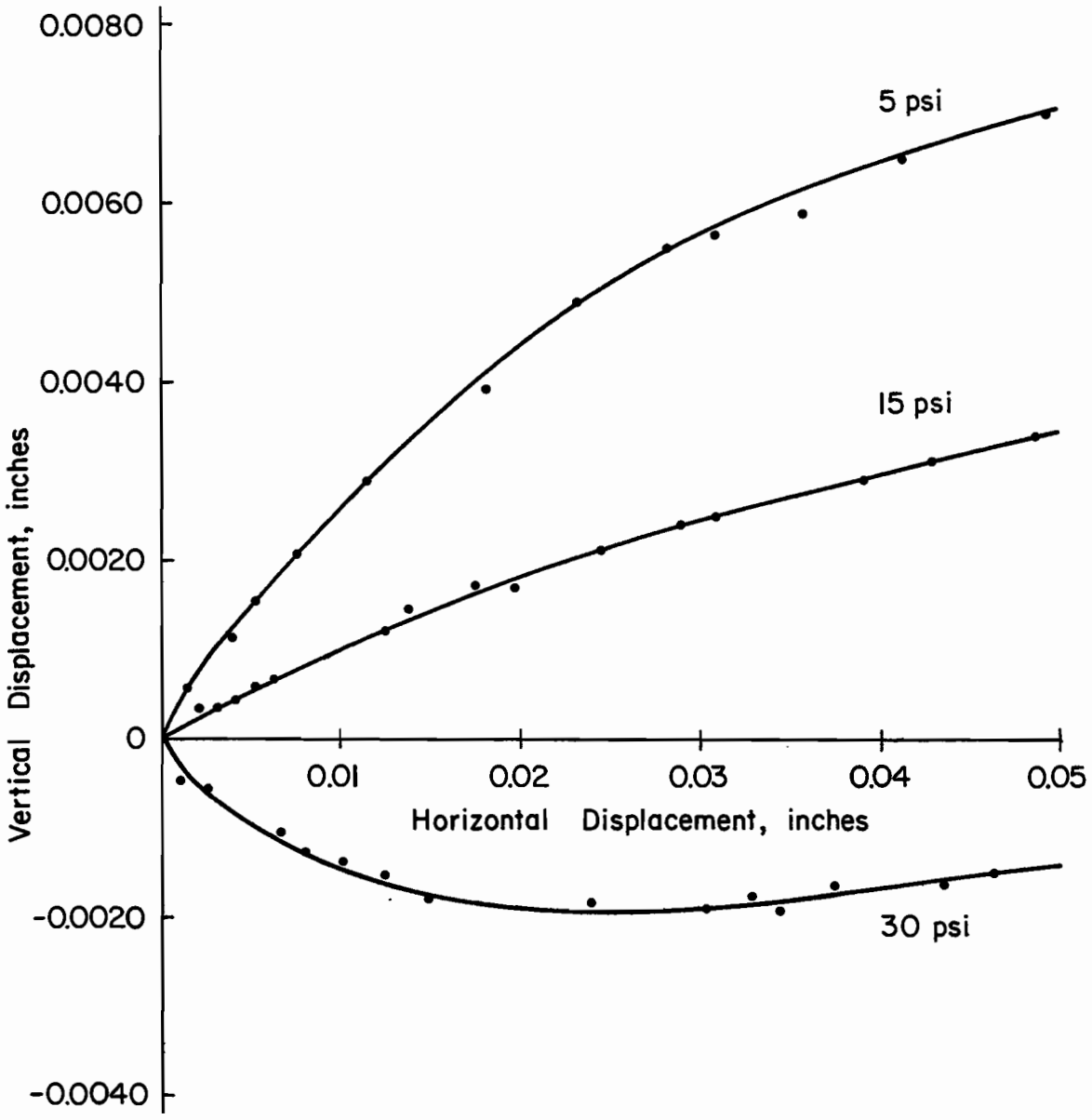

FIG. 21 - Vertical versus Horizontal Displacement - Backfill
(1 in. = 25.4 mm)

compacted to a dry unit weight of 113 pcf (17.7 kN/m^3) at a water content of 12.3%. These values match compaction specifications established by TSDHPT laboratory tests.

The compaction specifications for the clay backfill required field dry densities to be much lower than the maximum dry density obtained from the TSDHPT compaction test, and the specified water content was greater than the optimum water content obtained from the compaction test. These requirements were an effort to reduce the expansive activity of the clay.

DATA COLLECTION, INTERPRETATION AND RESULTS

Data Collection

Schedule.- It was anticipated that the retaining wall would be constructed and backfilled in early 1980. Soon thereafter, the paving would be completed and the project opened to traffic. With this sequence of events, the plan was to be at the site and closely monitor the effects of compaction and backfill heights on earth pressure and wall movement on a lift by lift basis. Measurements were to be made on a biweekly basis after backfilling was completed until the system stabilized. Then measurements would be made at intervals sufficient to determine seasonal effects. The effect of traffic loading was also to be monitored. With this systematic approach of obtaining measurements, the critical or maximum loading condition could be identified and be used for design modifications if necessary. The actual construction progress prevented this approach to data collection. The data collection schedule was modified so that inspection visits were made more or less on a monthly basis. The TSDHPT project inspector and the contractor's foreman were to notify the researchers of any construction operations to be performed concerning the instrumented wall.

Pressure Cell Readings.- Data collection began with pressure cell readings when the retaining wall footing was instrumented in November 1979. Typically, each cell was read three times for each set of observations. Additional readings were taken on a particular cell if the readings varied more than 0.2 psi (1.4 kPa). If the readings stabilized, that value was recorded; otherwise, the average value was

recorded. The pressure cell readings were estimated to 0.1 psi (0.69 kPa). Normally, the three cell readings were identical for a particular observation. Stem Cells 923 and 929 became inoperative early in 1981. Temperature measurements were made adjacent to Cells 930, 928, 927, 921, and 924 beginning in September of 1980.

Wall Movement.- Wall movement measurements began in August of 1980 when the stainless steel pads were attached to the front face of the stem and the plumb bob bracket was anchored to the wall. The inclinometer readings were read and recorded to an accuracy of 1 minute. Repetitive measurements gave consistent results for the first year, but significant variations in repetitive inclinometer measurements began to occur. The inclinometer had been damaged at the TTI Laboratory and evidently was not satisfactorily repaired. The plumb line readings were read and recorded to an accuracy of 1/64th of an inch (0.4 mm). Repetitive plumb line measurements yielded consistent results throughout the study. Horizontal and vertical wall movements were read and recorded to a precision of 0.001 ft (0.3 mm) beginning in November of 1980 when the concrete pier reference point was established.

Backfilling Sequence.- The height of backfill is an important factor in this study. Since backfilling was not carried out in a short time period, Fig. 22 is presented to show backfill heights with respect to the date each particular profile was first observed. The position of the backfill corresponding to initial measurements of pressure and movement can be observed. Pressure cell readings were obtained for several months before any backfill was placed. Also, the toe of the

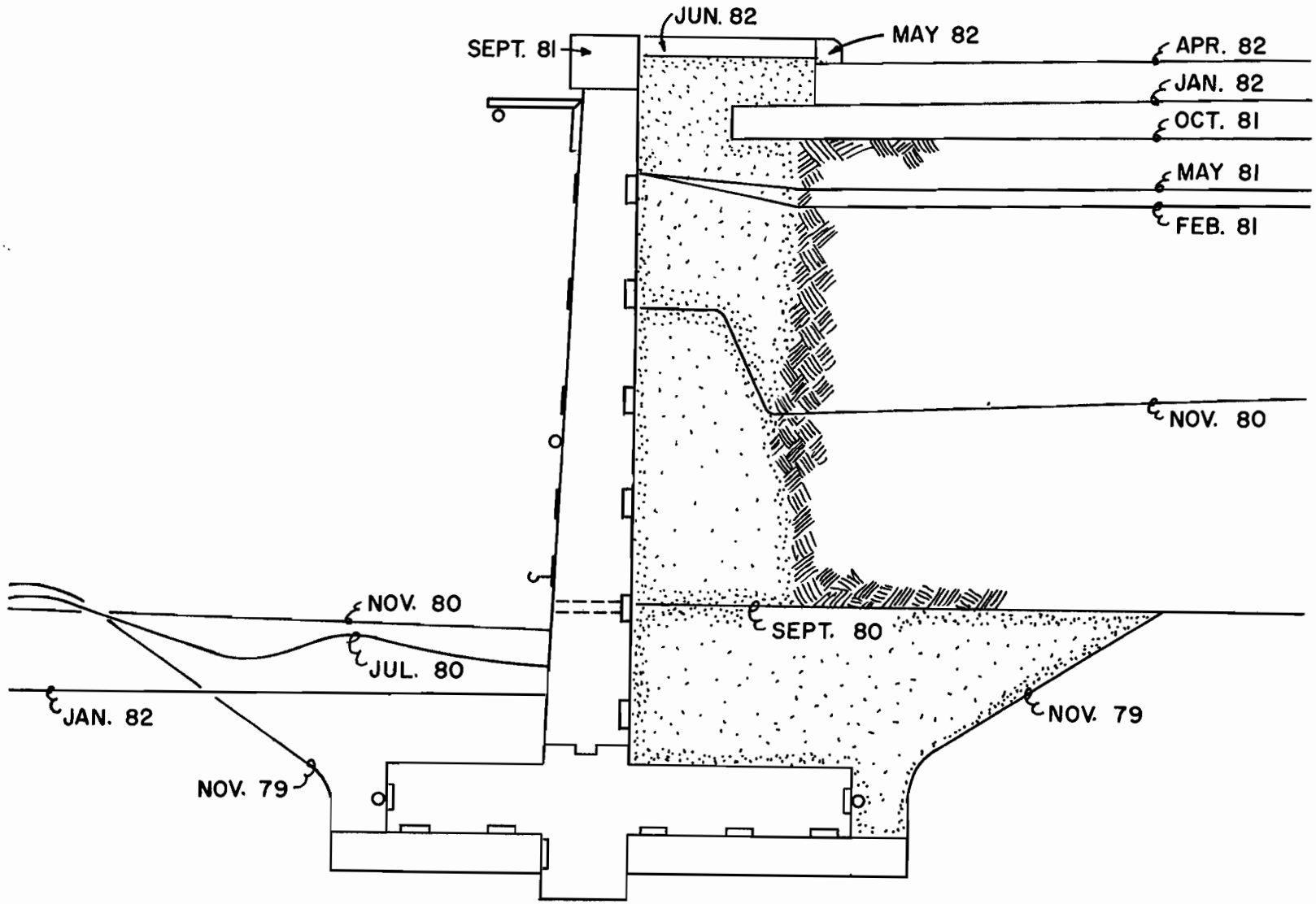

FIG. 22 - Construction Sequence

footing was covered with soil before wall tilt measurements were made and approximately half of the clay backfill was in place before horizontal and vertical wall movement measurements were made.

Data Interpretation

Total Earth Pressure.- Each Terra Tec Pneumatic pressure cell has a built-in preload reading, therefore the pressure cell readings do not give earth pressure directly. After loading, the earth pressure is obtained by subtracting the preload reading from the field pressure reading. This is expressed as

$$p_e = p_i - p_o \quad \ldots\ldots\ldots\ldots\ldots\ldots\ldots\ldots\ldots\ldots \quad (9)$$

in which p_e = the total earth pressure, p_i = the field pressure reading, and p_o = the preload reading. Each Terra Tec pressure cell was supplied with a test record form which contained the following information:

> "Each pneumatic total pressure sensor has a unique, built-in, offset (preload) value. The factory value for this specific pressure sensor is listed below...
>
> As a final installation step, a preload value reading should be recorded above. All subsequent data readings will be referenced to this base reading. This field value should be slightly different than the precise factory preload value. Corrected total pressure is computed by subtracting the field preload value from the in-ground values."

It is implied that the field preload is a constant for each individual pressure cell and should be approximately equal to the factory preload value. Typically, when pressure cells are set in place, preload

readings are obtained, and then the cells are covered with construction material so only one set of field preload readings are obtained.

Variation in Pressure Cell Readings.- The foregoing procedure was followed for the footing cells in this research program. The cells along the base of the footing were loaded with the weight of the concrete immediately after the preload readings were made. The cells on the heel and toe of the footing were partially exposed to the atmosphere so the preload condition existed until the backfill was placed. Six sets of footing cell readings were obtained during the five months the stem was being constructed. Eleven sets of preload readings were obtained for the stem cells. Five sets of readings were made when the cells were attached to the back face form, one set after the concrete was poured and was still fresh, and five sets after the concrete hardened and the stem forms were removed. No soil had been placed against the stem cells, so the preload condition existed through August of 1980. The magnitude of each pressure cell reading varied significantly during that time period.

This unexplained variation in cell readings prompted an investigation to determine the cause. The calibration of the readout unit was checked in the TTI laboratory. The manufacturer was consulted, but could not offer an explanation. Site conditions, including air temperature, barometric pressure, and soil moisture were recorded along with the regular measurements. The variation in cell readings seemed to correspond to the variation in air temperature, which led to the decision to install thermocouples. The cell readings continued to vary even after the backfill was in place. The measurements of field cell readings, temperatures and backfill heights with respect to time for

Cells 930, 928, 927 921, 924, and 935 are presented in Figs. 23 through 28. It is important to note the variation in stem cell readings during the preload period which was February through August of 1980 as shown in Figs. 23 through 26. The cell readings observed in June of 1980 show the dramatic change in stem cell readings made just prior to and just after the concrete was poured. The similarity between the cell reading and temperature curves is apparent in each of these figures.

Temperature and Pressure Cell Reading Relationship.- The particular relationship between temperature and pressure cell reading for each cell was established by analyzing the data obtained between February and October of 1981. The backfill heights were essentially constant during this period and 10 sets of observations were obtained. All the cells were covered with soil. As shown in Figs. 29 and 30, a linear relationship between temperature and cell reading was observed (solid line). The equation of the line which fit the temperature-cell reading data for each cell was computed by regression analysis. The slopes of the fitted lines indicate the effect of temperature on cell reading for each cell.

Temperature and Preload Pressure Relationship.- It was necessary to establish a temperature-preload relationship for each cell. Preload readings had been obtained, but no direct temperatures had been measured until September of 1980. At this time, stem Cells 930, 929, 928 and 927 were exposed to the atmosphere and a single point on the temperature-preload graph for these cells was obtained. It was assumed that the temperature-preload relationship is also linear. Furthermore, it was assumed that the slope of the temperature-preload graph is

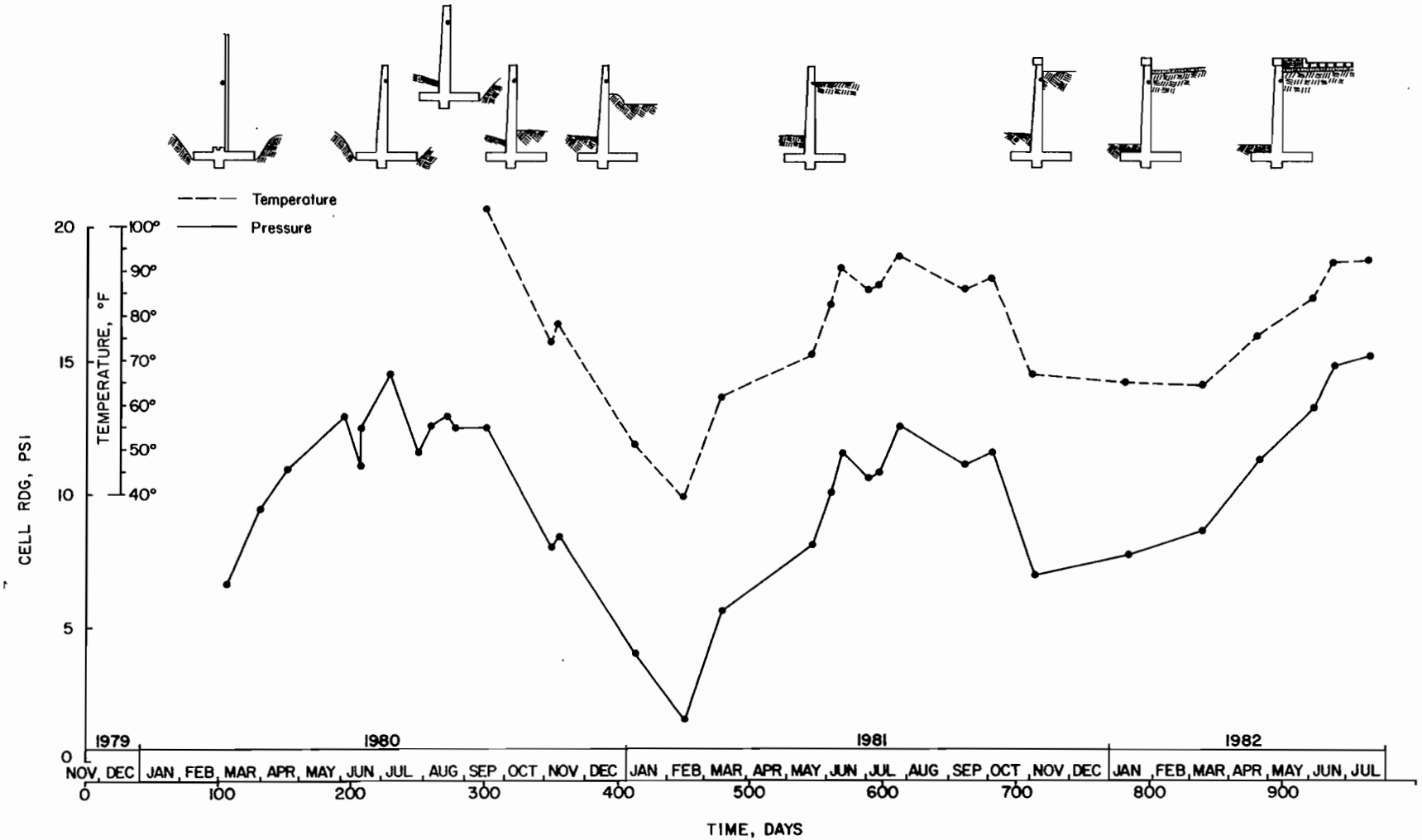

FIG. 23. - Cell 930: Pressure, Temperature, Backfill Measurements
(°C = 0.56 (°F - 32), 1 psi = 6.89 kPa)

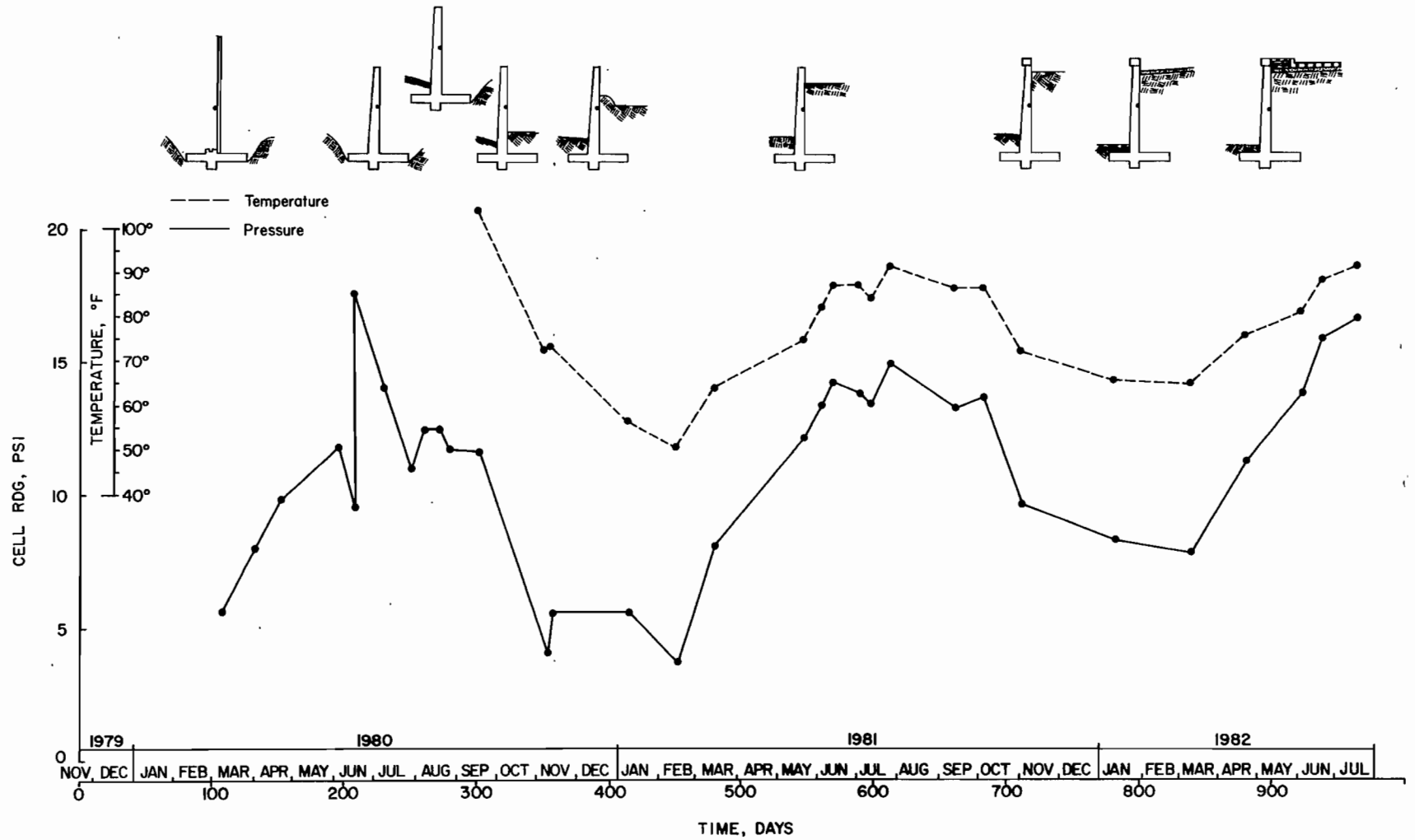

FIG. 24 - Cell 928: Pressure, Temperature, Backfill Measurements
(°C = 0.56 (°F - 32), 1 psi = 6.89 kPa)

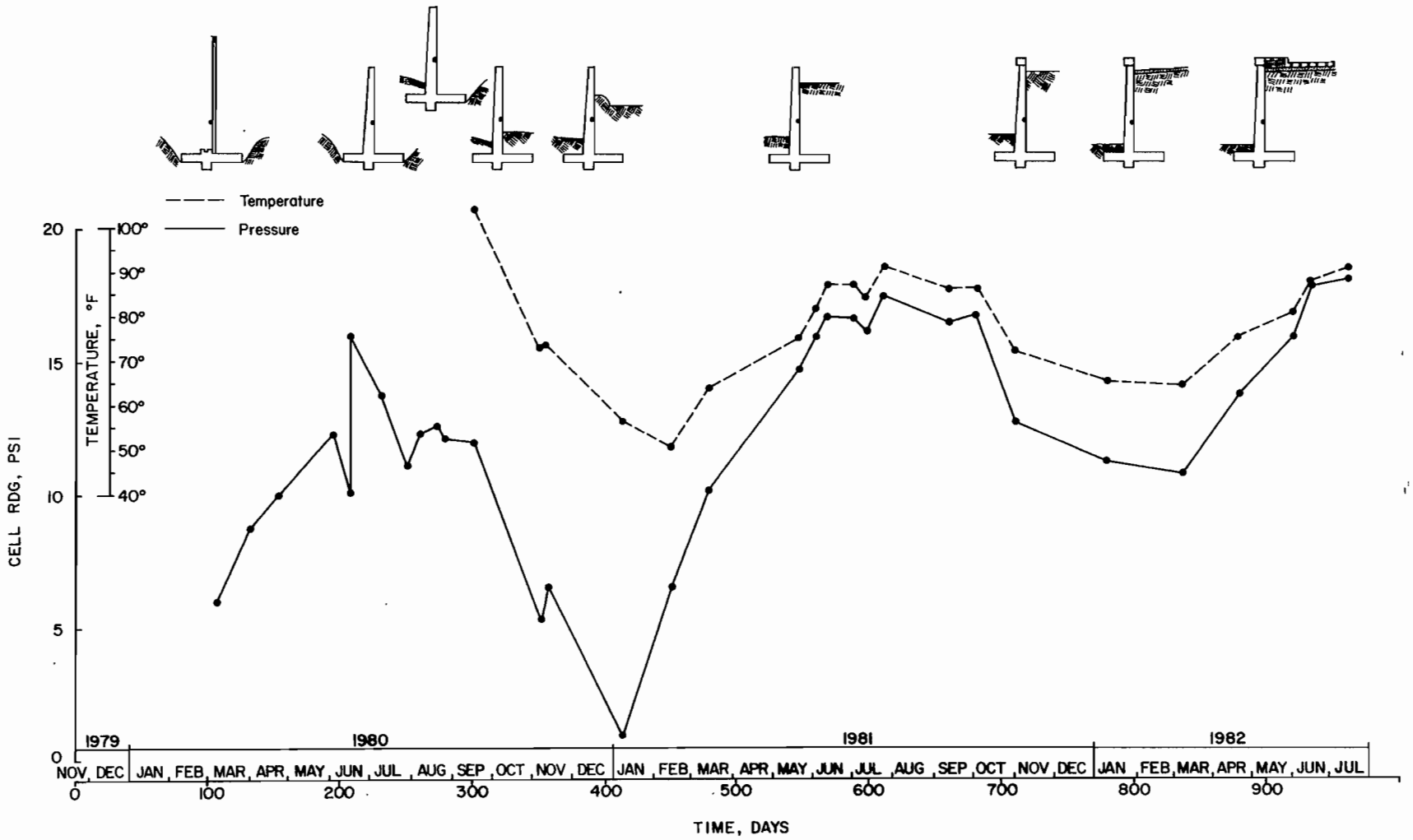

FIG. 25 - Cell 927: Pressure, Temperature, Backfill Measurements
(°C = 0.56 (°F - 32), 1 psi = 6.89 kPa)

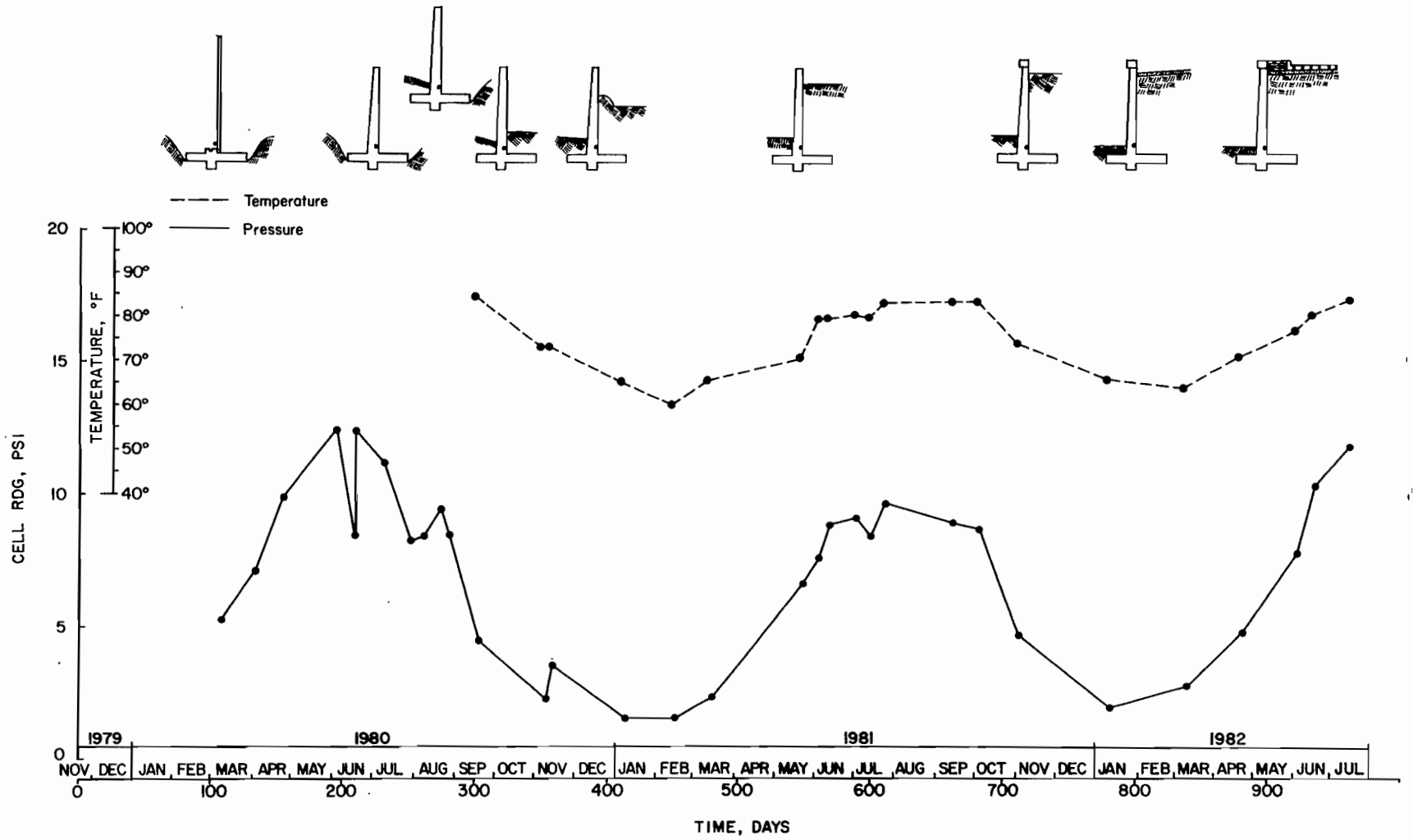

FIG. 26 - Cell 921: Pressure, Temperature, Backfill Measurements
(°C = 0.56 (°F - 32), 1 psi = 6.89 kPa)

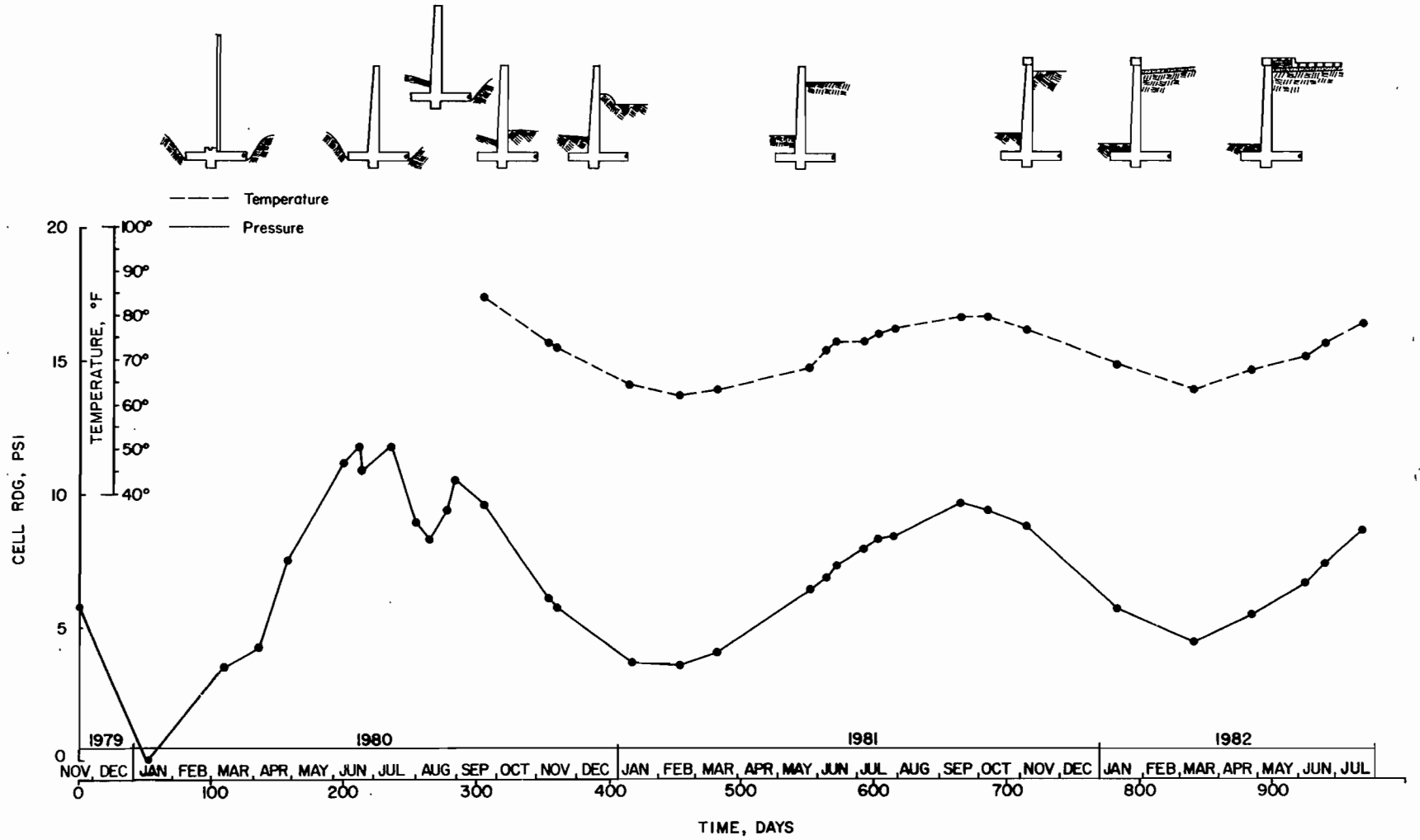

FIG. 27 - Cell 924: Pressure, Temperature, Backfill Measurements
(°C = 0.56 (°F - 32), 1 psi = 6.89 kPa)

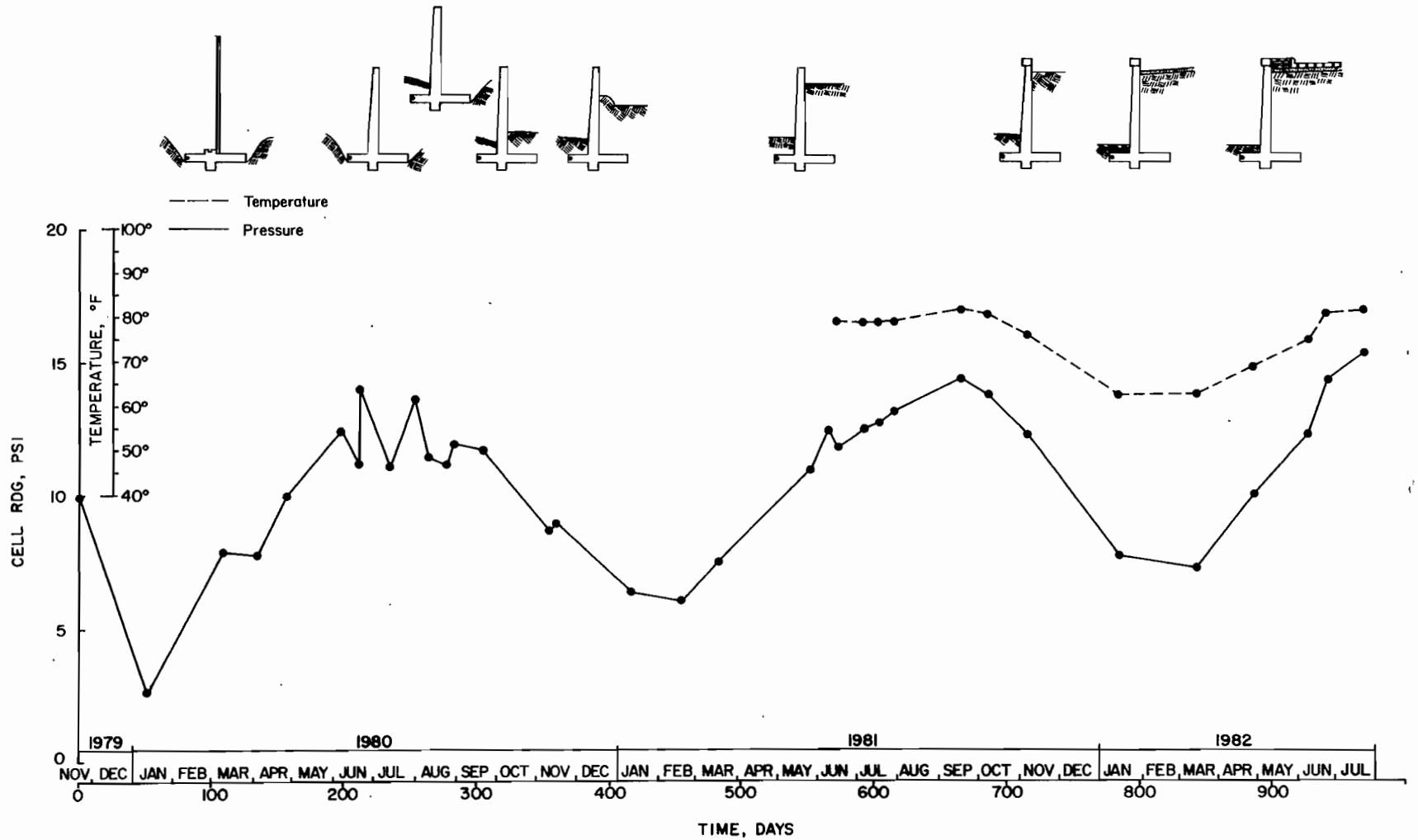

FIG. 28 - Cell 935: Pressure, Temperature, Backfill Measurements
(°C = 0.56 (°F - 32), 1 psi = 6.89 kPa)

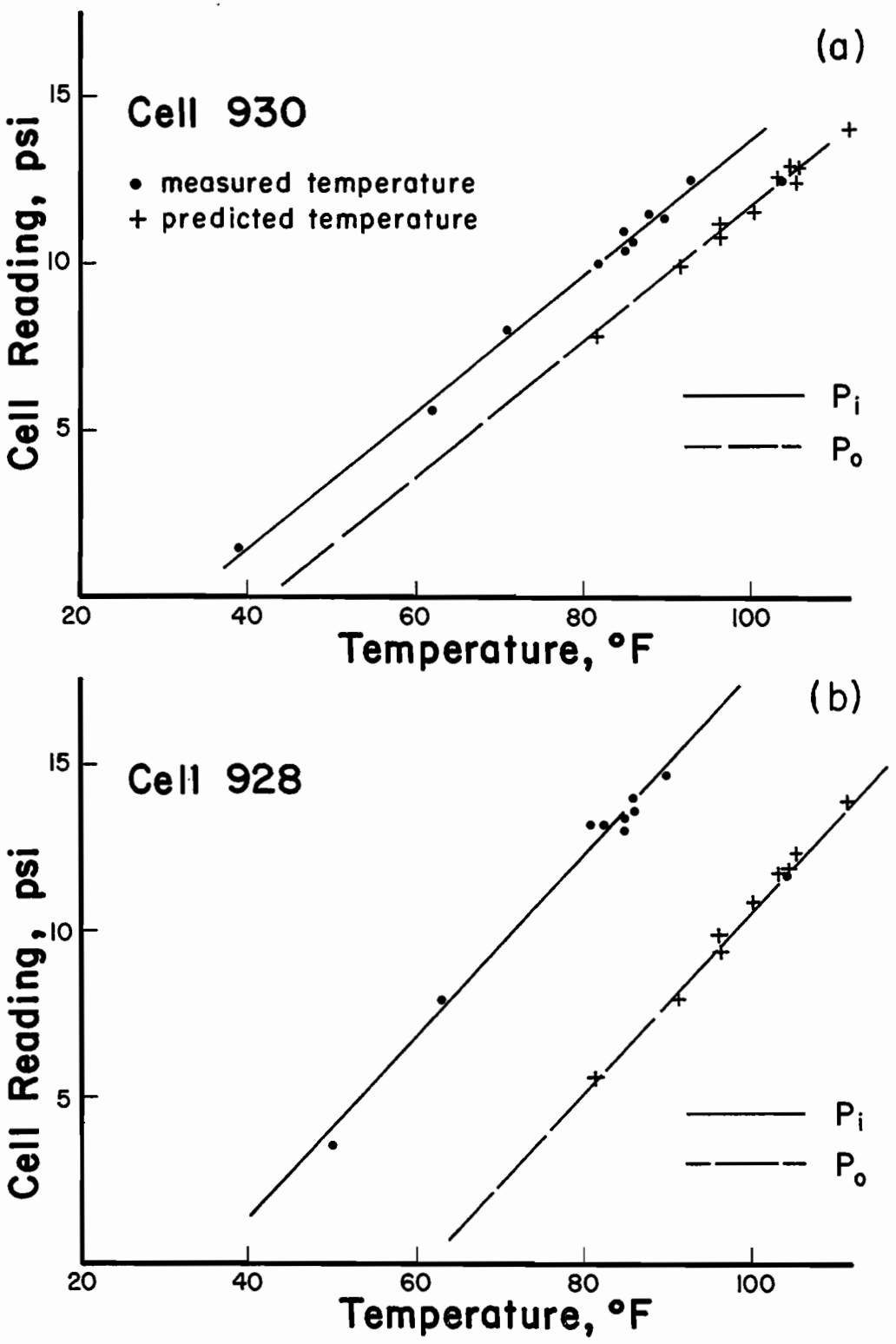

FIG. 29 - Cells 930 and 928: Temperature-Cell Reading Relationship (°C = 0.56 (°F - 32), 1 psi = 6.89 kPa)

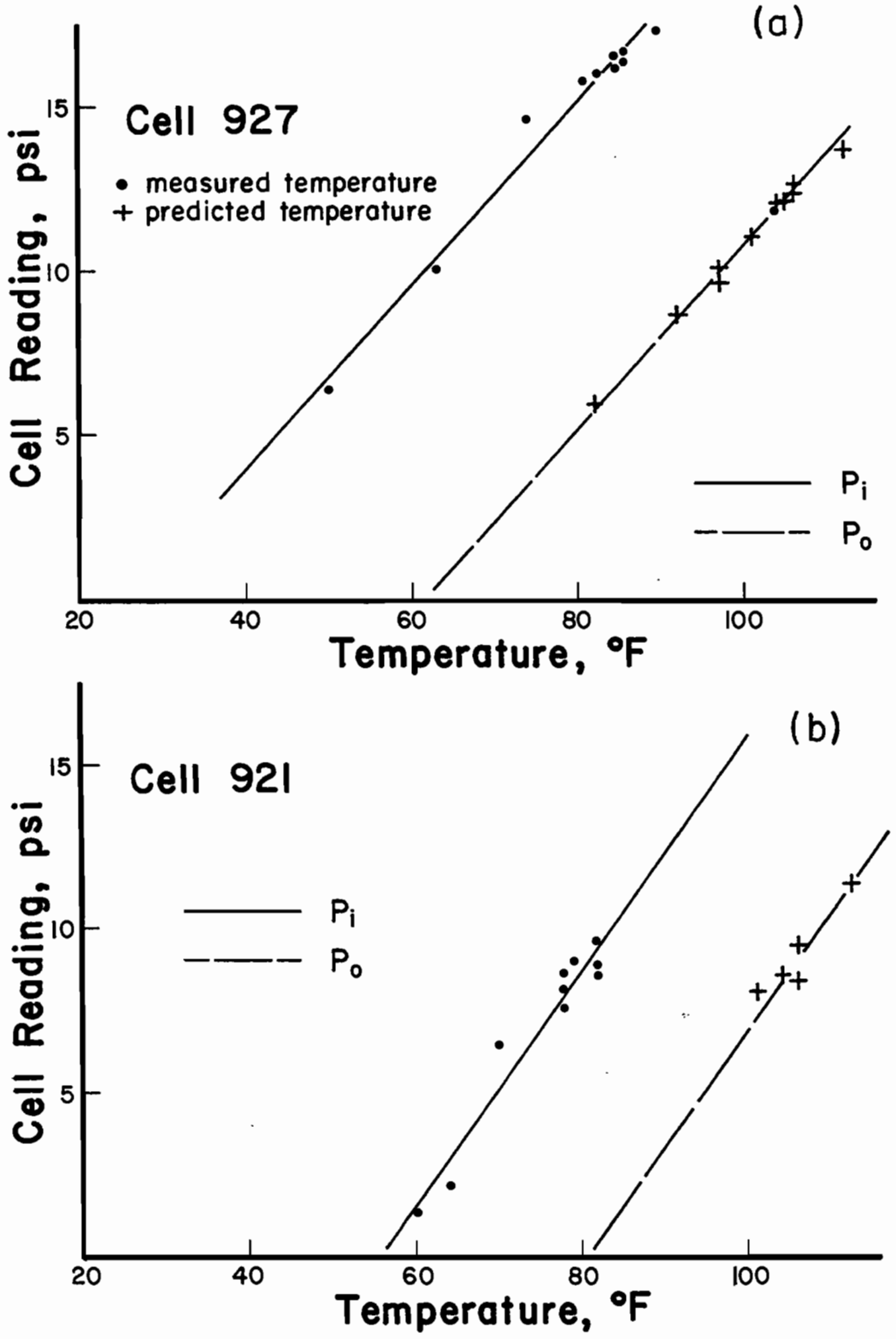

FIG. 30 - Cells 927 and 921: Temperature-Cell Reading Relationship (°C = 0.56 (°F - 32), 1 psi = 6.89 kPa)

parallel with the slope of the temperature-cell reading graph for each cell. These assumptions are illustrated in Fig. 29(a) and (b) and Fig. 30(a) which show the plot of temperature and cell reading, p_i, and the assumed temperature and preload, p_o, plot for Cells 930, 928, and 927. The preload curves pass through the single data point and are parallel with the cell reading curves. The total earth pressure is the difference between the measured cell pressure and the preload value at the measured temperature. An equation for preload pressure as a function of temperature, the equation of the dashed line, was determined for Cells 930, 928, and 927. These equations were then used to calculate the temperature for each day preload pressures were measured from March through August 1980. The three computed temperatures for these three cells for each particular day were found to be in close agreement. The maximum difference in computed temperature was 4°F (2.2°C) with an average difference of 1.7°F (1.0°C) for each day. These differences are within the precision expected if direct temperature measurements had been made.

The predicted temperatures are considered to apply to those cells that were exposed to the atmosphere, which include stem Cell 921 and Cells 924 and 935 which are on the face of the heel and toe respectively (see Fig. 13). The computed temperatures and measured preload readings, p_o, were plotted and a preload curve was established by fitting a line through these plotted points which was parallel to the temperature-cell reading, p_i, curve for each cell. These curves are shown in Fig. 30(b) and Fig. 31(a) and (b). The preload curve for Cell 921, Fig. 30(b), was established using the temperatures and preload readings

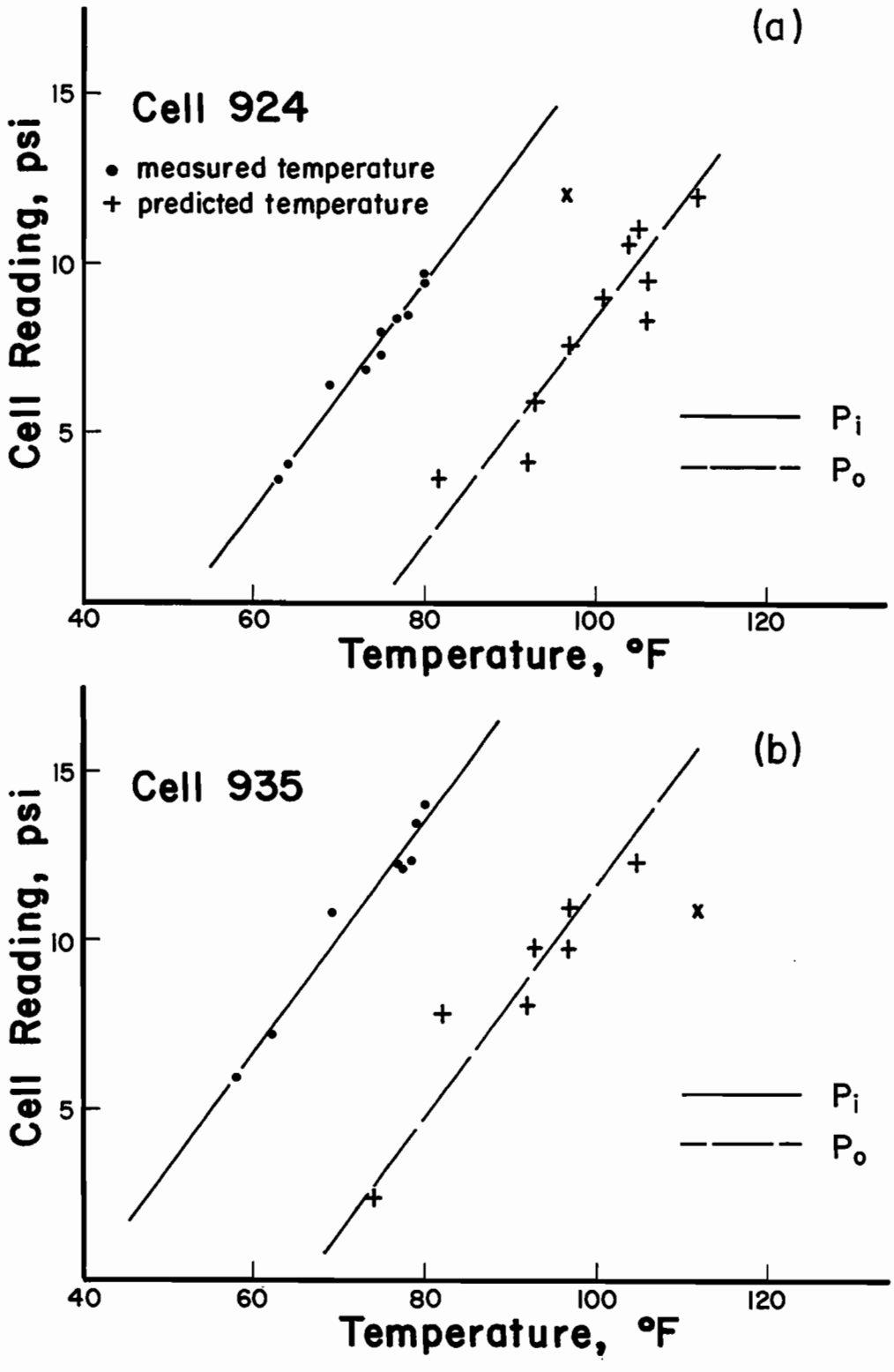

FIG. 31 - Cells 924 and 935: Temperature-Cell Reading Relationship (°C = 0.56 (°F - 32), 1 psi = 6.89 kPa)

taken from July through August of 1980 after the stem had been placed. The toe of the footing was covered with soil in late July of 1980 so the temperature-cell readings after this event were not used to establish the preload curve for cell 935. Confidence in the accuracy of the computed temperatures was enhanced by observing the data from stem Cells 923 and 929. Preload readings had been obtained for these cells from March through August 1980 and temperature-preload curves could be established. The points plotted along a straight line, which indicates the computed temperatures are correct, because errors in temperature would produce an erratic plot. The preload curves for these cells are not shown because they ceased to function after August 1980.

The cells on the base of the footing and in the key posed a special problem, because the computed temperatures, based on direct preload pressure and temperature readings on the top stem cells, could only be made back to March 1980, when the first stem cell readings were recorded. The preload condition for the footing Cells 926, 936, 938, 922 and 937 along the base and key, occurred when the first cell readings were taken in November 1979. Only the weight of the concrete loaded these cells when cell readings were taken in January 1980. The temperatures in November and January 1980 were predicted from the temperature-preload pressure relationship for Cells 924 and 935 on the face of the heel and toe respectively. The estimated temperature-preload curves for Cells 926, 936, 938, 922, and 937 are presented in Fig. 32 through Fig. 34. No preload curve is given for Cell 925 because of erratic cell readings for the first year of the study.

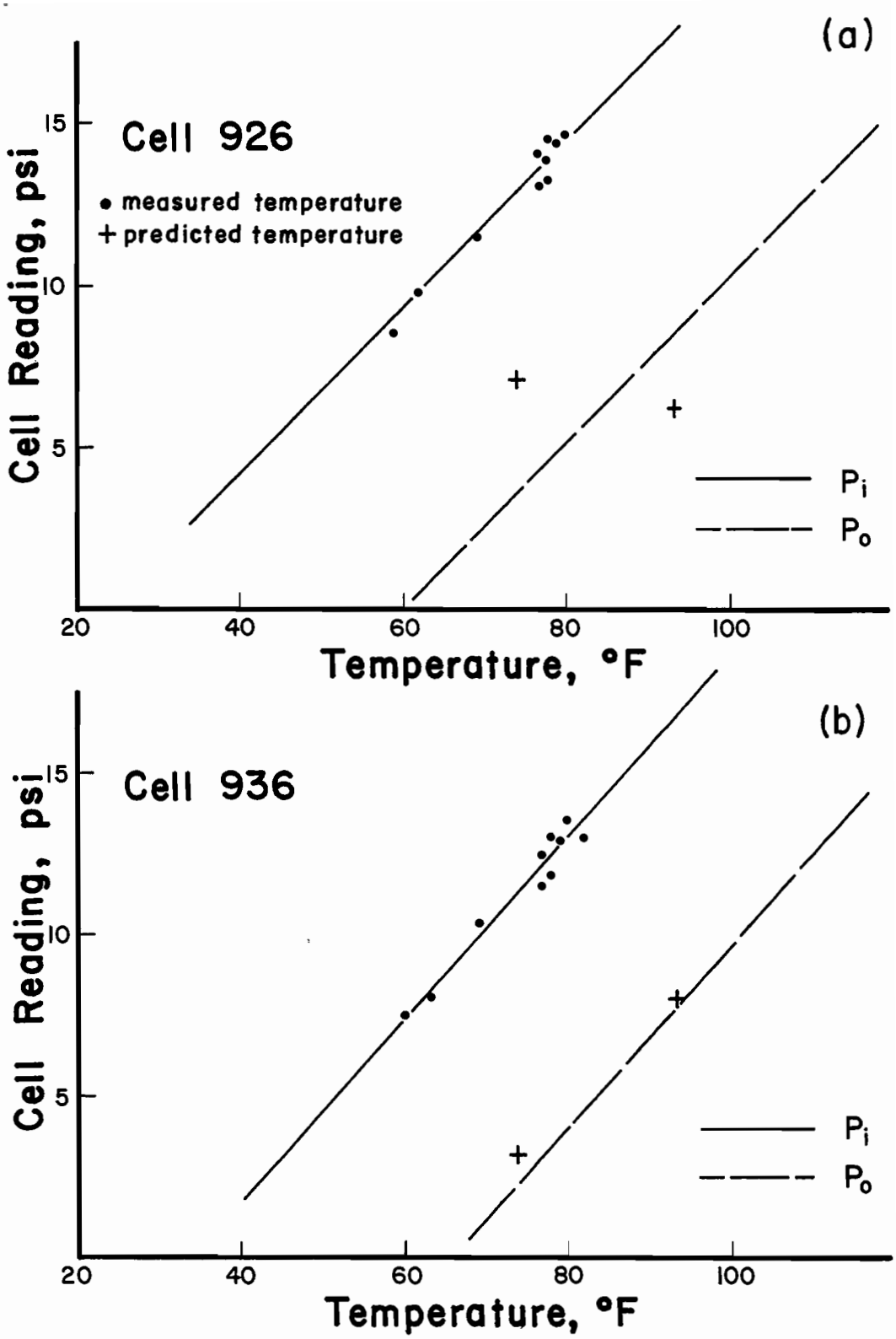

FIG. 32 - Cells 926 and 936: Temperature-Cell Reading Relationship (°C = 0.56 (°F - 32), 1 psi = 6.89 kPa)

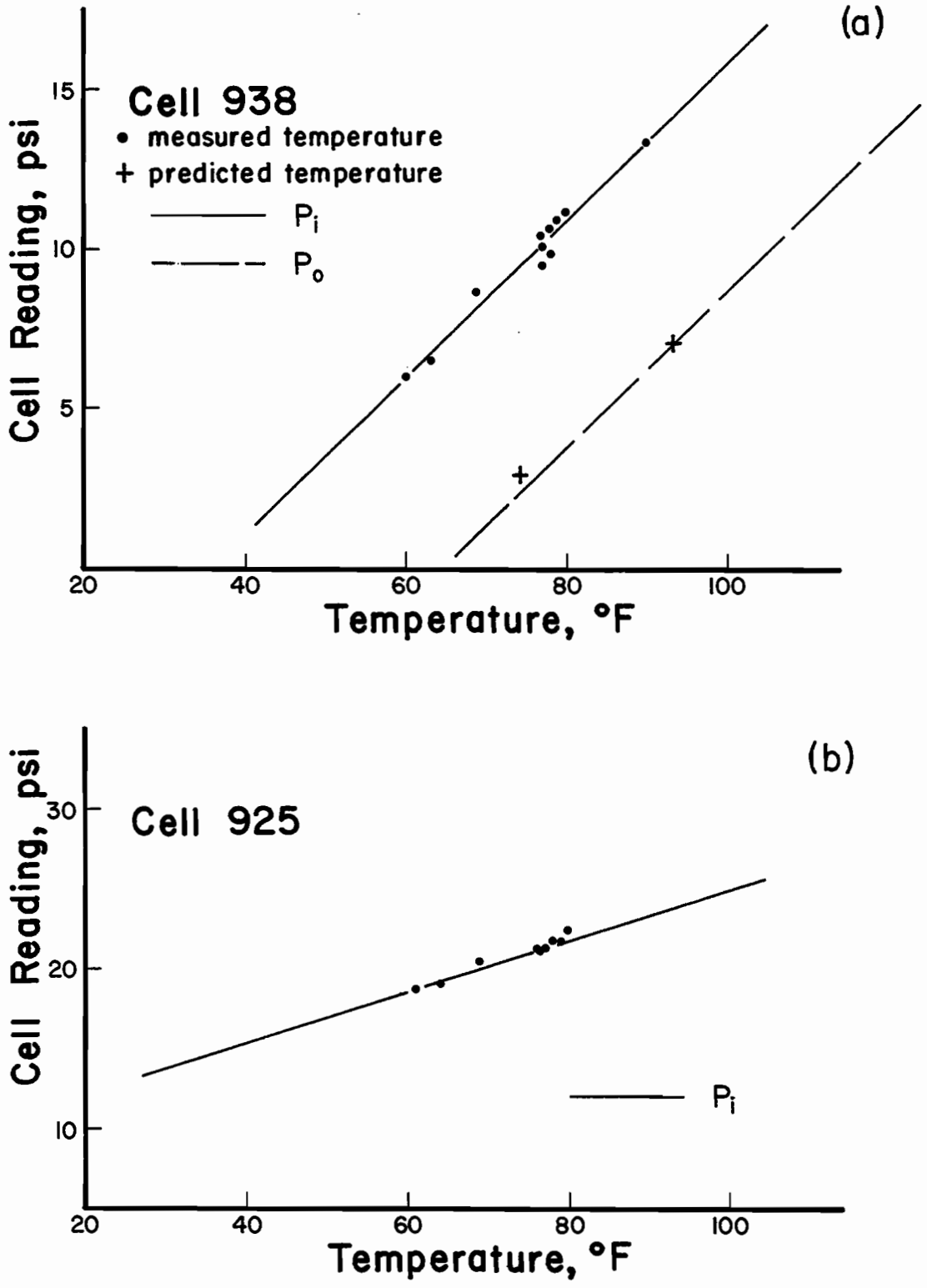

FIG. 33 - Cells 938 and 925: Temperature-Cell Reading Relationship (°C = 0.56 (°F - 32), 1 psi = 6.89 kPa)

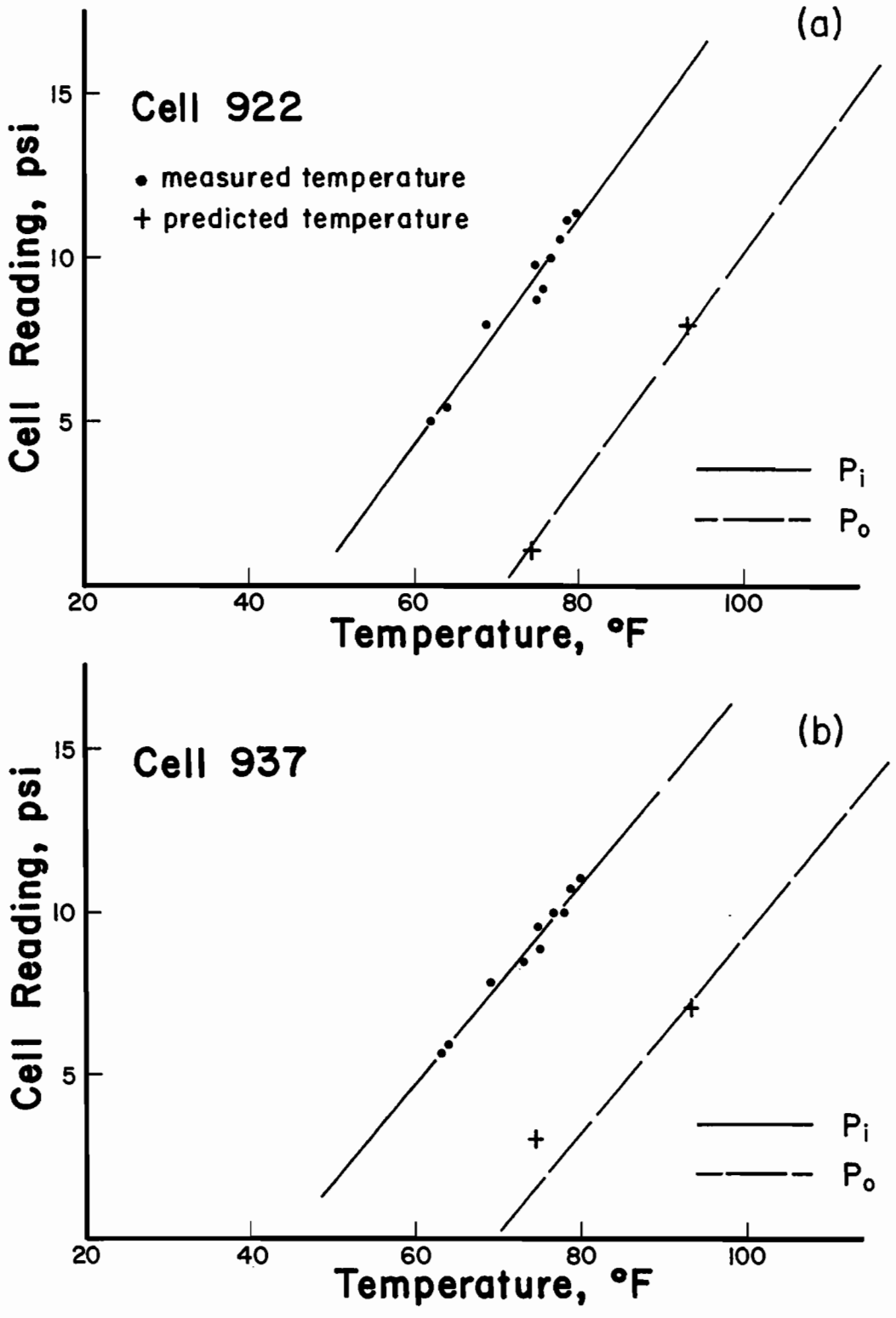

FIG. 34 - Cells 922 and 937: Temperature-Cell Reading Relationship (°C = 0.56 (°F - 32), 1 psi = 6.89 kPa)

Laboratory Temperature-Preload Pressure Tests.- Additional Terra Tec cells were obtained for a laboratory study, and preload readings were made throughout a temperature range overlapping those observed in the field. Cell 913 had been used in an earlier study and was available for testing. Cell 954 was purchased from Terra Tec primarily to investigate temperature variation. The cells were placed on a bed of sand and subjected to a constant temperature until the preload reading and temperature measured on the face of the cell stabilized. The results of these tests are given in Fig. 35. It should be noted that the preload readings are not constant with temperature and that the temperature-preload relationship is linear within the temperature range observed in the field study after the cells were covered with soil. The temperature response of Cell 913 changed for temperatures above 100°F (37.8 °C). Two curves are shown for Cell 954. The observed shift in preload reading with respect to temperature occurred after reversing the gas flow through the cell when testing the cell for linearity. This may be significant, because it is the manufacturer's recommended procedure for reviving cells that fail to respond. This procedure is used to open the piston valve if it becomes stuck in the closed position. Also, gas is "backflushed" through the return line to blow out water that has entered the tubing. Cell 954 was backflushed a second time after the temperature-preload tests were completed. The effect of the second backflushing was to return the temperature-preload relationship to that which was first observed. Cell 913 was backflushed and ceased to function. It is concluded that the effect of backflushing is unpredictable and should be performed only as a last resort.

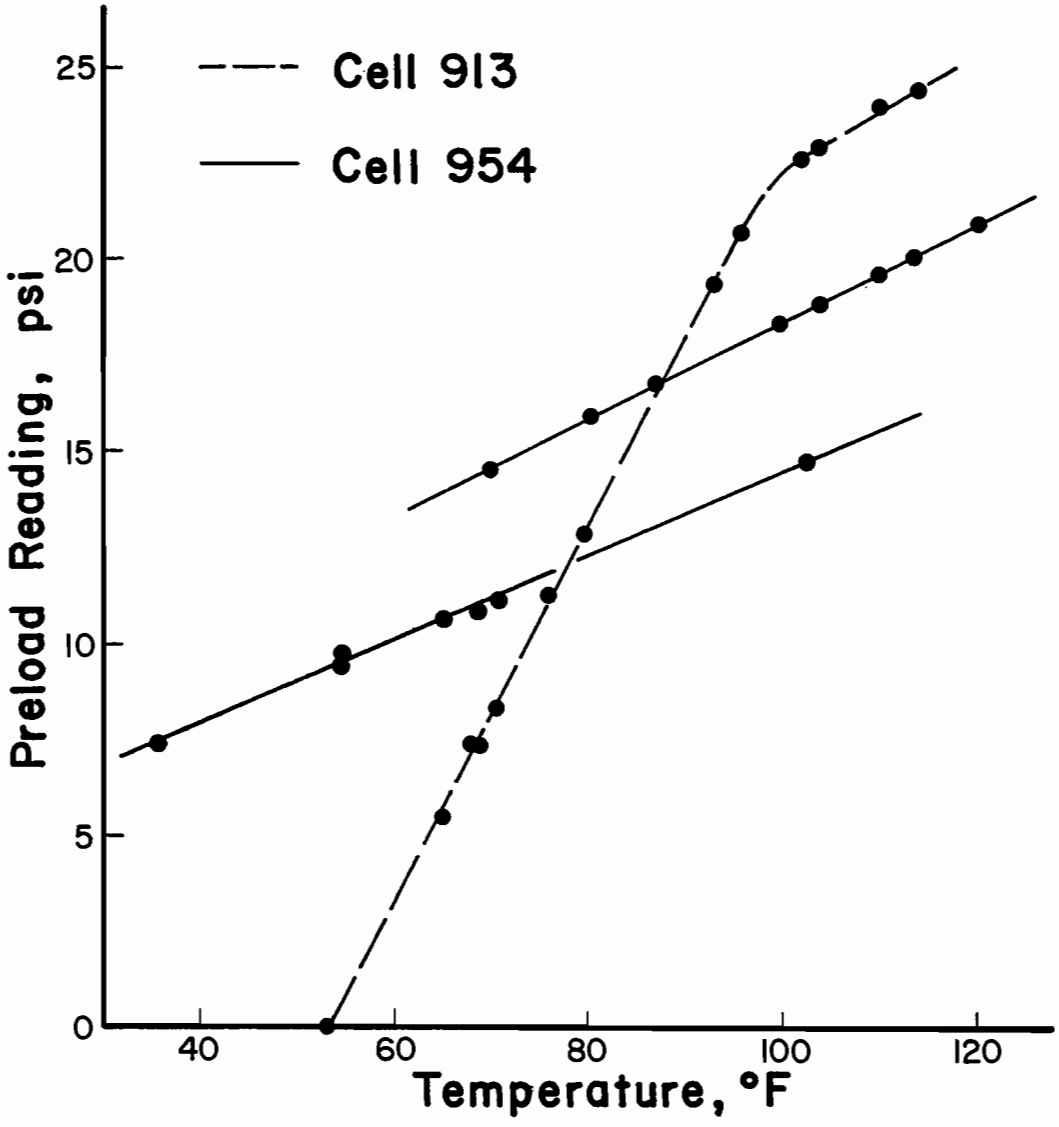

FIG. 35 - Laboratory Temperature-Preload Relationship
(°C = 0.56 (°F - 32), 1 psi = 6.89 kPa)

The backflushing procedure was performed on cells which failed to respond during the field performance study. Cells 923 and 929 ceased to function and did not register after backflushing. Cells 928, 927, and 921 failed to respond and did register after backflushing in January of 1980, Feburary of 1981, and January of 1982 respectively.

After extensive data analysis, the temperature-preload relationship for each pressure cell was established. The temperature-preload relationships established give the best consistency for each cell and for cell to cell comparisons. It is important to note that the temperature-preload relationship is linear throughout the temperature range observed. Also, backflushing is considered to have had negligible effect on the temperature-preload response.

In summary, the total earth pressure is obtained by subtracting the field preload pressure from the field pressure cell reading. The field preload pressure was found to vary with temperature. Evidence from field observations and laboratory tests indicates that the preload pressure varies linearly for the temperature range measured in the field study. The temperature preload relationship for each cell used in the research study is shown in Figs. 29 through 34.

Wall Movement.- As shown in Fig. 36, the wall movement was primarily established with respect to Pad E where direct horizontal, vertical and tilt movements were measured. The movements at Pads A through D were computed using the plumb line readings and the position of Pad E.

The position of Pad E was determined from horizontal tape measurements and leveling. The horizontal movement of the wall at

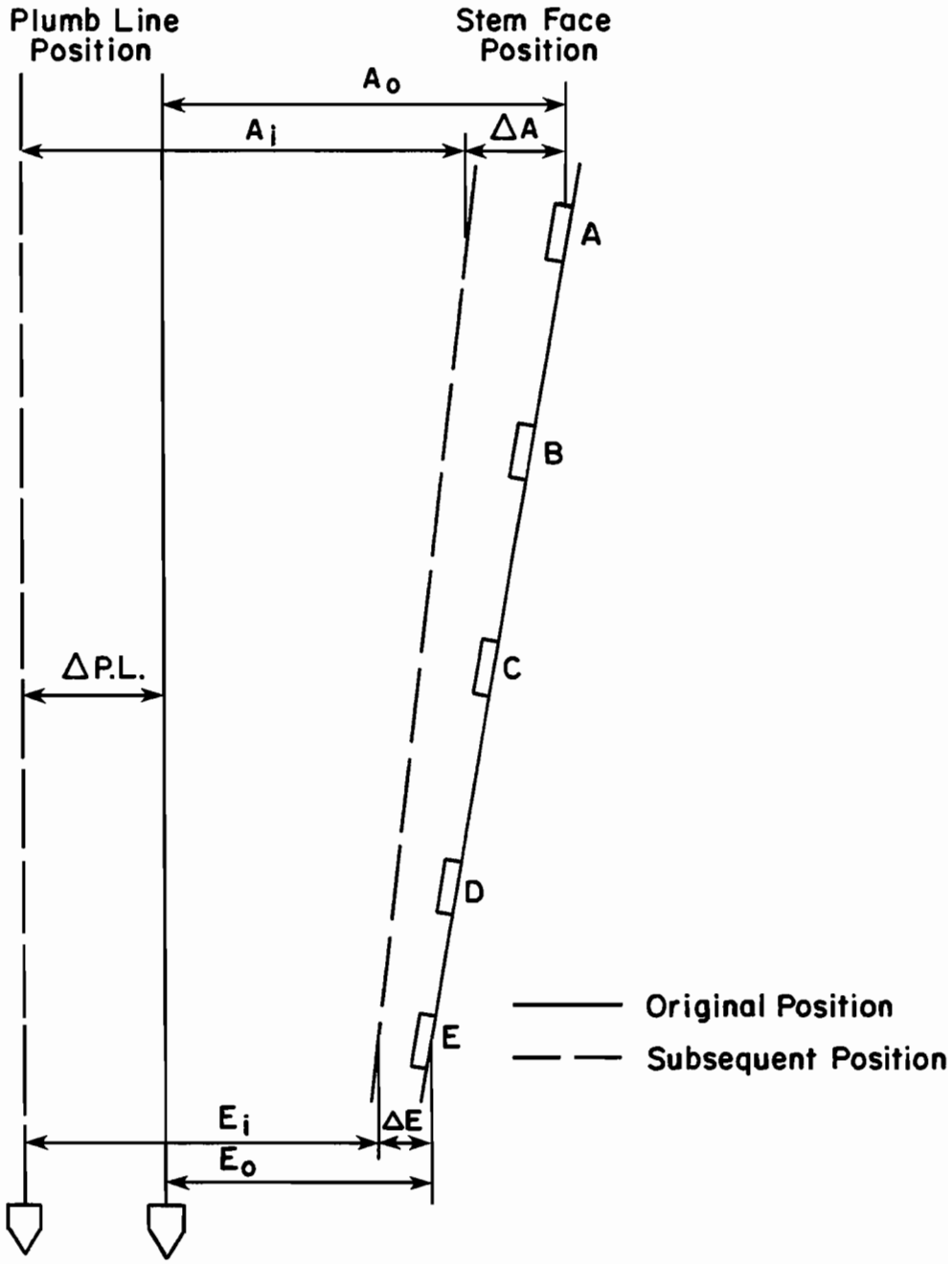

FIG. 36 - Horizontal Wall Movement Analysis

Pad E is the difference between the initial horizontal distance from the hook adjacent to Pad E and the reference point and subsequent horizontal distance measurements (see Fig. 16). The vertical movement at Pad E is the difference in rod readings between the hook and the reference point.

The horizontal movement of Pads A through D is the sum of the horizontal movement of the plumb line and the difference between the original plumb line reading and subsequent plumb line readings for each pad. The movement of the plumb line is the sum of the horizontal movement at Pad E and the change in plumb line readings at Pad E. This is illustrated in Fig. 36 where ΔE is a direct horizontal measurement. The horizontal movement of the plumb line, $\Delta P.L.$, is computed as follows

$$\Delta P.L. = \Delta E + E_i - E_o \quad \ldots\ldots\ldots\ldots\ldots\ldots\ldots\ldots \quad (10)$$

The horizontal movement of the wall at the remaining pads is illustrated using Pad A. The horizontal movement at Pad A, ΔA, is computed as follows

$$\Delta A = \Delta P.L. + A_o - A_i \quad \ldots\ldots\ldots\ldots\ldots\ldots\ldots\ldots \quad (11)$$

The horizontal movement of the stem at Pads B, C, and D are computed using the same procedures. The horizontal wall movements have a precision of 0.002 ft (0.6 mm).

Wall tilt is computed using the difference in plumb line readings at each pad, and the distance between the plumb bob support and each pad. This is illustrated in Fig. 37 for Pad E and explained as follows: the angular rotation or tilt angle, θ, is defined by

$$\theta = \frac{\Delta Rdg_E}{R_E} \quad \ldots\ldots\ldots\ldots\ldots\ldots\ldots\ldots\ldots\ldots \quad (12)$$

where ΔRdg_E is the difference between the original plumb line reading and subsequent plumb line readings for Pad E, and R_E is the distance between the radius point and Pad E. The original plumb line position and the subsequent plumb line position are considered to be coincidental which places the radius point at the same position as the plumb bob support. The computed values of the tilt angle at each pad agree within 0.5 minutes of arc for a set of measurements. The computed values of wall tilt are verified with the inclinometer measurements. The tilt angle values computed from plumb line readings are more precise and considered more accurate than those obtained from inclinometer measurements.

Results

Earth Pressure.- Total earth pressure is obtained by subtracting the preload pressure reading from the field pressure cell reading as explained previously. A significant finding in this research study is that the preload reading varies with temperature. The logical consequence of this evidence is that the preload pressure can be determined only if a corresponding temperature is measured or can be accurately estimated; therefore, the total earth pressure can be determined only

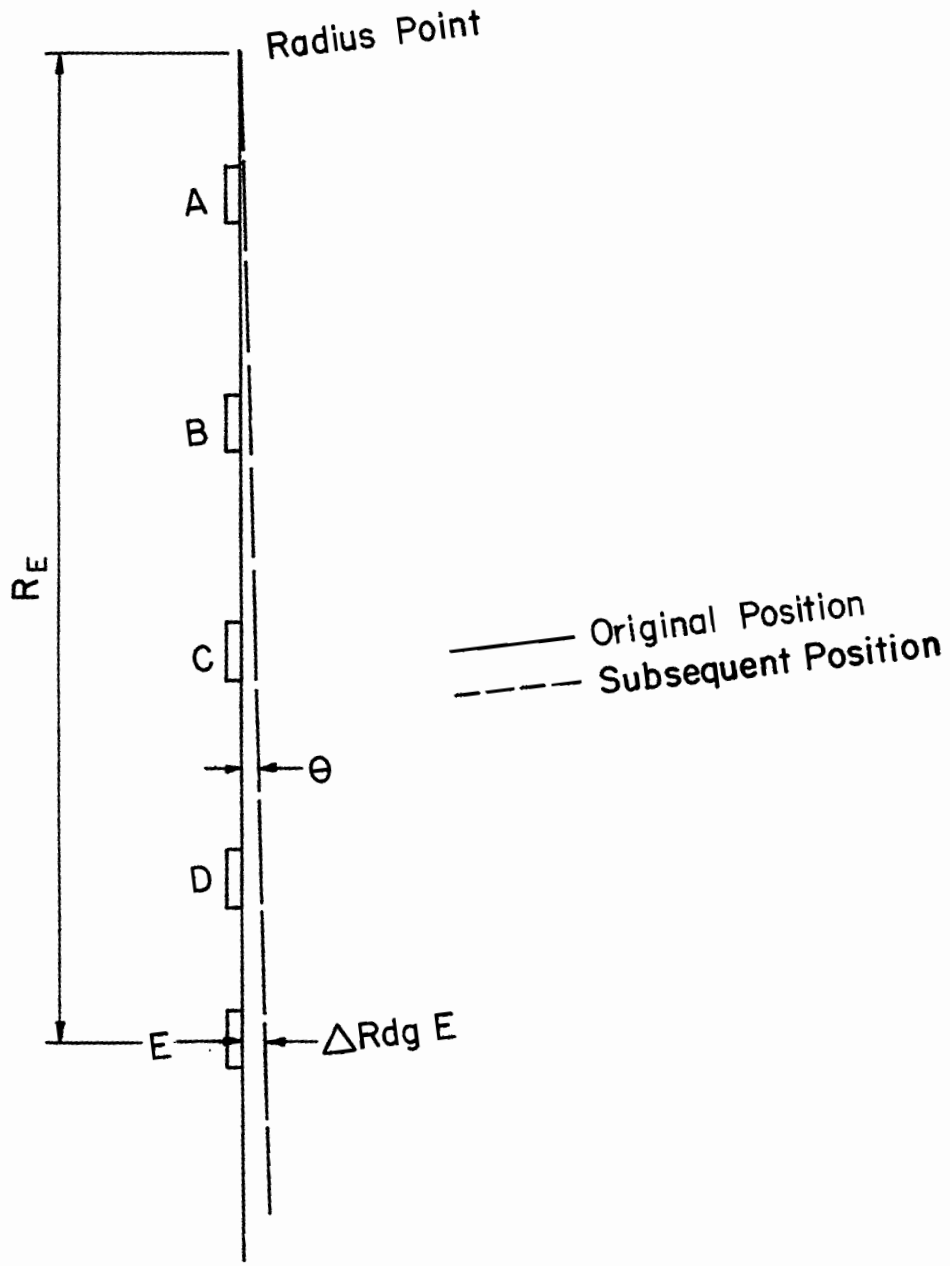

FIG. 37 - Wall Tilt Analysis

when the corresponding temperature is known. Complete data, to include field pressure cell readings, measured or estimated temperatures, measured or computed preload pressures and total earth pressures are tabulated in Appendix No. III for each pressure cell.

Earth Pressure, Stem Cells.- Total earth pressures for the stem cells are summarized in Table 1. Stem Cells 929 and 923 are omitted because these cells ceased to function before earth pressures were measured. Backfill was not placed against the backface of the stem through August of 1980, so prior to that date the earth pressure should be zero. A second set of values for earth pressures was not tabulated for June 16, 1980 after the concrete was placed and was still fresh, because these readings were not applicable.

There are some anomalies which deserve special attention. Cell 930 was not covered with soil until February of 1981, but positive earth pressures were observed in November 1980 and January 1981. A possible explanation is that a compressive stress on the cell was developed due to bending caused by the friction on the back face of the stem from compaction as observed by Ingold (10). The earth pressures for Cell 921 are significantly different from zero from March 7 through June 16, 1980, before the stem concrete had been placed. The earth pressures for Cell 921 between July 9 and August 26, 1980 were approximately zero after the stem concrete had been placed, but no backfill had been placed against the backface of the stem during this time period. A possible explanation is that cell reading response changed after the concrete was placed. Another possible anomaly is the effect on earth pressure readings after backflushing. The earth pressure for

TABLE 1. - Total Earth Pressure, Stem Cells
(1 psi = 6.9 kPa)

Date	Time, days	Total Earth Pressure, psi 930	928	927	921
7 Mar 80	180	0.0	0.0	+ 0.2	+ 4.9
1 Apr 80	133	- 0.5	- 0.3	+ 0.3	+ 3.0
22 Apr 80	154	0.0	+ 0.1	+ 0.2	+ 4.2
4 Jun 80	197	+ 0.4	- 0.1	+ 0.1	+ 3.9
16 Jun 80	209	+ 0.2	- 0.2	0.0	+ 2.7
16 Jun 80	209	*	*	*	*
9 Jul 80	232	+ 0.2	+ 0.2	- 0.3	- 0.6
29 Jul 80	252	- 0.1	+ 0.1	0.0	+ 0.9
8 Aug 80	262	- 0.2	+ 0.3	- 0.1	- 0.6
20 Aug 80	274	+ 0.1	+ 0.3	+ 0.1	+ 0.5
26 Aug 80	280	+ 0.1	+ 0.1	+ 0.3	+ 0.8
18 Sep 80	303	0.0	0.0	0.0	+ 3.0
6 Nov 80	352	+ 1.7	+ 1.0	+ 2.2	+ 5.0
11 Nov 80	357	+ 1.2	+ 2.3	+ 3.2	+ 6.3
7 Jan 81	414	+ 2.3	**+ 6.8	+ 3.0	+ 7.5

TABLE 1. - (Continued)

Date	Time Days	Total Earth Pressure, psi 930	928	927	921
12 Feb 81	450	+ 2.3	+ 6.6	**+ 9.6	+ 8.7
12 Mar 81	478	+ 1.7	+ 7.4	+ 9.6	+ 8.1
20 May 81	547	+ 2.3	+ 8.4	+ 11.1	+ 10.3
2 Jun 81	560	+ 2.1	+ 7.8	+ 10.3	+ 8.5
10 Jun 81	568	+ 1.8	+ 7.3	+ 9.8	+ 9.6
30 Jun 81	588	+ 1.9	+ 6.9	+ 9.6	+ 9.6
9 Jul 81	597	+ 1.9	+ 7.3	+ 9.9	+ 9.1
23 Jul 81	611	+ 2.3	+ 6.9	+ 9.4	+ 9.1
10 Sep 81	660	+ 2.5	+ 6.5	+ 9.7	+ 8.4
1 Oct 81	681	+ 2.3	+ 6.9	+ 10.9	+ 8.1
29 Oct 81	709	+ 2.1	+ 6.7	+ 9.9	+ 7.2
6 Jan 82	778	+ 3.2	+ 7.3	+ 10.3	**+ 7.6
4 Mar 82	835	+ 4.3	+ 7.0	+ 10.1	+ 8.8
15 Apr 82	877	+ 4.7	+ 7.7	+ 10.3	+ 8.6
26 May 82	918	+ 5.0	+ 8.5	+ 10.8	+ 9.6
10 Jun 82	933	+ 4.9	+ 8.8	+ 10.6	+ 10.7
7 Jul 82	960	+ 5.2	+ 8.3	+ 10.1	+ 11.1

* - Unknown

** - Backflushed to obtain response

Cell 928 on January 7, 1981 is not consistent with the earth pressures reported in November 1980 when the backfill height was the same. The cell was backflushed on the January 1981 date. Cell 927 was backflushed on February 12, 1981 and a significant increase in earth pressure has been observed since that date, but a significant increase in backfill corresponds to this event. Cell 921 was backflushed in January 1982. No significant variation in earth pressure was observed prior to or after this date. The effect of backflushing cannot be determined conclusively based on field and laboratory observations.

Earth Pressures, Vertical Footing Cells.- Table 2 contains the earth pressures for the cells on the vertical faces of the footing. Cell 924 and Cell 935 are located on the heel and toe of the footing and Cell 938 is located on the key of the footing. Earth pressures are not tabulated if temperature measurements or accurate estimates are not available. Cell 924 was partially exposed to the atmosphere until September 1980 so earth pressures are tabulated for all dates except June 16, 1980. Cell 935 was covered with soil in July 1980 so no valid temperature estimates could be made until September 1980 when temperature measurements began. The temperature estimated for the stem cells on June 16, 1980 is not considered valid for the footing cells because the stem cells were shaded by the forms and Cells 924 and 935 were not. It is important to note that a temperature difference of $3^{o}F$ (1.67^{o}) will cause a cell reading change on the order of 1 psi (6.89 kPa). No earth pressures are tabulated between March and August of 1980 for Cell 938, because no accurate temperatures can be estimated during this time

TABLE 2. - Total Earth Pressure, Heel, Toe and Key
(1 psi = 6.9 kPa)

Date	Time, days	Total Earth Pressure, psi 924 heel	935 toe	938 key
20 Nov 79	0	- 0.2	+ 0.6	+ 0.2
9 Jan 80	50	+ 0.3	- 0.3	+ 0.4
7 Mar 80	108	+ 1.2	+ 2.3	*
1 Apr 80	133	- 1.5	- 1.2	*
22 Apr 80	154	+ 0.3	- 0.8	*
4 Jun 80	197	+ 1.0	- 1.0	*
16 Jun 80	209	*	*	*
16 Jun 80	209	*	*	*
9 Jul 80	232	- 0.4	- 4.8	*
29 Jul 80	252	+ 0.3	*	*
8 Aug 80	262	- 0.7	*	*
20 Aug 80	274	+ 0.5	*	*
26 Aug 80	280	+ 0.8	*	*
18 Sep 80	303	+ 6.7	+ 5.3	+ 6.7
6 Nov 80	352	+ 6.4	+ 6.1	+ 6.4
11 Nov 80	357	+ 6.4	+ 6.4	+ 6.3
7 Jan 81	414	+ 7.1	+ 7.2	+ 6.4

TABLE 2. - (Continued)

Date	Time days	Total Earth Pressure, psi 924 heel	935 toe	938 key
12 Feb 81	450	+ 7.5	+ 8.6	+ 7.0
12 Mar 81	478	+ 7.7	+ 8.7	+ 7.0
20 May 81	547	+ 8.3	+ 9.8	+ 7.6
2 Jun 81	560	+ 7.5	+ 8.5	+ 6.4
10 Jun 81	568	+ 7.3	**+ 7.4	+ 6.7
30 Jun 81	588	+ 8.0	+ 8.4	+ 7.1
9 Jul 81	597	+ 7.7	+ 8.5	+ 7.3
23 Jul 81	611	+ 7.5	+ 8.8	+ 7.2
10 Sep 81	660	+ 0.0	+ 9.6	+ 7.3
1 Oct 81	681	+ 7.8	+ 9.0	+ 7.0
29 Oct 81	709	+ 7.9	+ 9.3	+ 7.6
6 Jan 82	778	+ 7.7	+ 9.2	+ 7.4
4 Mar 82	835	+ 8.1	+ 8.7	+ 7.0
15 Apr 82	877	+ 7.4	+ 9.5	+ 6.9
26 May 82	918	+ 7.7	+ 9.6	+ 7.0
10 Jun 82	933	+ 7.7	+ 10.2	+ 7.1
7 Jul 82	960	+ 7.8	+ 10.2	+ 6.9

* - No temperature data for preload determination

** - Low due to thermocouple installation

period. The earth pressure readings should be zero prior to September 1980 for Cell 924, prior to July 1980 for Cell 935, and in November 1979 for Cell 938. These dates correspond to the preload condition for each of the cells respectively. The observed variation from zero pressure readings for Cells 924 and 935 is attributed to the fact that the cells were partially covered with soil which sloughed off the face of the excavation. This soil, though loose, probably provided an insulation effect which caused the estimated temperatures to be slightly in error.

Earth Pressure, Horizontal Footing Cells.- The earth pressures for the cells located along the base of the footing are presented in Table 3. No accurate temperature estimate could be made before September 1980 when temperature measurements were begun, so earth pressures are not given before this date except for the preload condition in November 1979 and the approximate preload condition in January 1980. The earth pressures for November 1979 should be zero for these cells. All but Cell 926 satisfy this requirement. The cell readings for Cell 926 were not consistent with the other cells early in the study, but became less erratic after backfilling. It should be noted that the earth pressures change very slightly between September 1980 and July 1982. This implies that the earth pressures along the base of the footing are not significantly affected by the backfill height which increased by a factor of 4.5 during this time period. The temperature-preload pressure relationship could not be established for Cell 925 so earth pressures could not be obtained.

TABLE 3. - Total Earth Pressure, Footing Cells
(1 psi = 6.9 kPa)

Date	Time, days	Total Earth Pressure, psi 926	936	922	937
20 Nov 79	0	- 1.6	+ 0.1	+ 0.1	+ 0.1
9 Jan 80	50	+ 4.2	+ 0.8	- 0.2	+ 1.6
7 Mar 80	108	*	*	*	*
1 Apr 80	133	*	*	*	*
22 Apr 80	154	*	*	*	*
4 Jun 80	197	*	*	*	*
16 Jun 80	209	*	*	*	*
16 Jun 80	209	*	*	*	*
9 Jul 80	232	*	*	*	*
29 Jul 80	252	*	*	*	*
8 Aug 80	262	*	*	*	*
20 Aug 80	274	*	*	*	*
26 Aug 80	280	*	*	*	*
18 Sep 80	303	+ 9.0	+ 7.9	+ 6.4	+ 7.7
6 Nov 80	352	+ 8.8	+ 7.4	+ 6.9	+ 6.7
11 Nov 80	357	+ 8.7	+ 7.5	+ 7.0	+ 6.8
7 Jan 81	414	+ 9.3	+ 8.3	+ 7.8	+ 6.9

TABLE 3. - (Continued)

Date	Time, days	Total Earth Pressure, psi 926	936	922	937
12 Feb 81	450	+ 10.0	+ 9.1	+ 8.0	+ 7.3
12 Mar 81	478	+ 9.9	+ 8.9	+ 7.8	+ 7.4
20 May 81	547	+ 10.5	+ 9.5	+ 8.5	+ 7.9
2 Jun 81	560	+ 9.4	+ 8.3	+ 7.2	+ 7.3
10 Jun 81	568	+ 9.4	+ 8.4	+ 7.2	+ 7.0
30 Jun 81	588	+ 10.2	+ 9.2	+ 8.2	+ 7.7
9 Jul 81	597	+ 10.4	+ 9.2	+ 7.8	+ 7.5
23 Jul 81	611	+ 10.7	+ 9.6	+ 8.0	+ 7.3
10 Sep 81	660	+ 10.3	+ 9.5	+ 8.6	+ 7.7
1 Oct 81	681	+ 9.8	+ 9.1	+ 8.0	+ 7.4
29 Oct 81	709	+ 9.7	+ 8.7	+ 8.2	+ 7.3
6 Jan 82	778	+ 10.4	+ 9.4	+ 8.2	+ 7.1
4 Mar 82	835	+ 9.4	+ 9.1	+ 8.4	+ 7.5
15 Apr 82	877	+ 9.5	+ 8.8	+ 7.4	+ 6.8
26 May 82	918	+ 9.5	+ 8.8	+ 7.7	+ 7.1
10 Jun 82	933	+ 9.6	+ 9.3	+ 8.0	+ 7.3
7 Jul 82	960	+ 10.1	+ 10.2	+ 8.2	+ 7.6

* - No temperature data for preload determination

Pressure Distribution, Heel Side.- The distribution of earth pressures is an important consideration in the design of retaining walls. Design should be based on the maximum pressures. This condition occurred after the backfill and paving of the Left Frontage Street Ramp was completed and includes the earth pressures observed from April 15 through July 7, 1982.

The minimum to maximum values of earth pressures obtained during this time period for the stem cells and the cell on the heel of the footing are presented in Fig. 38. The pressure distribution is linear for those cells which were above the natural ground surface - Cells 930, 928 and 927. The linear distribution projected to the surface results in a earth pressure of 2 psi (13.8 kPa) which is consistent with the earth pressures measured near the surface when the backfill height was at the same level as Cells 928 and 930. This probably represents a portion of the residual lateral earth pressure due to compaction. The indicated linear increase in lateral pressure with depth would be developed using a coefficient of earth pressure equal to one. The pressures decrease appreciably at Cell 921 at the base of the stem and Cell 924 on the heel. These cells were completely covered with sand which was dumped into the void created by the footing excavation and then the sand was compacted lightly. The relatively low compactive effort and sand backfill contribute to the lower pressures measured at these cells. Also, arching probably occurred between the stem and footing and the face of the footing and face of the excavation, which reduced the pressures measured at these cells.

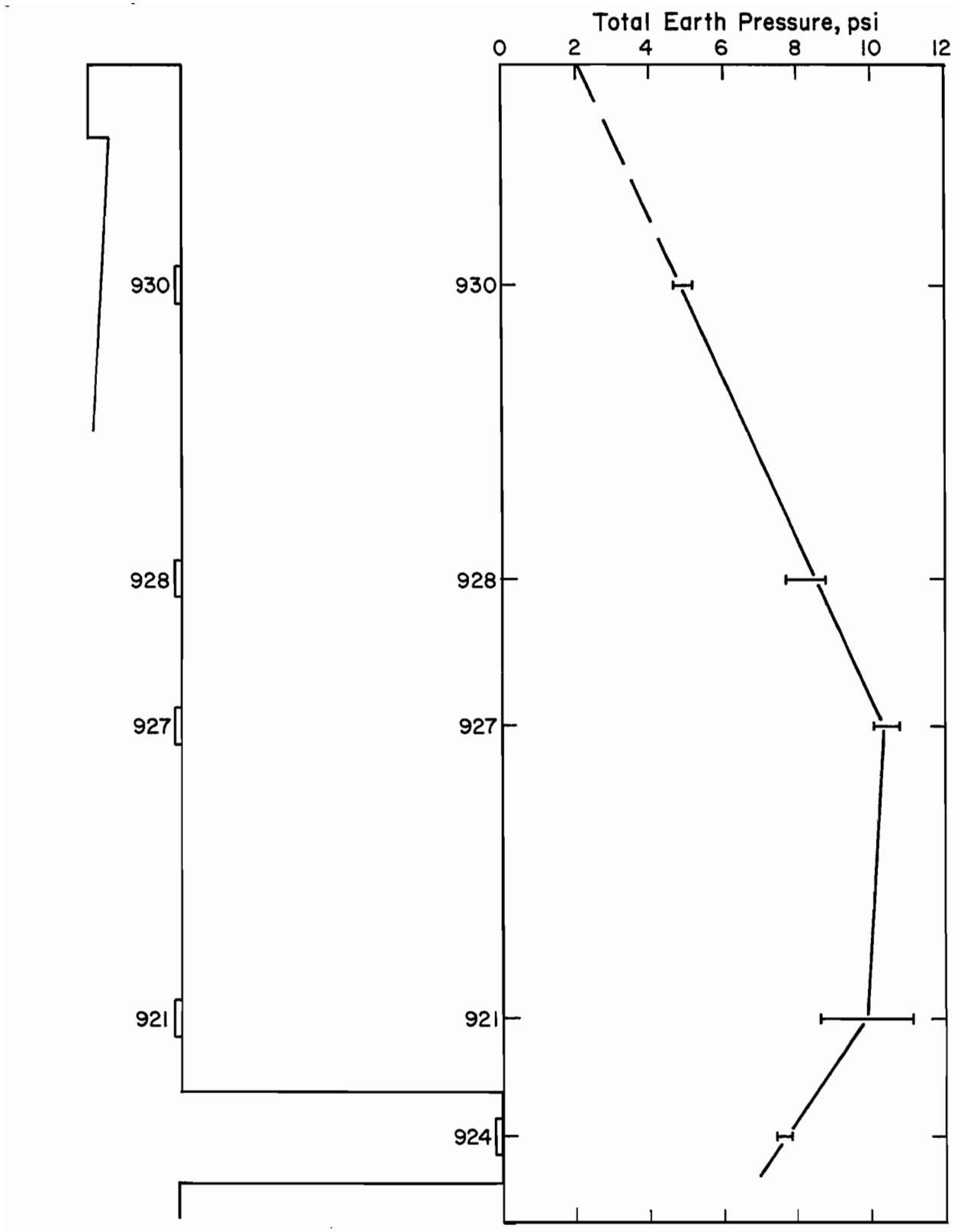

FIG. 38 - Lateral Earth Pressure Distribution, April-July, 1982 (1 psi = 6.89 kPa)

Pressure Distribution, Toe Side.- The pressure on the toe side of the wall was measured at the face of the toe and the face of the key only. Assuming the pressure distribution is similar to the top portion of the pressure distribution shown in Fig. 38, the coefficient of earth pressure would be 3.5 above the base of the footing. The coefficient of earth pressure at the key would be 2.5 if the effect of compaction is neglected. The earth pressure coefficients given above are consistent with the earth pressures between April and June 1982 in Table 2, and the depth of backfill for these dates.

Pressure Distribution, Base of Footing.- The earth pressure distribution along the base of the footing observed between April 15, 1982 through July 7, 1982 is shown in Fig. 39. The pressure decreases linearly from a maximum at the toe to a minimum at the heel of the footing. The pressure distribution corresponding to September 1980, when the backfill heights on each side of the stem were approximately the same, was nonlinear with greater pressures at the heel and toe and lower pressures near the center. The distribution became linear as the backfill height behind the wall increased.

Accuracy of Earth Pressures.- The accuracy of the earth pressures depends on the accuracy of the measured field pressures and the corresponding preload pressures. Field pressure measurements were repeated and consistent readings typically observed for each date readings were obtained. The procedure of backflushing is assumed to have no effect on the field pressure readings.

The preload pressures were found to be highly temperature dependent. Nominally, the precision of the preload pressure is 0.33 psi/^{0}F

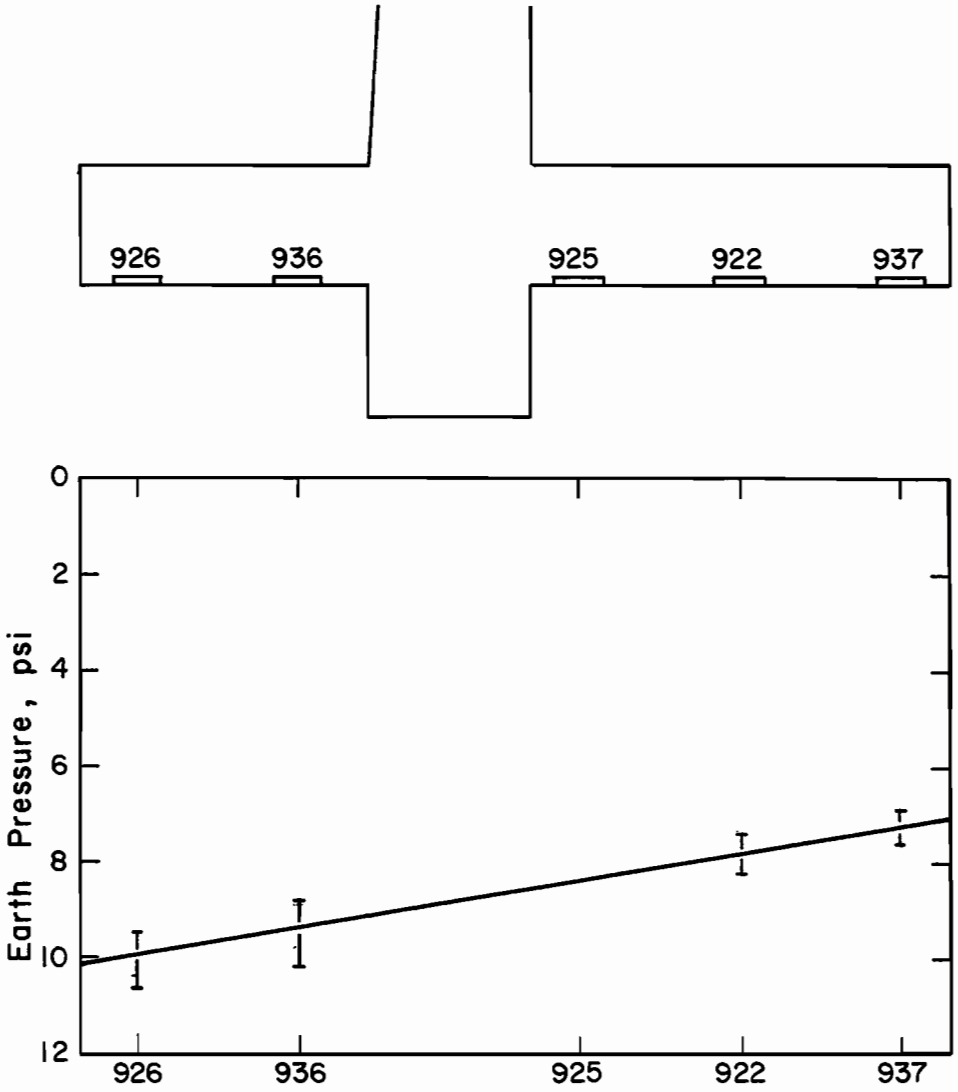

FIG. 39 - Earth Pressure Distribution on Footing Base, April-July, 1982 (1 psi = 6.89 kPa)

(4.14 kPa/^{o}C). The precision of measured temperatures is about 1.5^{o}F (0.12^{o}C).

The overall accuracy of the earth pressures is a function of the several factors discussed previously. The indicated precision of earth pressures as presented in Tables 1 through 3 is apparently inconsistent with the precision implied in the previous discussion. The tabulated values of earth pressures are consistent with direct observations and best estimates of temperature. It is believed that the best indicator of the precision of the earth pressures for each cell is the range of measured values corresponding to a particular backfill height. This is shown graphically in Figs. 38 and 39. The effect of pressure redistribution with time and cell linearity are also incorporated in the range of earth pressures shown.

Wall Movement.- The wall movement was measured in separate components of horizontal movement, vertical movement and tilt. The horizontal movement at the stainless steel pads is presented in Table 4. The negative sign indicates movement towards the heel. The horizontal movements were computed from the direct horizontal movement at Pad E and the plumb line readings as described previously. Direct horizontal measurements were begun in November 1980. Plumb line readings and inclinometer readings were taken earlier in August 1980. There was no change in either the plumb line readings or inclinometer readings between August and November which indicates that no tilt occurred during that time. The horizontal movement values given in Table 4 and illustrated in Fig. 40 represent minimum values because some translation probably occurred since 7 ft (2.13 m) of backfill had been placed

TABLE 4. - Horizontal Movement at Pads
(1 ft = 305 mm)

Date	Time, days	Horizontal Movement, feet A	B	C	D	E
6 Nov 80	352	0	0	0	0	0
11 Nov 80	357	0	0	- 0.001	0	- 0.002
7 Jan 81	414	0.013	0.013	0.012	+ 0.011	0.009
12 Feb 81	450	0.044	0.039	0.035	+ 0.035	0.025
12 Mar 81	478	*	*	*	*	0.031
20 May 81	547	0.069**	0.060**	0.054**	0.047**	0.042
2 Jun 81	560	0.072	0.064	0.055	0.049	0.043
10 Jun 81	568	0.071	0.062	0.057	0.048	0.044
30 Jun 81	588	0.076	0.069	0.062	0.053	0.049
9 Jul 81	597	0.078	0.070	0.062	0.055	0.049
23 Jul 81	611	0.080	0.072	0.065	0.058	0.051
1 Oct 81	660	*	*	*	*	0.054
10 Sep 81	681	0.088	0.078	0.070	0.061	0.053
29 Oct 81	709	0.091	0.081	0.072	0.062	0.056
16 Jan 82	778	0.108	0.098	*	0.076	0.069
4 Mar 82	835	0.112	0.100	*	0.078	0.078
15 Apr 82	877	0.122	0.110	*	0.088	0.080
26 May 82	918	0.128	0.116	*	0.093	0.085
10 Jun 82	933	0.130	0.119	*	0.094	0.086
7 Jul 82	960	0.132	0.120	*	0.095	0.087

* - No measurements
** - Less precise scale used

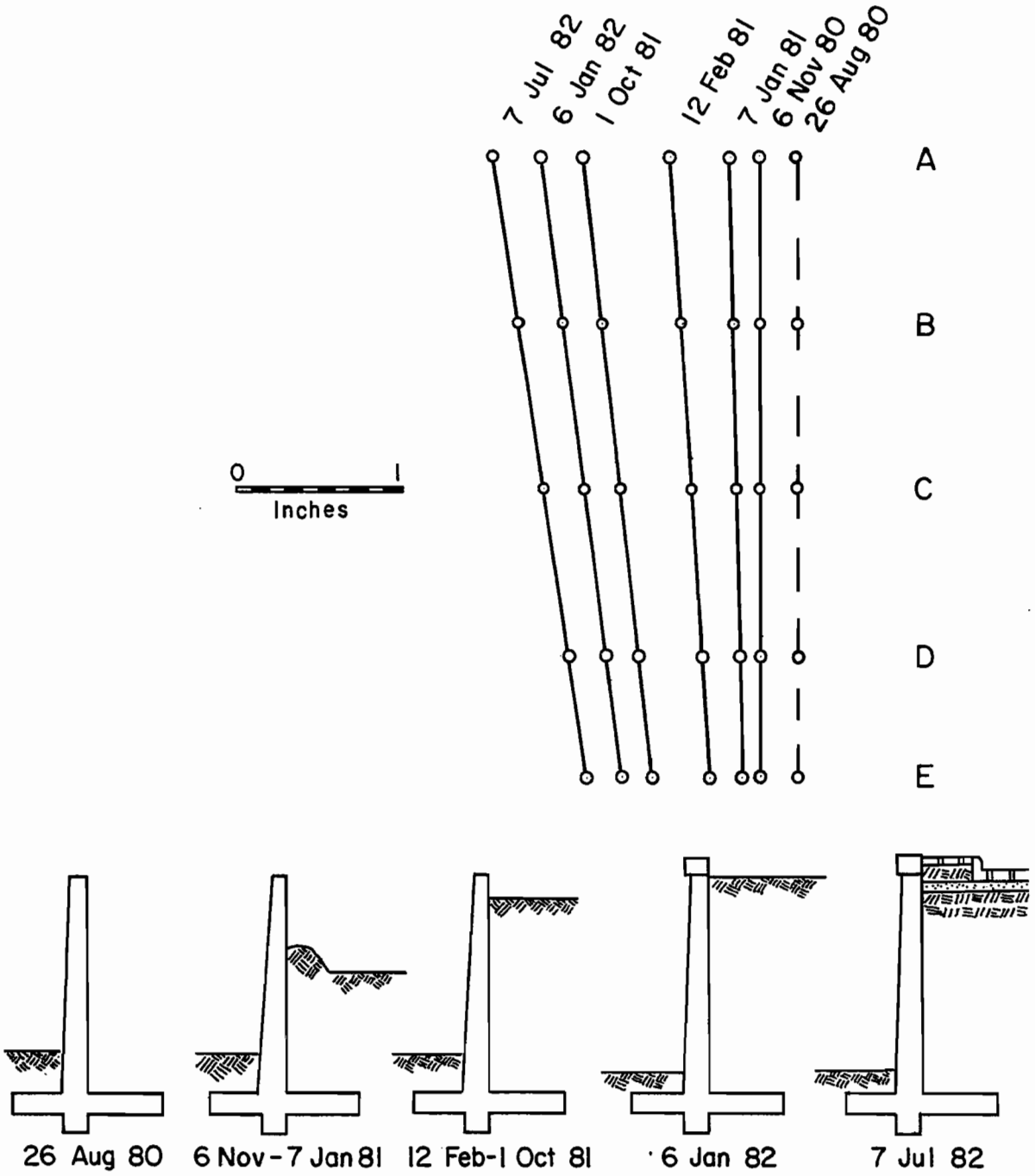

FIG. 40 - Horizontal Wall Movement and Tilt
(1 in. = 25.4 mm)

during that time span. Plumb line readings could not be obtained in March and September of 1981 so no horizontal movements are tabulated for Pads A through E on these dates. Pad C was vandalized in January 1982. The horizontal wall movement with respect to particular dates and backfill heights is shown graphically in Fig. 40. It can be seen that the stem remained rigid.

The wall tilt is also indicated in Fig. 40. The computed tilt for the six dates shown, in minutes of arc, are 00, 01, 07, 15, 19 and 21 respectively. The inclinometer readings verify these values. It should be pointed out that the front face of the stem is on a batter so the impression that the wall is overturning, as indicated by Fig. 40, is not correct.

The vertical wall movement was measured directly at Pad E. The total settlement was 0.034 ft (10 mm) measured between November 1980 and July 1982. This represents a minimum value, since some settlement probably occurred prior to November when vertical movement measurements began. The relatively low settlement was expected because the footing is supported by a stabilized sand overlying a stiff preconsolidated clay.

TEST WALL DESIGN

District 12 TSDHPT Design

Wall Proportions.- The as-built proportions and dimensions of the test wall have been given in Fig. 11. These proportions are representative of those obtained using current design procedures. A cross section of unit width is used in the design procedures.

Geotechnical Properties.- The geotechnical properties of the foundation soil are determined from laboratory tests and/or correlations from the TSDHPT cone penetration test. Spread footings without piling or pier suppports are considered appropriate for clay foundation soils which have an undrained shear strength greater than 2000 psf (95.8 kPa) (13). The backfill is assumed to be a granular soil with a unit weight of 115 pcf (18.1 kN/m^3). The equivalent fluid method is the basis for this design procedure. An equivalent fluid unit weight, γ_e, equal to 40 pcf (6.3 kN/m^3) for horizontal backfill is specified.

Gravity Forces.- The gravity forces due to the weight of the structure and the soil above the base of the footing are computed as the product of the unit weight of the material and the appropriate area (areas 1, 2, 3, 4 and 5) as indicated in Fig. 41. A live load, an equivalent uniform surcharge, equal to 2 ft (0.61 m) of backfill is included in the TSDHPT design. The weight of the key is neglected.

Lateral Forces.- The lateral force due to the equivalent surcharge is

$$P_{hs} = \gamma_e H_s H \quad \ldots\ldots\ldots\ldots\ldots\ldots\ldots\ldots\ldots\ldots \quad (13)$$

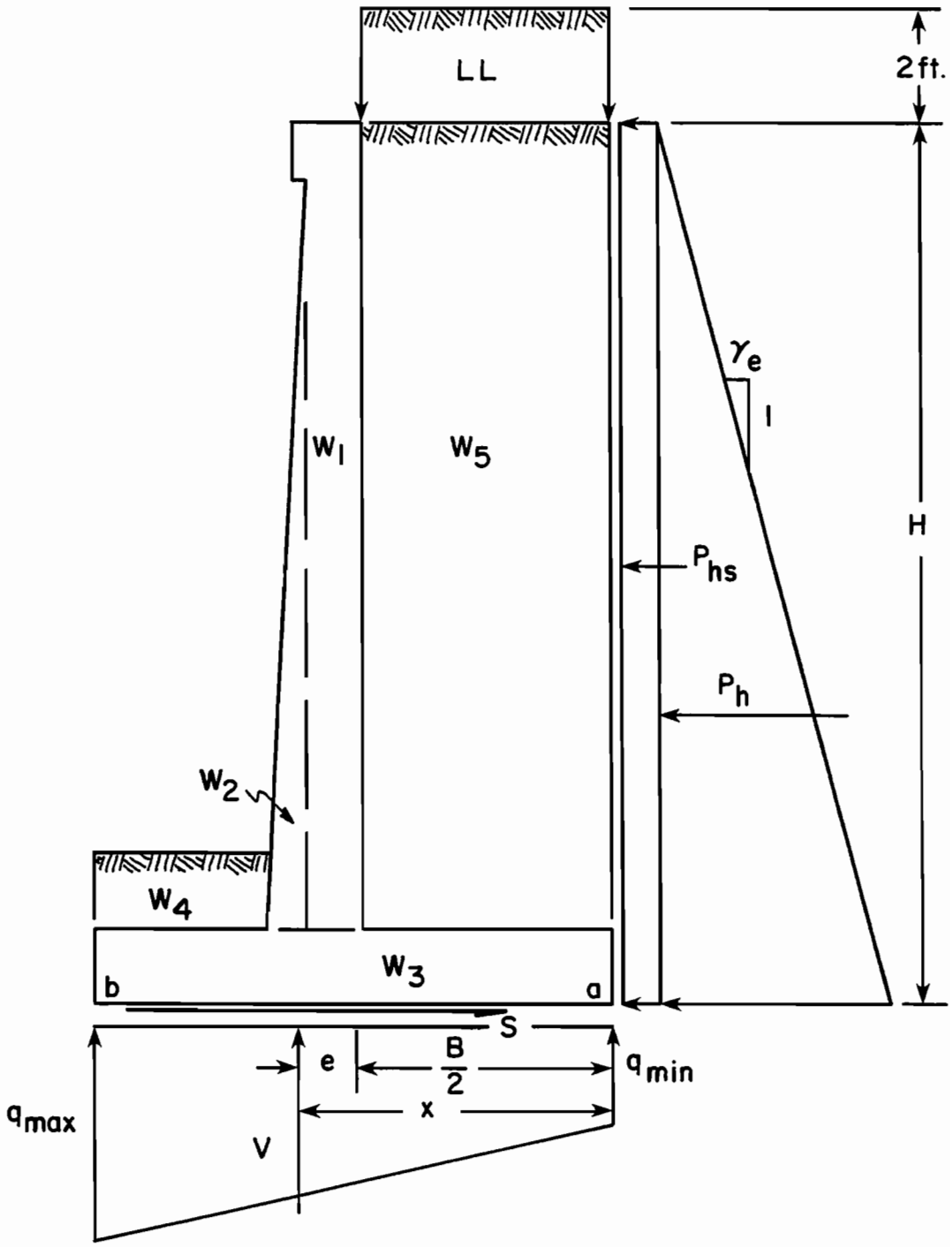

FIG. 41 - Free Body Diagram, District 12 TSDHPT Design
(1 ft = 0.305 m)

in which H_s = 2 ft (0.61 m) and H = the design height. The lateral force due to the equivalent fluid is computed using Eq. 7, repeated here for reference

$$P_h = \frac{\gamma_e H^2}{2} \quad \ldots\ldots\ldots\ldots\ldots\ldots\ldots\ldots\ldots\ldots\ldots\ldots \quad (7)$$

The lateral forces on the toe side of the wall are conservatively considered to be zero in the TSDHPT design.

Footing Pressure.- The maximum and minimum footing pressures acting on the base of the footing are computed using Eq. 8 discussed previously and repeated here for ready reference

$$q = \frac{V}{B}\left(1 \pm \frac{6e}{B}\right) \quad \ldots\ldots\ldots\ldots\ldots\ldots\ldots\ldots\ldots\ldots\ldots\ldots \quad (8)$$

Reviewing, V is the sum of the gravity forces and e is the difference between x and B/2. Moments are taken about the bottom of the heel, point a, in order to obtain the value of x. These terms are shown in Fig. 41.

Stability.- The stability against sliding is achieved by the shear force that develops in the foundation soil beneath the footing and the lateral force acting on the front side of the wall. The TSDHPT design assumes the slip surface occurs along the base of the footing and neglects the beneficial effects of the key with respect to the increased slip surface length and the lateral force on the face of the key, as well as the front face of the toe and stem. The specifications state that the allowable bearing capacity of the foundation soil must

not be exceeded to assure stability against bearing failure. The wall is considered stable against overturning if e is less than B/6.

Structural Design.- The District 12 TSDHPT design standard includes the size and placement of steel reinforcement in the retaining wall. The structural analysis is based on allowable stresses of 1 200 and 20 000 psi (8 300 and 138 000 kPa) for the concrete and steel respectively.

Drainage.- The provision for drainage, as discussed previously, is weep holes on 10 ft (3.05 m) centers for the test wall design. Lateral drains are sometimes used (14).

Construction.- Construction was governed by TSDHPT specifications. Only one TSDHPT field representative was assigned to the project.

Comparison with Study Results

Wall Proportions.- The as-built wall dimensions agree with the project plans and specifications within acceptable tolerances. Had the designer anticipated a clay backfill, the width of the footing would have been considerably larger, based on current design procedures.

Geotechnical Properties.- The foundation soil properties are consistent with those assumed in the TSDHPT design. The clay backfill is significantly different than the granular backfill assumed in the design. By comparison, the γ_e value for a horizontal stiff clay backfill material is 120 pcf (18.8 kN/m^3) (8,23).

Gravity Forces.- The calculations for gravity forces are summarized in Table 5. The forces were computed by multiplying the unit weight of the material by the appropriate area. The dimensions used in

the area computations are found in Fig. 11. The differences in gravity forces W_4 and W_5 are due to the use of the measured unit weight of the backfill material and the assumed design value. No surcharge was applied so the measured value is zero. The tabulated values of the measured resultant gravity force V were obtained by summing measured gravity forces W_1 through W_5 and computing the area of the measured footing distribution given in Fig. 39. The difference in these values (12.70 and 11.07) may be attributed to measurement errors. There is possibly a vertical component of resistance to movement on the face of the toe. The assumption that the value of V is approximately equal to the gravity forces is valid.

TABLE 5. - Design and Measured Gravity Forces
(1 kip/ft = 14.6 kN/m)

Force Kip/foot	District 12 TSDHPT		Measured	
W_1	0.150(1.00)(14.0)	= 2.10	0.150(1.00)(14.0)	= 2.10
W_2	0.150(0.67)(13)/2	= 0.65	0.150(0.67)(13)/2	= 0.65
W_3	0.150(9.0)(125)	= 1.69	0.150(9.0)(1.25)	= 1.69
W_4	0.115(3.0)(1.3)	= 0.45	0.128(3.0)(1.3)	= 0.50
W_5	0.115(4.33)(14.0)	= 6.97	0.128(4.33)(14)	= 7.76
LL	0.115 (4.33)(2.0)	= 1.00	NA	= 0
V	$W_1+W_2+W_3+W_4+W_5+LL$	= 12.76	$W_1+W_2+W_3+W_4+W_5$	= 12.70
V	NA		Area Fig. 39	= 11.07

Lateral Forces.- The computations for lateral forces are summarized in Table 6. These calculations are based on TSDHPT design procedures, wall dimensions from Fig. 11, measured lateral pressures and horizontal equilibrium.

TABLE 6. - Design and Measured Lateral Forces
(1 kip/ft = 14.6 kN/m)

Force kip/foot	District 12 TSDHPT	Measured
P_{hs}	$40(2)(15.25) = 1.22$	NA = 0
P_h	$40(15.25)^2/2 = 4.65$	Area of Fig. 38 = 16.43
P_{toe}	Assume = 0	$1.42(1.25)$ = 1.77
P_{key}	Assume = 0	$1.00(1.33)$ = 1.33
S	$P_{hs} + P_h = 5.87$	$P_h - P_{toe} - P_{key} = 13.33$

The lateral force due to the equivalent surcharge, P_{hs}, used in the TSDHPT design is due to a live load. The live load is zero in the measured column as no live loads were applied during the course of the study.

A significant difference between the design and measured values of the force, P_h, was observed. This difference is partially attributed to the difference between the granular backfill anticipated by the designer and the clay backfill used in the construction plus residual lateral stresses induced by compaction. In fact, had the designer

used an equivalent fluid unit weight corresponding to stiff clay, the computed value of P_h would increase by a factor of three, which better agrees with the measured value. The measured value of P_h was determined as the resultant of the lateral pressure distribution of Fig. 38.

The TSDHPT design conservatively omits the force that develops on the face of the toe and neglects the force which develops on the front face of the key. Therefore, these forces are shown as zero in Table 6. The measured pressure on the face of the toe is approximately 3.5 times larger than the measured pressure on the back face of the stem at the same depth of backfill. The measured pressure on the front face of the key is less than the pressure on the toe of the footing. This may be due to restricted relative movement of the key against the soil. The adhesion of the soil to the base of the footing in front of the key probably reduced the effect of the movement of the key into the soil. This drag effect on the key cell was enhanced because the cell was placed at the top of the key. Also, little residual stress due to compaction was developed on the face of the key.

The shear force, S, tabulated in Table 6 reflects the horizontal force necessary to achieve horizontal equilibrium. Lateral pressures were not measured on the front face of the stem due to the 1.3 ft (0.40 m) of backfill above the top of the footing, so the value of 13.33 in the measured column probably overestimates the magnitude of the shear force needed for horizontal equilibrium. Despite this fact, a significant difference between design and measured lateral forces exists.

Footing Pressure.- The pressure distribution on the base of the

footing is determined using Eq. 8. The point of application of V is determined by summing moments about the base of the heel, point a in Fig. 41. The summation of moments yields the distance x which is used to determine the eccentricity, e (see Fig. 41). Thus, the terms in Eq. 8 are evaluated. The computations of moments are presented in Table 7 for both the TSDHPT design and measured gravity and lateral forces. The forces given in Table 5 and Table 6 are repeated in Table 7 for ready reference. The moment arms can be verified by referring to Fig. 11 and Fig 41. P_{toe} and P_{key} are considered to act at the center of the toe and key respectively. Dual moment arms are tabulated for P_h and S. The moment arms for P_h, 5.08 and 6.41, correspond to the locations of the centroid of the pressure distributions shown in Fig. 41 and Fig. 38 respectively. The moment arms for S which are 0 and 1.33 correspond to the assumed location of S. The TSDHPT design assumes that S acts along the base of the footing. It is assumed for this text that S acts on a horizontal plane through the base of the key for the measured condition as shown in Fig. 8(c). The summation of moments is also tabulated in Table 7.

The computations of x, e and q based on moments of the TSDHPT design forces and measured forces, as well as the measured footing pressure distribution are given in Table 8. Significant differences among the x and e values were obtained. The TSDHPT values are consistent with the assumed granular backfill and design standard from which the test wall was constructed. The x and e values based on the moments of the measured forces are consistent with current design procedures and show a need to redesign the footing width. These values indicate

TABLE 7. - Moments About Base of Heel

(1 kip/ft = 14.6 kN/m, 1 ft = 0.305m, 1 $\frac{kip \cdot ft}{ft}$ = 4.45 $\frac{kN \cdot m}{m}$)

Symbol	Force kip/foot		Moment Arm	Moment kip•foot/foot	
	TSDHPT	Measured	Feet	TSDHPT	Measured
W_1	2.10	2.10	4.63	10.14	10.14
W_2	0.65	0.65	5.55	3.61	3.61
W_3	1.69	1.69	4.50	7.61	7.61
W_4	0.45	0.50	7.50	3.38	3.75
W_5	6.97	7.76	2.17	15.12	16.84
LL	1.00	0	2.17	2.17	0
P_{hs}	1.22	0	7.63	9.30	0
P_h	4.65	16.43	5.08/6.41	23.64	105.32
P_{toe}	0	1.77	0.63	0	-1.12
P_{key}	0	1.33	0.67	0	0.89
S	5.87	13.33	0/1.33	0	17.33
V	12.86	12.70	x	-12.86x	-12.70x

Sum of Moments	TSDHPT	Measured
	74.97 - 12.86x	164.77 - 12.70x

TABLE 8. - Footing Pressure Calculations

(1 ft = 0.305 m, 1 ksf = 47.9 kPa)

x e q	Calculations: x, e, q		Measured Pressure Distribution Fig. 39
	TSDHPT (moments)	Measured (moments)	
x, feet	74.97/12.86 = 5.83	164.77/12.70 = 12.97	Centroid Area = 4.77
e, feet	5.83- 4.50 = 1.33	12.97- 4.50 = 8.47	4.77-4.50 = 0.27
q_{max}, ksf	$\frac{12.86}{9.0}\left[1 + \frac{6(1.33)}{9.0}\right] = 2.70$	NA	10.1/6.94 = 1.46
q_{min}, ksf	$\frac{12.86}{9.0}\left[1 + \frac{6(1.33)}{9.0}\right] = 0.16$	NA	7.0/6.94 = 1.01

that the point of application of V is beyond the toe of the footing! Current design procedures would require the heel projection to be extended 6.0 ft (1.83 m) in order to reduce the eccentricity to a value of B/6 or less. The increased heel extension cited above is of the same order of magnitude that would be required if the design had been based on a clay backfill as was used in construction. The anomalous values of x and e based on the measured footing pressure distribution deserve special attention. These values indicate that the point of application of V is near the center of the footing despite the large lateral forces. This condition cannot be explained by current design procedures, which infers significant design parameters are neglected. Respective maximum and minimum footing pressures also differ. The TSDHPT values agree with the assumptions made in the TSDHPT design standard. The pressure distribution is nearly triangular. The pressure distributions cannot be obtained for the measured forces using Eq. 8, as this equation only applies if e is less than or equal to B/6. This condition indicates an extremely large contact pressure of the toe, and tensile values over a significant portion of the base of the footing. The measured footing pressure distribution is nearly uniform as shown in Fig. 39. The computations shown in Table 8 for the measured footing pressure distribution are simply the conversion of units of the measured maximum and minimum pressures. The Table 8 values can also be obtained using Eq. 8 for this case.

Stability.- A satisfactory design is achieved if the resisting lateral forces exceed those which tend to translate the wall horizontally, the bearing capacity is not exceeded and the tendency to

overturn is resisted. Safety factors are applied to ensure that the wall will remain stable. The conventional safety factor definition is the ratio of factors which cause stability to factors which cause instability.

Sliding is resisted by the lateral forces on the toe side of the wall and the maximum shear force that can develop within the foundation soil or along the base of the footing. The maximum shear force that can develop in the clay foundation soil, S_{max}, can be estimated by

$$S_{max} = c_u L \quad \ldots \ldots \ldots \ldots \ldots \ldots \ldots \ldots \ldots \ldots \quad (14)$$

in which c_u = the undrained shear strength and L = the length of the slip surface. The minimum value of L is the footing width B while the measured value of c_u is 3.17 ksf (152 kPa). The evaluation of the safety factor against sliding is given in Table 9. The length of the slip surface used in the computations is 9.0 ft (2.74 m) even though a slightly larger value can be justified because of the key (see Fig. 8). The magnitudes of the lateral forces are taken from Table 6. The computed safety factors are greater than 1.5 which is commonly used (1,8,10,11,19,23).

The stability against bearing failure is achieved if the maximum footing pressure imposed is less than the shear strength of the foundation soil. The bearing capacity is obtained using the same criteria as that for spread footings. The ultimate bearing capacity of clay in terms of undrained conditions can be conservatively estimated,

neglecting the surcharge term as, (23)

$$q_{ult} = 5.14\ c_u \quad \text{(15)}$$

TABLE 9. - Safety Factor Against Sliding

(1 kip/ft = 14.6 kN/m)

Lateral Force kip/foot	Dictrict 12 TSDHPT	Measured
S_{max}	3.17(9.0) = 28.53	3.17(9.0) = 28.53
P_{toe}	0	1.77
P_{key}	0	1.33
Sum, (resist)	28.53	31.63
P_{hs}	1.22	0
P_h	4.65	16.43
P_{key}	0	*
Sum (cause)	5.87	16.43
Safety Factor	28.53/5.87 = 4.86	31.63/16.43 = 1.93

* - Not measured

The evaluation of the safety factor against bearing failure is given in Table 10. The calculated safety factors against bearing failure are much greater than 3.0 which is typically specified for clay foundation soils (1,8). The measured settlement at the face of the stem was only 0.41 in. (10 mm) which is tolerable. Excessive settlement is not expected for preconsolidated clays.

TABLE 10.- Safety Factor Against Bearing Failure
(1 ksf = 47.9 kPa)

Soil Pressure ksf	TSDHPT	Measured
q_{max}	2.70	1.46
q_{ult}	5.14(3.17) = 16.29	
Safety Factor	16.29/2.70 = 6.0	16.29/1.46 = 11.2

There are two commonly used methods for checking the stabilitity against overturning as described previously. In one method, the wall is considered stable if the eccentricity is less than B/6 (8,11,23), or 1.50 ft (0.46 m) in this case. Inspection of Table 8 reveals that the TSDHPT design and measured footing pressure distribution satisfy this requirement (1.33 and 0.27 are less than 1.50). The eccentricity based on the moments of the measured forces fails this requirement (8.47 is much greater than 1.50). The TSDHPT design is based on a granular backfill, so it does not apply. The eccentricity based on moments of measured forces is consistent with current design procedures and predicts overturning, even though the test wall is stable as indicated by the eccentricity of the measured footing distribution. These observations infer that the current design procedures neglect a significant component of stability.

Many designers determine the stability against overturning by summing moments about the base of the toe, point b in Fig. 41. Only the forces above the base of the footing are considered. The safety

factor against overturning is defined as the ratio of moments that resist overturning, M_r, to moments that cause overturning, M_o. The minimum value of this safety factor often used is 2.0 (1,10,19). A summary of the calculations for the safety factor against overturning is given in Table 11. Calculations similar to those shown in Table 7 were performed.

TABLE 11. - Safety Factor Against Overturning

($1 \frac{kip \cdot ft}{ft} = 4.45 \frac{kN \cdot m}{m}$)

Moment Type	TSDHPT kip•foot/foot	Measured kip•foot/foot
M_r	74.15	73.90
M_o	32.93	105.32
Safety Factor	74.15/32.93 = 2.25	73.90/105.32 = 0.70

The TSDHPT design is satisfactory as expected, but is not applicable. The stability calculations based on current design procedures predict that the wall should overturn, because the safety factor is less than 1.0. This is contrary to the observed performance of the wall and suggests that modification of current design procedures for overturning stability is warranted.

Structural Design.- The structural analysis is not a part of this report, but significant differences between bending moments and shear stresses obtained in the TSDHPT design and those due to the measured pressure distributions undoubtedly exist. The bending moments in the stem probably approach design capacity since the measured lateral

pressures are about three times greater than those used in design. Similarly, the footing is likely to be overdesigned due to the difference between the design and measured pressure distributions.

Drainage.- The drainage system used in the design was presented previously, and no measurements were made to evaluate its effectivenesss.

Construction.- The significant departures from specifications are the use of clay as backfill and the extremely slow construction progress. The field technician considered the sand blanket to be a satisfactory "cushion" for the earth pressures imposed by the clay backfill. The contractor often abandoned the project for months at a time, thereby stalling the construction and study progress.

Analysis of Comparisons

Wall Proportions.- The wall proportions typically used in current design procedures are generally satisfactory, based on the stability of the test wall and cantilever walls in general. For clay foundation soils, a logical modification in current design procedures would involve sizing the footing width as a function of sliding stability instead of assuming a trial width, then correcting if necessary.

Geotechnical Properties.- This field study can be used as the basis for a rational design procedure for using clay as the backfill material. The unit weights of the backfill and foundation soil must be established. Also, the undrained shear strength of the foundation soil must be determined. These soil properties are typically required in current design procedures.

Gravity Forces.- The current procedure for calculating gravity

forces is satisfactory. A recommended modification is to include the weight of the key and the weight of the foundation soil above the bottom of the key with the gravity forces. In other words, the free body diagram should be extended to the base of the key, especially if lateral forces on the key are considered. Since no traffic loads were measured in the study, the equivalent surcharge currently used is assumed to be a satisfactory approximation.

Lateral Forces, Heel Side.- The uniform equivalent surcharge would cause a uniform lateral pressure as used in current design procedures. Compaction of the backfill in lifts causes large lateral pressures. The measured pressure distribution can be approximated as a trapezoid. For simplicity, the trapezoid can be broken down into a rectangle and a triangle, where the rectangular distribution can be conveniently described as that induced by compaction, and the triangular distribution as that due to lateral earth pressure. The measured uniform pressure was 2 psi (14 kpa). The measured coefficient of earth pressure on the heel side of the wall, K_h, was unity for a significant portion of the triangular pressure distribution. The resultant force of the trapezoidal pressure distribution, as described, overestimates the measured lateral force by 15 to 20%. The moment of the resultant force of the trapezoidal distribution is about 5% more than the moment of the measured resultant force. Therefore, the trapezoidal pressure distribution is reasonably accurate and conservative.

No pressure measurement was made on the heel side of the key, but it can be approximated as the product of K_h and the vertical

pressure at the middepth of the key. This is consistant with the measurement on the toe side of the key. The pressure distribution can be assumed to be uniform.

Lateral Forces, Toe Side.- TSDHPT design procedures assume these forces to be zero. The lateral pressure was measured at the face of the toe of the footing only. Assuming a trapezoidal pressure distribution as observed on the heel side, the earth pressure coefficient on the toe side, K_t, is 3.5 based on the measured pressure.

The measured lateral pressure on the toe side of the key corresponds to the product of the vertical pressure at the middepth of the key and an earth pressure coefficient of 2.5. The pressure distribution can be assumed to be uniform.

Footing Pressure.- The measured pressure distribution along the base of the footing varied approximately linearly as assumed in the conventional design. The significant difference is that the measured distribution is more nearly uniform. Measured toe and heel pressures are within 18% of a uniform pressure distribution. The TSDHPT design procedures yield toe and heel pressures 89% more and less than a uniform pressure. The resultant of the measured pressure distribution, V, is 13% less than the weight of the material above the footing, so can be conservatively taken to be equal.

Stability.- The stability against sliding is considered to be the most influential in proportioning the footing width for the conditions of the field study. The lateral forces on the heel side of the wall are likely to be overestimated, as described previously.

Settlement and bearing failures typically are not problems for

footings on preconsolidated clays.

Perhaps the most significant observation of the study is that the test wall is stable against overturning even though the conventional method of summing moments about the toe indicates that an unstable condition exists. This can be explained by evaluating the basic assumptions inherent with this method. The structure and the soil above the footing are assumed to rotate rigidly about the toe, much like tipping over a refrigerator about its edge. This analogy is not consistent with measured movements. The wall translated and rotated simultaneously until the backfilling was complete and then rotated slightly about the center of the base of the footing which indicates a point of rotation. Also, rotation about the toe assumes a loss of contact between the footing and the soil except at the toe. Rotation about the center of the footing and the measured pressure distribution indicate contact throughout the width of the footing. The resulting deformation in the foundation soil would be resisted by the shearing strength of the foundation soil which is interpretated as the component of stability that is neglected in current design procedures.

The resistance of the foundation soil to deform can be interpretated as a couple, equal and opposite vertical forces, applied at the heel and toe of the footing; therefore the moment arm is equal to the footing width. The couple would resist overturning and explain the nearly uniform pressure distribution observed on the base of the footing and wall stability.

The magnitude of the couple must be established. It is conceivable that rotation about the center of the base of the footing, as

observed, would develop a semicircular slip surface through the foundation soil with a radius of B/2. The resultant force along this slip surface, F, would be expressed as

$$F = \frac{\tau \pi B}{2} \quad \ldots\ldots\ldots\ldots\ldots\ldots\ldots\ldots\ldots\ldots\ldots\ldots \quad (16)$$

in which τ = the average shear stress along the slip surface required for equilibrium. The moment arm of F is B/2. These concepts are illustrated in Fig. 42.

Structural Design.- The structural components of the cantilever retaining wall should be designed based on the pressure distributions measured in the study. Wall proportions will be essentially unchanged, but significant reinforcing steel requirements are expected.

Drainage.- The effectiveness of the drainage system was not quantitatively evaluated. Water was often observed dripping from the weep holes and no significant change in total pressure was measured for a particular backfill height which indicates that hydrostatic pressures did not build up behind the wall.

Construction.- The use of clay backfill was accepted by the TSDHPT field technician, but not anticipated by the design engineer. This situation is likely to be common in practice. The construction delays were inexcusable. Action should be taken to ensure that it is not economically prudent to habitually exceed contract time schedules.

$$F = \tau \pi \frac{B}{2}$$

$$M_A = F\left(\frac{B}{2}\right) \text{ or } \frac{F}{2}\left(B\right)$$

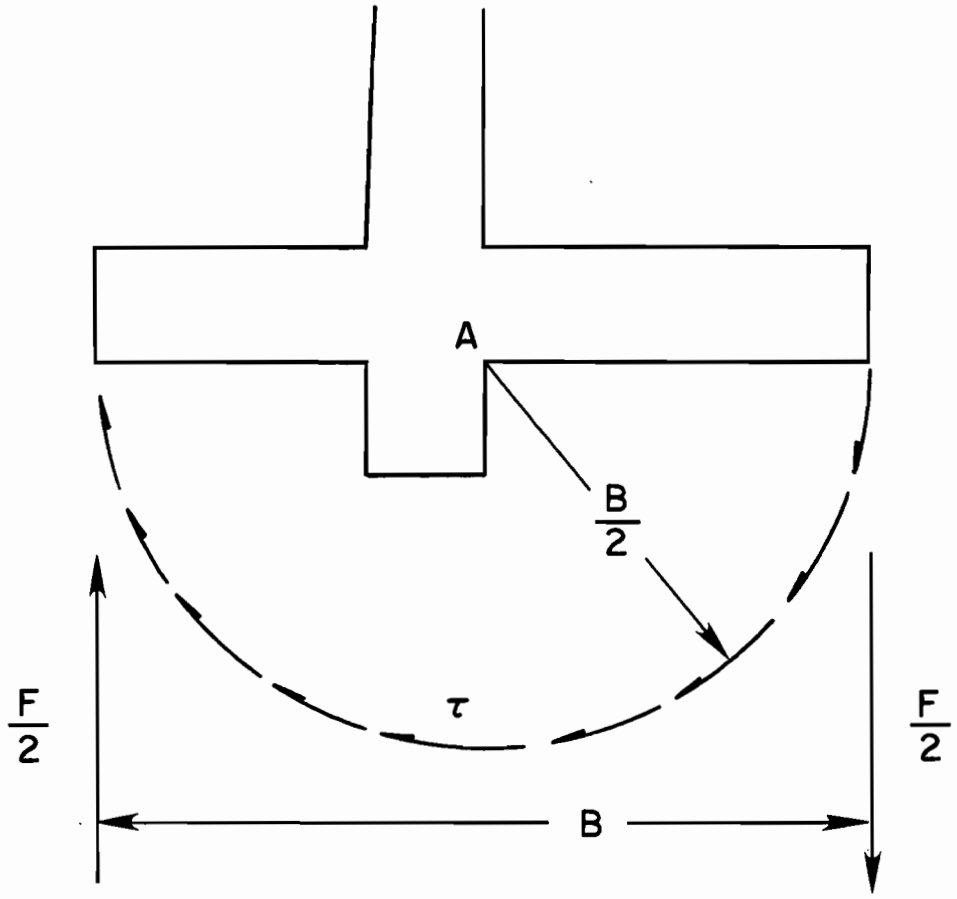

FIG. 42 - Foundation Soil Resistance to Deformation

PROPOSED DESIGN PROCEDURES

Application

The following design procedures are based on the results from this full scale field performance study of a typical cantilever retaining wall. The design procedures are a modification of the currently used procedures so that calculated values will correspond with those measured in this study.

In particular, the proposed design procedures will apply to cantilever walls founded on a preconsolidated clay with horizontal clay backfill. The concepts are general and can be extended to various soil conditions if appropriate adjustments are made based on current knowledge and further verification from field studies.

Wall Proportions

The proportions of the proposed wall section are given in Fig. 43 and much of the following discussion will relate to this figure. A cross section one unit wide is used in the proposed design procedure.

Wall Height.- The wall height is a function of the particular site requirements. The design height, H, is the vertical distance between the bottom of the footing and the top of the stem. The bottom of the footing on the toe side should have about 3 ft (0.91 m) of cover for protection (1), therefore, the total height of the wall is the sum of the required difference in elevation between the surfaces on the heel and toe sides and 3 ft (0.91 m). The proposed design is considered appropriate for design heights up to 20 ft (6.10 m).

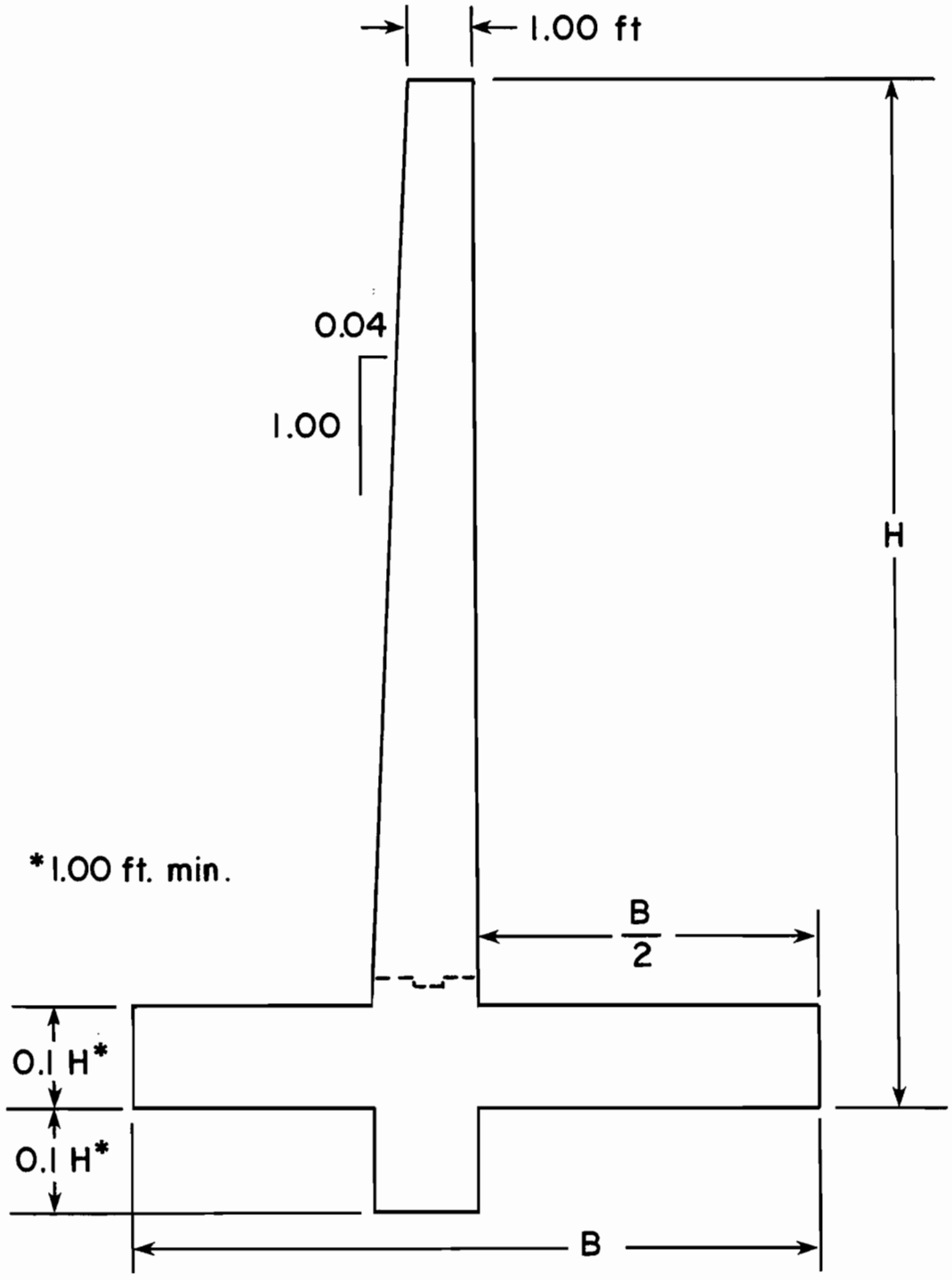

FIG. 43 - Proposed Wall Proportions
(1 ft = 0.305 m)

Stem.- The front face of the stem should be battered to give the illusion that the walls remain vertical after tilting. A satisfactory horizontal to vertical ratio is 0.04 to 1.00. The top of the stem should be 1.00 ft (0.305 m) wide to provide an adequate opening for placing concrete and cover for reinforcing steel.

Footing.- The footing should be attached to the stem such that the center of the footing coincides with the back face of the stem. The stem should be keyed into the footing. The trial thickness of the footing should be 0.1 H but not less than 1.00 ft (0.305 m). The footing width will be determined in the design procedures.

Key.- The key should be directly beneath the stem. This provides a convenient point for anchoring the stem reinforcing steel. The depth of the key should be about 0.1 H, but not less than 1.00 ft. (0.305 m). The width of the key should be approximately the width of the base of the stem. From a practical viewpoint, the width of the key will probably be the width of a backhoe bucket.

Geotechnical Properties

Foundation Soil.- The proposed design assumes the wall is founded on a deep preconsolidated clay deposit. This infers that settlement will be negligible if the applied footing stresses are lower than the preconsolidation pressure of the clay. This assumption can be verified by performing consolidation tests on the foundation soil and then computing the settlement based on predicted footing pressures. The undrained shear strength of the foundation clay should be obtained by appropriate laboratory or field testing for the short term stability analysis. The long term stability of the wall is a function of the

drained shear strength of the foundation soil which may be less than the undrained shear strength for stresses below the preconsolidation pressure. The drained shear strength of preconsolidated clays particularly applies to deep seated slope failures which is beyond the scope of the proposed design procedures, but this probably is not a significant problem based on the lack of such failures on TSDHPT projects. The total unit weight should also be determined accurately.

Backfill.- The total unit weight of the backfill soil is required. The use of clay backfill is consistent with the field study upon which the proposed design is based. Compaction below the maximum dry density should be specified. This reduces the lateral pressure induced by compaction and possible expansion of the clay. A blanket of granular material against the back face of the stem should be included for drainage. A granular backfill material should be used if available, and standard compaction should be specified.

Applied Forces

The retained soil may support structural loads which should be included in the design. Live loads, such as traffic, may be approximated by an equivalent uniform surcharge. Based on current practice, the equivalent surcharge can be considered as an additional height of backfill, H_S.

The free body diagram for the proposed design is given in Fig. 44. Much of the following discussion explains the details of this figure.

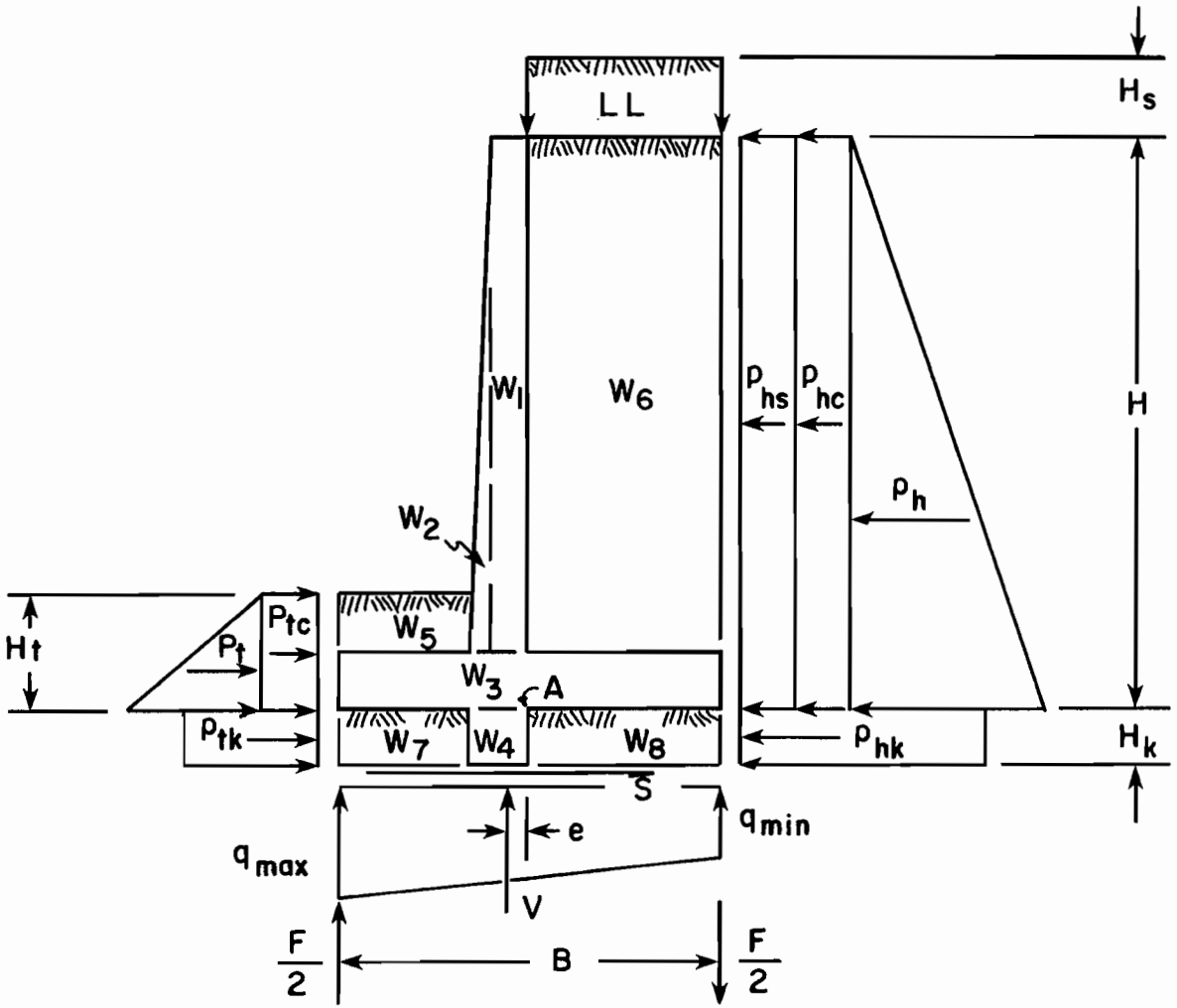

FIG. 44 - Free Body Diagram, Proposed Design

Horizontal Equilibrium

The retaining wall must be in horizontal equilibrium, so the horizontal forces must add to zero. The width of the footing is determined in this portion of the design procedure.

Lateral Forces, Heel Side.- The lateral forces on the heel side of the wall which must be evaluated are those induced by the live load surcharge, compaction, backfill along the design height and the foundation soil along the key. The lateral force due to the equivalent surcharge, P_{hs}, is obtained by

$$P_{hs} = K_h \gamma H_s H \quad \ldots \ldots \ldots \ldots \ldots \ldots \ldots \ldots \ldots \ldots \quad (17)$$

in which K_h = the coefficient of earth pressure on the heel side of the wall, γ = the unit weight of the backfill soil and H = the design height of the wall. K_h was measured to be 1.0 in this study. Field performance studies with granular backfill indicate K_h values equal to or greater than the at rest coefficient of earth pressure, K_o, (7,14,25). Recently published literature recommend the use of K_o in lateral earth pressure computations (1,4,10). A conservative alternative is to treat the structure as a nonyielding wall, since the current construction practice of backfilling and compacting in lifts tends to cancel the effect of wall movement (16). Earth pressure coefficients for nonyielding walls have been published for various types of soils and compaction methods (26). H_s is generally taken to be 2 ft (0.61 m)(19).

The lateral force due to compaction, as described previously, is

$$P_{hc} = CH \quad \ldots \quad (18)$$

in which C = the lateral earth pressure induced by compaction. C was measured to be about 0.288 ksf (13.8 kPa) in this study. A uniform lateral pressure due to compaction is proposed by Ingold (9) for cohesionless soils.

The lateral earth pressure on the design height causes a lateral force of

$$P_h = \frac{K_h \gamma H^2}{2} \quad \ldots \quad (19)$$

The terms in this equation have been described previously.

The lateral force on the key, P_{hk}, can be estimated by

$$P_{hk} = K_h \left[\gamma (H + H_s) + \frac{\gamma_{fnd} H_k}{2}\right] H_k \quad \ldots \quad (20)$$

in which H_k = the height of the key and γ_{fnd} = the unit weight of the foundation soil. This equation represents a uniform pressure distribution along the face of the key with a magnitude equal to the lateral pressure at the middepth of the key.

Lateral Force, Toe Side.- The lateral forces on the toe side of the wall are those induced by compaction, backfill above the base of the footing and foundation soil against the key. The lateral force due to compaction is obtained by

$$P_{tc} = CH_t \quad \ldots \quad (21)$$

in which H_t = the vertical distance from the base of the toe to the ground surface.

The lateral force due to the backfill on the front of the wall is

$$P_t = \frac{K_t \gamma H_t^2}{2} \quad \ldots \quad (22)$$

in which K_t = coefficient of earth pressure on the toe side of the wall. The value of K_t measured in this study is 3.5.

Based on the measurements of this study, the lateral force on the toe side of the key, P_{tk}, can be estimated as

$$P_{tk} = K_{tk} \left(\gamma H_t + \frac{\gamma_{fnd} H_k}{2}\right) H_k \quad \ldots \quad (23)$$

in which K_{tk} was measured to be 2.5. This equation is consistent with a uniform pressure distribution equal in magnitude to the lateral pressure at the middepth of the key.

Horizontal Shear.- Horizontal equilibrium is achieved by the shear force which is developed in the foundation soil. Consider that the shear force, S, acts horizontally at the base of the key. For equilibrium

$$S = P_{hs} + P_{hc} + P_h + P_{hk} - P_{tc} - P_t - P_{tk} \quad \ldots \quad (24)$$

The shear force, S, has previously been defined as the product of the undrained shear strength of the foundation soil and the length of the slip surface, Eq. 14. Therefore, the retaining wall will be in horizontal equilibrium if the length of the slip surface and shear strength of the foundation soil are sufficiently large.

Footing Width.- From Fig. 44, it can be seen that the length of the slip surface corresponds to the footing width, B. It is desirable to have the potential of developing a horizontal shear force that exceeds the value of S necessary for equilibrium. This is accomplished by using a design value, S_d, 1.5 times greater than S, needed for equilibrium, which expressed in equation form is

$$S_d = 1.5\ S \quad \ldots\ldots\ldots\ldots\ldots\ldots\ldots\ldots \quad (25)$$

The footing width can then be computed as

$$B = \frac{S_d}{c_u} \quad \ldots\ldots\ldots\ldots\ldots\ldots\ldots\ldots \quad (26)$$

The computed value of B should be rounded up to the nearest integral foot for simplicity in construction and to ensure an adequate horizontal slip surface length.

Stability Against Sliding.- The safety factor against sliding, SF_s, in terms of horizontal shear forces is

$$SF_s = \frac{c_u B}{S} \quad \ldots\ldots\ldots\ldots\ldots\ldots\ldots\ldots \quad (27)$$

By design procedure, this ratio will exceed 1.5. It should be emphasized that the proposed design procedure is not based on limit equilibrium, i.e., the lateral forces predicted do not correspond to failure conditions, but maximum values observed in a field performance study. It is probable that at failure conditions the lateral forces on the toe side of the wall would be greater than those predicted and the lateral forces on the heel side would be less than those predicted. The safety factor obtained from Eq. 27 expresses quantitatively an assurance that the equilibrium shear stress in the foundation soil (τ) is less than the shear strength of the soil, c_u.

Vertical Equilibrium

The vertical forces on the wall must equal zero for vertical equilibrium. The stability against bearing failure is obtained in this portion of the design procedure.

Gravity Forces.- The weights of the material above the bottom of the key and the live load surcharge as shown in Fig. 44 must be obtained. The weight structure, W_c, is obtained by

$$W_c = \gamma_{con}(A_1 + A_2 + A_3 + A_4) \quad \text{. (28)}$$

in which γ_{con} = the unit weight of concrete and A_1 through A_4 = the area per unit width of each of the components of the wall section.

The weight of the backfill, W_{bkf} is

$$W_{bkf} = \gamma(A_5 + A_6) \quad \text{. . . . . (29)}$$

and the weight of the foundation soil, W_{fnd}, is

$$W_{fnd} = \gamma_{fnd}(A_7 + A_8) \quad \ldots \quad (30)$$

in which A_5 through A_8 = the area per unit width of the appropriate soil component.

The weight of the equivalent surcharge, LL, is

$$LL = \frac{\gamma H_s B}{2} \quad \ldots \quad (31)$$

The terms in this equation have been defined previously.

The weights of each of the components of W_c, W_{bkf} and W_{fnd} should be computed and tabulated separately because the moment of each gravity force will be needed in subsequent computations. The total downward vertical force, W, is

$$W = W_1 + W_2 + W_3 + W_4 + W_5 + W_6 + W_7 + W_8 + LL \quad \ldots \quad (32)$$

Forces on Base of Footing.- The forces acting on the base of the footing include the reaction to the gravity forces, V, and the forces which form the couple developed by the foundation soil. For vertical force equilibrium, V is equal in magnitude to the total gravity force, W, so

$$V = W \quad \ldots \quad (33)$$

The forces forming the couple, F/2, are equal and opposite so do not enter into the computations involving vertical force equilibrium.

Footing Pressure.- Based on the results of this study, the pressure distribution will decrease linearly from a maximum value, q_{max}, at the toe to a minimum value, q_{min}, at the heel. The maximum and minimum footing pressures are

$$q_{max} = \frac{1.18V}{B} \text{ and } q_{min} \frac{0.82V}{B} \quad \ldots\ldots\ldots\ldots\ldots\ldots \quad (34)$$

Stability Against Bearing Failure.- The maximum footing pressure should not exceed the ultimate bearing capacity, q_{ult}, of the foundation soil. For clays, q_{ult} can be conservatively estimated using Eq. 15 and repeated here as

$$q_{ult} = 5.14\, c_u \quad \ldots\ldots\ldots\ldots\ldots\ldots\ldots\ldots \quad (15)$$

The safety factor against bearing failure SF_b is

$$SF_b = \frac{q_{ult}}{q_{max}} \quad \ldots\ldots\ldots\ldots\ldots\ldots\ldots\ldots \quad (35)$$

A safety factor of 3 is recommended. Excessive settlement is not likely if the maximum footing pressure is less than the preconsolidation pressure of the foundation soil.

Moment Equilibrium

The moments of the forces acting on the free body diagram must equal zero for moment equilibrium. The moment arm of each of the

forces and the magnitude of the shear force F must be determined. The stability against overturning is determined in this part of the design procedure.

Moment Center.- The study results indicate that point A in Fig. 44 is near the center of rotation. This establishes a logical point about which moments can be summed.

Moment Arms.- The forces previously computed pass through the centroid of the corresponding area of the pressure distribution diagram. The determination of the moment arm for those forces which have a rectangular or triangular pressure distribution is straightforward. The moment arm for V is the eccentricity, e, which is computed as

$$e = x - \frac{B}{2} \quad \ldots\ldots\ldots\ldots\ldots\ldots\ldots\ldots\ldots\ldots \quad (36)$$

where x is the distance from the heel of the footing to the point of application of V. This is the position of the centroid of the footing pressure distribution which is computed as follows:

$$x = \frac{q_{min}(\frac{B^2}{2}) + (q_{max} - q_{min})(\frac{B^2}{3})}{V} \quad \ldots\ldots\ldots\ldots\ldots\ldots \quad (37)$$

Couple Developed by Foundation Soil.- Rotation of the wall about the center of the base of the footing is resisted by the shear strength of the foundation soil. The couple developed in the foundation is equal to the moment of the shear force, F, which acts on a semicircular slip surface with radius B/2 (see Fig. 42). F was

previously defined by Eq. 16, and is repeated here for convenience

$$F = \frac{\tau \pi B}{2} \quad \ldots\ldots\ldots\ldots\ldots\ldots\ldots\ldots\ldots\ldots \quad (16)$$

in which τ = the average shear stress on the semicircular slip surface necessary to maintain moment equilibrium. The magnitude of τ is unknown, but can be determined by summing moments about point A.

Moments.- The moments of the forces can be summed for those that resist overturning, M_r, and those that cause overturning, M_o. If an equation is written for moment equilibrium ($M_r = M_o$), the only unknown will be the magnitude of τ.

Stability Against Overturning.- The wall is stable against overturning if τ is less than c_u. The safety factor against overturning, SF_o, is expressed as

$$SF_o = \frac{c_u}{\tau} \quad \ldots\ldots\ldots\ldots\ldots\ldots\ldots\ldots\ldots\ldots \quad (38)$$

A safety factor of 2 is recommended.

Structural Design

The structural design of the cantilever wall should be performed after a footing width has been determined which meets the required safety factors for sliding, bearing failure and overturning. The structural components are loaded with the pressure distributions presented previously. Some modification of the wall proportions may be indicated, such as the thickness of the footing.

Drainage

Drainage must be provided by any of the conventional methods. If a sand blanket is used, a suggested minimum width is 2 ft (0.61 m) with weep holes at 5 ft (1.5 m) intervals.

Construction

The performance of the wall should be monitored during construction. The minimum compaction necessary to reduce settlement and develop the required strength of clay backfill should be specified. Lateral pressures in excess of those predicted by the proposed design could occur if standard compaction specifications are required because increased compactive effort will induce larger lateral compaction pressures and expansion pressures in clay backfill. The proposed lateral pressure computations are probably appropriate for granular backfills if standard compaction specifications are followed.

Example Design Problem

The preceding procedure is illustrated in the following example problem. Consider that an earth retaining structure is required to separate horizontal surfaces by a vertical distance of 12 ft (3.66 m).

Wall Proportions

Dimensions: Refer to Fig. 43.

Design Height, $H = 12.0 + 3.0 = 15.0$ ft

Footing and Key Height, $H_k = 0.1(15.0) = 1.50$ ft

Stem Base and Key Width = $0.04(15.0-1.50) + 1.00 = 1.54$ ft

Geotechnical Properties

Foundation Soil:

Shear Strength, $c_u = 3$ ksf

Unit Weight, $\gamma_{fnd} = 0.125$ kcf

Backfill and Blanket Drain:

Unit Weight, $\gamma = 0.120$ kcf

Applied Forces

Equivalent Surcharge:

Surcharge Height, $H_s = 2.0$ ft

Horizontal Equilibrium

Lateral Forces, Heel Side: Refer to Fig. 44.

Surcharge, $P_{hs} = 1.0(0.120)(2.0)(15.0) = 3.60$ (17)

Compaction, $P_{hc} = 0.288(15) = 4.32$ (18)

Earth Pressure, $P_h = \frac{1.0(0.120)(15.0)^2}{2} = 13.50$ (19)

Key, $P_{hk} = 1.0\ [0.120(15.0+2.0) + 0.125(\frac{1.50}{2})]\ (1.50) = 3.20$ (20)

Summation, $P_{hs} + P_{hc} + P_h + P_{hk} = 24.62$ kip/ft

Lateral Forces, Toe Side: Refer to Fig. 44

Compaction, $P_{tc} = 0.288(3.0) = 0.86$ (21)

Earth Pressure, $P_t = \frac{3.5(0.120)(3.0)^2}{2} = 1.89$ (22)

Key, $P_{tk} = 2.5\ [0.120(3.0)+0.125\ (\frac{1.50}{2})]\ (1.50) = 1.70$ (23)

Summation, $P_{tc} + P_t + P_{tk} = 4.45$ kip/ft

Horizontal Equilibrium (Con't)

Horizontal Shear:

$$\text{Equilibrium Shear, } S = 24.62 - 4.45 = 20.17 \text{ kip/ft} \quad (24)$$

Footing Width:

$$\text{Design Shear, } S_d = 1.5(20.17) = 30.26 \text{ kip/ft} \quad (25)$$

$$\text{Footing Width, } B = \frac{30.26}{3} = 10.09 \text{ ft} \quad (26)$$

Let B = 11.00 ft

Stability Against Sliding:

$$\text{Safety Factor, } SF_s = \frac{3.0(11.00)}{20.17} = 1.6 > 1.5 \quad (27)$$

Vertical Equilibrium

Gravity Forces: Refer to Figs. 43 and 44.

$W_1 = 0.150(13.5)(1.00) = 2.03$

$W_2 = \frac{0.150(0.54)(13.5)}{2} = 0.55$

W_c, (28)

$W_3 = 0.150(11.00)(1.50) = 2.48$

$W_4 = 0.150(1.50)(1.54) = 0.35$

$W_5 = 0.120(3.96)(1.5) = 0.71$

W_{bkf}, (29)

$W_6 = 0.120(13.5)(\frac{11.00}{2}) = 8.91$

$W_7 = 0.125(3.96)(1.50) = 0.74$

W_{fnd}, (30)

$W_8 = 0.125(\frac{11.00}{2})(1.50) = 1.03$

Surcharge, $LL = 0.120(2.0)(\frac{11.00}{2}) = 1.32$ (31)

Summation, $W = W_c + W_{bk} + W_{fnd} + LL = 18.12$ kip/ft (32)

Vertical Equilibrium (Con't)

Forces on Base of Footing:

Resultant, $V = W = 18.12$ kip/ft (33)

Couple Forces, $\frac{F}{2}$ are equal and opposite

$$F = \tau\pi \left(\frac{11.00}{2}\right) = 17.28\tau \text{ ft}$$

Footing Pressure:

Toe Pressure, $q_{max} = \frac{1.18(18.12)}{11.00} = 1.94$ ksf

(34)

Heel Pressure, $q_{min} = \frac{0.82(18.12)}{11.00} = 1.35$ ksf

Stability Against Bearing Failure:

Bearing Capacity, $q_{ult} = 5.14(3.0) = 15.42$ ksf (15)

Safety Factor, $SF_b = \frac{15.42}{1.94} = 7.95 > 3.0$ (35)

Moment Equilibrium

Moment Center:

Center of Base of Footing, point A Fig. 44.

Moment Arms: Refer to Fig. 44.

Point A to Centroids of Pressure Distributions

$$e = \frac{\frac{(1.35)(11.0)^2}{2} + \frac{(0.59)(11.0)^2}{3}}{18.12} - \frac{11.00}{2} = 0.32 \text{ ft} \qquad (36)$$

Moments that Resist Overturning, M_r:

P_{hk}, $3.20\ (\frac{1.50}{2})$ = 2.40

P_{tc}, $0.86\ (\frac{1.5}{2})$ = 0.65

P_t, $1.89\ (\frac{3.0}{3})$ = 1.89

W_3, $2.48\ (0)$ = 0

W_6, $8.91\ (\frac{5.50}{2})$ = 24.50

W_8, $1.03\ (\frac{5.50}{2})$ = 2.83

LL, $1.32\ (\frac{5.50}{2})$ = 3.63

V, $18.12(0.32)$ = 5.80

$\frac{F}{2}$, $(\frac{17.28\,\tau}{2})(11.00)$ = 95.04

Summation, $M_r = 41.70\ \frac{\text{kip}\cdot\text{ft}}{\text{ft}} + 95.04\,\tau\ \text{ft}$

Moment Equilibrium (Con't)

Moments that Cause Overturning, M_o:

P_{hs}, $3.60\ (\frac{15.0}{2})$ $= 27.00$

P_{hc}, $4.32\ (\frac{15.0}{2})$ $= 32.40$

P_h, $13.50\ (\frac{15.0}{3})$ $= 67.50$

P_{tk}, $1.70\ (\frac{1.50}{2})$ $= 1.28$

S, $20.17\ (1.50)$ $= 30.26$

W_1, $2.03\ (\frac{1.00}{2})$ $= 1.02$

W_2, $0.55\ (1+\frac{0.54}{3})$ $= 0.65$

W_4, $0.35\ (\frac{1.54}{2})$ $= 0.27$

W_5, $0.71\ (1.54+\frac{3.96}{2})$ $= 2.50$

W_7, $0.74\ (1.54+\frac{3.96}{2})$ $= 2.60$

Summation, $M_o = 165.48\ \frac{kip \cdot ft}{ft}$

$M_r = M_o$

$41.70 + 95.04\tau = 165.48$

Equilibrium Shear Stress, $\tau = \frac{165.48-41.70}{95.04} = 1.30$ ksf

Stability Against Overturning:

Safety Factor, $SF_o = \frac{3.00}{1.30} = 2.31 > 2$ (38)

CONCLUSIONS AND RECOMMENDATIONS

The basic objective of this study has been met. Indicated modifications in current design procedures have been proposed based on the field performance study.

Conclusions

Measurements.- The basic measurements performed included earth pressures, wall movement, backfill soil profiles and geotechnical properties. Conclusions concerning these measurements are discussed below.

The earth pressure cells used in this study had a preload reading different from zero which was found to vary with temperature for both field and laboratory conditions. The accuracy of the measured earth pressures was primarily dependent upon the predicted preload pressures. After accounting for the temperature-induced preload variation, the net earth pressure is found to be relatively constant at a particular backfill height and cell location.

The pressure cells were backflushed if no response to normal cell reading procedures was observed. The effect of backflushing on cell readings could not be definitely established.

The wall movement measurement systems yielded satisfactory results. Construction procedures prevented horizontal and vertical movement measurements from being made until a portion of the backfill had been placed, so the reported movements are probably less than those which actually occurred. The tilt measurements probably represent actual movements because the initial measurements were made when the

toe extension was covered and no backfill had been placed on the heel extension.

Backfill soil profiles were established at each observed change in backfill height. The geotechnical properties of the backfill and foundation soil were obtained from laboratory testing and supplemented with data from TSDHPT soil reports and from the project inspector. These parameters were established to the normal standard of care and accuracy.

Results.- The measured earth pressures on the heel side of the test wall were greater than those predicted by current design procedures. This phenomenon was attributed to the construction practice of compacting the backfill in relatively thin lifts. A lateral earth pressure of 2 psi (14 kPa) was observed at the backfill surface and the lateral pressure increased linearly with depth to about the natural ground surface, then decreased from natural grade down to the heel. The proposed design procedure considers a uniform pressure distribution and a triangular distribution that increases linearly from the ground surface to the base of the footing. This should conservatively overestimate the lateral pressure on the heel side of the retaining wall. The proposed uniform pressure is 2 psi (14 kPa) and the earth pressure coefficient is unity; both are probably related to compactive effort.

The measured lateral pressure on the toe was about 3.5 times greater than the pressure measured on the heel side of the stem at the same depth. This indicates that a significant contribution to stability is potentially available if the toe side is backfilled prior

to backfilling the heel side of the wall. Therefore, this procedure should be required and verified by field inspection.

The key contributed to the stability of the wall; it undoubtedly affected the performance of the test wall, and therefore the proposed design parameters. Use of the proposed design procedures should predict the wall behavior more accurately if a key is included.

The measured earth pressures along the base of the footing were more uniform than would be expected from current design procedures. This is attributed to the foundation soil resistance to deformation. This contribution to stability has previously been omitted but should be considered in future designs, as proposed.

The total horizontal movement of the midpoint of the stem was about 0.007H which exceeds published movements necessary to develop the active state of stress (26). This was not observed and is explained in terms of current construction practice. The net movement of the stem at any vertical position is that which occurs after the backfill is above that position. In other words, the net movement is zero at the backfill surface, therefore the net movement is much less than the total movement. The earth pressures may reduce to the active state if sufficient movement can occur after construction is complete. The wall must be stable during construction so the at rest movement and earth pressure conditions are more applicable than active stress conditions. The vertical movement (settlement) and tilt were relatively small in magnitude as expected for the stiff preconsolidated foundation soil.

The lateral earth pressures were found to be directly proportional

to the unit weight and height of the backfill. The undrained shear strength of the foundation soil was used in the proposed design because it is the appropriate strength parameter during construction and generally is conservative.

Recommendations

Measurements.- The earth pressures should be measured with two methods or types of pressure sensors in order to verify results. Unanticipated problems would not be as likely to influence both types of pressure sensors, or at least to the same degree. Laboratory calibrations should be performed to determine the accuracy and response of each cell under the environmental conditions the pressure sensors will experience. The effects of backflushing should be investigated. Temperature sensors should be installed adjacent to pressure sensors that are found to be temperature dependent. Field calibrations should be performed for those factors found to be significant in the laboratory.

A more complete set of data would be obtained if the pressure sensors are placed along cross sections near the ends of the test panel as well as a section along the center line. Sensors should also be placed on the top of the footing, front face of the stem and on the bottom and back face of the key, in order to obtain a more complete pressure distribution on all bearing surfaces.

The wall movement should be measured at the cross sections where the pressure sensors are located. Direct translation measurements should be made from points near the top and bottom of the stem at each location. Vertical movements should be measured on the stem and near

the toe of the footing. Pads attached to the front face of the stem for tilt measurements should be made of stainless steel. Corrosion and distortion of the pads will be minimized because of the corrosion resistance of this material and because the thermal properties of steel and concrete are almost identical.

The geotechnical properties of the foundation soil and backfill must be obtained. The backfill heights should be measured when changes occur.

Construction Control.- The successful completion of a field performance study will be enhanced if the researchers have some control over the construction procedures. The project specifications should include penalties if the construction is not completed before the study terminates, if the construction procedures prohibit instrumentation installation and calibration, or if the instrumentation is damaged.

Additional Studies.- The proposed design modifications are based on a single field performance study. The accuracy of the proposed parameters can be improved by additional studies on walls with similar proportions and soil conditions. The general application of the proposed design procedures should be based on studies of walls with different proportions and various foundation soils and types of backfill.

APPENDIX I. - REFERENCES

1. Bowles, J. E., Foundation Analysis and Design, 2nd. ed., McGraw-Hill Book Co., New York, 1977, pp. 321-333, 374-375, 377-405.

2. Broms, B., "Lateral Earth Pressures Due to Compaction of Cohesionless Soil," Proceedings, Fourth Budapest Conference on Soil Mechanics, Budapest, Hungary, 1971, pp. 373-384.

3. Carder, D. R., Pocock, R. G., and Murray, R. T., "Experimental Retaining Wall Facility - Lateral Stress Measurements with Sand Backfill," Report 766 Transportation and Road Research Laboratory, Crowthorne, England, 1977, pp. 1-8.

4. Casagrande, L., "Comments on Conventional Design of Retaining Structures," Journal of the Soil Mechanics and Foundations Division, ASCE, Vol 99, No. SM2, Proc. Paper 9568, February, 1973, pp. 181-198.

5. Corbett, D. A., Coyle, H. M., Bartoskewitz, R. E., and Milberger, L. J., "Evaluation of Pressure Cells for Field Measurements of Lateral Earth Pressures on Retaining Walls," Research Report No. 169-1, Texas Transportation Institute, Texas A&M University, September, 1971.

6. Coyle, H. M., Bartoskewitz, R. E., and Milberger, L. J., "Field Measurements of Lateral Earth Pressures on a Cantilever Retaining Wall," Research Report No. 169-2, Texas Transportation Institute, Texas A&M University, September 1972.

7. Felio, G., "Monitoring of a Bridge Abutment Founded on a Granular Compacted Fill," thesis presented to Carleton University, at Ottawa, Canada, in 1980, in partial fulfillment of the requirements for the degree of Master of Engineering, pp. 241-251,277-343.

8. Huntington, W. C., Earth Pressures and Retaining Walls, John Wiley and Sons, Inc., New York, 1957, pp. 1-7, 53-73, 139-142, 218-234, 283-290, 294-300, 314-320, 385, 390-393, 406-409.

9. Ingold, T. S., "Retaining Wall Performance During Backfilling," Journal of the Geotechnical Division, ASCE, Vol. 105, No. GT5, Proc. Paper 14580, May, 1979, pp. 613-626.

10. McCarthy, D. F., Essentials of Soil Mechanics and Foundations, 2nd. ed., Reston Publishing Company, Inc., Reston, Virginia, 1982, pp. 507-519.

11. Peck, R. B., Hanson, W. E., and Thornburn, T. H., Foundation Engineering, 2nd. ed., John Wiley and Sons, Inc., New York, 1974, pp. 415-428.

12. Prescott, D. M., Coyle, H. M., and Bartoskewitz, R. E., "Field Measurements of Lateral Earth Pressures on a Pre-Cast Panel Retaining Wall," Research Report No. 169-3, Texas Transportation Institute, Texas A&M University, September, 1973.

13. Prikryl, W., "Measurements of Earth Pressures for the Design Modification of Cantilever Retaining Walls," thesis presented to Texas A&M University, at College Station, Texas, in 1979, in partial fulfillment of the requirements for the degree of Master of Science.

14. Schulze, L. W., Coyle, H. M., and Bartoskewitz, R. E., "Field Measurements of Earth Pressure on a Cantilever Retaining Wall," Research Report No. 236-1, Texas Transportation Institute, Texas A&M Unversity, January, 1981.

15. Sims, F. A., Forrester, G. R., and Jones, C. J. F., "Lateral Earth Pressures on Retaining Walls," Journal of the Institution of Highway Engineers, England, Vol. 17, No. 6, June, 1970, pp. 1930.

16. Sims, F. A., and Jones, C. J. F., "Comparison between Theoretical and Measured Earth Pressures Acting on a Large Motorway Retaining Wall," Journal of the Institute of Highway Engineers, England, Vol. 21, No. 12, December, 1974, pp. 26-29.

17. Sowers, G. F., Robb, A. D., Mullis, C. H., and Glenn, A. J., "The residual Latral Earth Pressures Produced by Compacting Soils," Proceedings, Fourth International Conference on Soil Mechanics and Foundations Engineering, Rotterdam, Vol. 3, 1957, pp. 243-247.

18. Stiles, J. W., "Practical Aspects of Cantilever Retaining Wall Design," Highway Research Record No. 302, Washington, D. C., 1970, pp. 87-88.

19. Teng, W. C., Foundation Design, Prentice-Hall, Inc., Englewood Cliffs, New Jersey, 1962, pp. 337-341.

20. Terzaghi, K., "Old Earth Pressure Theories and New Test Results," Engineering News Record, Vol. 85, No. 14, September, 1920, pp. 632-637.

21. Terzaghi, K., "Large Retaining Wall Tests, Part 1," Engineering News Record, Vol. 112, February, 1934, pp. 136-140.

22. Terzaghi, K., "A Fundamental Fallacy in Earth Pressure Computations," Journal of the Boston Society of Civil Engineers, April, 1936, pp. 71-88.

23. Terzaghi, K., and Peck, R. B., Soil Mechanics in Engineering Practice, 2nd. ed., John Wiley and Sons, Inc., New York, 1967, pp. 219, 361-378.

24. Weiler, W. A., Jr., and Kulhawy, F. H., "Factors Affecting Stress Cell Measurements in Soil," Journal of the Geotechnical Division, ASCE, Vol. 108, No. GT12, Proc. Paper 17558, December, 1982, pp. 1529-1548.

25. Wright, W. V., Coyle, H. M., and Bartoskewitz, R. E., "New Retaining Wall Design Criteria Based on Lateral Earth Pressure Measurements." Research Report No. 169-4F, Texas Transportation Institute, Texas A&M University, August, 1975.

26. Wu, T. H., "Retaining Walls," Foundation Engineering Handbook, Winterkorn, H. F., Fang, H. Y., editors, Van Nostrand Reinhold Company, New York, 1975, pp. 402-417.

APPENDIX II. - NOTATION

The following symbols are used in this paper:

A_n = area per unit width of component, n, n = 1, 2, . .;

A, B, C, D, E, = stainless steel pads;

A_i, B_i, C_i, D_i, E_i = subsequent plumb line reading on pad;

A_o, B_o, C_o, D_o, E_o = original plumb line reading on pad;

B = footing width;

C = uniform lateral pressure attributed to compaction;

c_u = undrained shear strength;

e = eccentricity;

F = resultant shear force on semicircle slip surface;

H = design height;

H_a = vertical distance from ground surface to base of footing for active stress conditions;

H_k = height of key;

H_p = vertical distance from ground surface to base of footing for passive stress conditions;

H_s = height of equivalent live load surcharge;

H_t = vertical distance from ground surface to base of footing, toe side of wall;

K_a = coefficient of earth pressure, active state of stress;

K_h = coefficient of earth pressure, heel side of wall;

K_{hk} = coefficient of earth pressure, heel side of key;

K_o = coefficient of earth pressure, at rest state of stress;

K_p = coefficient of earth pressure, passive state of stress;

K_t = coefficient of earth pressure, toe side of wall;

K_{tk} = coefficient of earth pressure, toe side of key;

L = length of slip surface below footing;

LL = gravity force due to uniform live load surcharge;

M_o = sum of moments that cause overturning;

M_r = sum of moments that resist overturning;

P_a = lateral force due to active earth pressure;

P_h = lateral force attributed to earth pressure, heel side;

P_{hc} = lateral force attributed to compaction, heel side;

P_{hk} = lateral force, heel side of key;

P_{hs} = lateral force due to live load surcharge;

P_p = lateral force due to passive state of stress;

P_t = lateral force attributed to earth pressure, toe side;

P_{tc} = lateral force attributed to compaction, toe side;

P_{tk} = lateral force, toe side of key;

p_e = total earth pressure;

p_i = pressure cell reading;

p_o = preload cell reading;

q_{max} = maximum pressure on footing base;

q_{min} = minimum pressure on footing base;

q_{ult} = bearing capacity of foundation soil;

R = resultant force on Coulomb/Rankine failure surface;

R_E = radial distance from bracket to pad E;

S = shear force required for horizontal equilibrium;

S_d = shear force for design;

SF_b = safety factor against bearing failure;

SF_o = safety factor against overturning;

SF_s = safety factor against sliding;

V = vertical force required for equilibrium;

W = sum of gravity forces;

W_{con} = weight of retaining wall;

W_{bkf} = weight of backfill above footing;

W_{fnd} = weight of foundation soil below footing;

W_n = weight of component n, n = 1, 2, 3, . . .;

W_w = weight of soil in assumed failure wedge;

W_I = weight of soil between vertical plane and back face of wall, Rankine theory;

x = distance from heel to point of application of V;

α = angle at base of stem between horizontal and the backface of stem;

β = angle between horizontal and backfill surface;

γ = unit weight of backfill;

γ_{con} = unit weight of concrete;

γ_e = unit weight of equivalent fluid;

γ_{fnd} = unit weight of foundation soil;

ΔA, ΔB, ΔC, ΔD, ΔE, = horizontal movement of pads;

$\Delta P.L.$ = horizontal movement of plumb line;

ΔRdg_E = change in plumb line reading at Pad E;

δ = wall friction angle;

θ = tilt angle;

τ = shear stress on semicircular slip surface required for moment equilibrium;

ϕ = angle of shear resistance; and

ψ = wall friction angle, Rankine condition.

APPENDIX III. - EARTH PRESSURE DETERMINATION

The total earth pressure, p_e, is determined by subtracting the preload pressure, p_o, from the field pressure cell reading p_i, as described in the text. It was observed that the preload pressures and the field pressure cell readings varied with temperature. The temperature response of each cell was obtained by regression analysis of the ten direct temperature-field pressure cell readings for each cell obtained between February and October of 1981 as shown in Figs. 29 through 34 when there was little change in the backfill profile. The average R-square value was 0.97 for the temperature and field pressure cell reading relationships. A similar temperature response was assumed to exist for the preload pressures of each cell. This assumption has been verified by studies recently reported in the literature (7, 24). An equation for predicting the preload pressure as a function of temperature was derived for each cell based on the regression analysis, measured preload pressures, and measured or predicted temperatures that correspond to preload pressure readings. These equations along with the pertinent field study data and computed pressures are presented in Table III.1 through Table III.11. The date, elapsed time and field cell readings are tabulated in the first three columns for each cell that functioned throughout the duration of the study. The temperatures prior to September of 1980 were computed as described in the text. Since September of 1980, direct temperatures were measured adjacent to Cells 930, 928, 927, 921 and 924 (see Fig. 13) by thermocouples. An additional theremocouple was installed adjacent to Cell 935 on June 10,

1981 so direct temperature measurements were obtained since that date. Temperatures at the remainder of the footing cells; 926, 936, 938, 922 and 937 (see Fig. 13) were obtained by interpolation. The tabulated preload pressures were obtained by solving the equation given in the table title. Note that some computed preload values are negative, but the corresponding earth pressure is consistent with those with the same backfill profile.

TABLE III.1 - Cell 930, $p_o = -8.68 + 0.2027T$

($^oC = 0.56(^oF-32)$, 1 psi = 689 kPa)

Date	Time Days	Cell Reading p_i, psi	Temperature, ^oF	Preload p_o, psi	Earth Pressure p_e, psi
20 Nov 79	0	NA	NA	NA	NA
9 Jan 80	50	NA	NA	NA	NA
7 Mar	108	7.9	82	7.9	0.0
1 Apr	133	9.5	92	10.0	- 0.5
22 Apr	154	11.0	97	11.0	0.0
4 Jun	197	13.0	105	12.6	+ 0.4
16 Jun	209	11.2	97	11.0	+ 0.2
16 Jun	209	12.5	*	*	*
9 Jul	232	14.2	112	14.0	+ 0.2
29 Jul	252	11.7	101	11.8	- 0.1
8 Aug	262	12.6	106	12.8	- 0.2
20 Aug	274	12.9	106	12.8	+ 0.1
26 Aug	280	12.5	104	12.4	+ 0.1
18 Sep	303	12.4	104	12.4	0.0
6 Nov	352	8.0	74	6,3	+ 1.7
11 Nov	357	8.3	78	7.1	+ 1.2
7 Jan 81	414	4.0	51	1.7	+ 2.3
12 Feb	450	1.5	39	- 0.8	+ 2.3

* Unknown

TABLE III.1 - Continued

Date	Time Days	Cell Reading p_i, psi	Temperature, ^oF	Preload p_o, psi	Earth Pressure p_e, psi
12 Mar 81	478	5.6	62	3.9	+ 1.7
20 May	547	8.0	71	5.7	+ 2.3
2 Jun	560	10.0	82	7.9	+ 2.1
10 Jun	568	11.4	90	9.6	+ 1.8
30 Jun	588	10.4	85	8.5	+ 1.9
9 Jul	597	10.7	86	8.8	+ 1.9
23 Jul	611	12.5	93	10.2	+ 2.3
10 Sep	660	11.0	85	8.5	+ 2.5
1 Oct	681	11.5	88	9.2	+ 2.3
29 Oct	709	6.8	66	4.7	+ 2.1
6 Jan 82	778	7.5	64	4.3	+ 3.2
4 Mar	835	8.4	63	4.1	+ 4.3
15 Apr	877	11.0	74	6.3	+ 4.7
26 May	918	12.9	82	7.9	+ 5.0
10 Jun	933	14.5	90	9.6	+ 4.9
7 Jul	960	14.8	90	9.6	+ 5.2

TABLE III.2 - Cell 928, $p_o = -16.45 + 0.2697\ T$

($^oC = 0.56(^oF-32)$, 1 psi = 6.89 kPa)

Date	Time Days	Cell Reading p_i, psi	Temperature, ^oF	Preload p_o, psi	Earth Pressure p_e, psi
20 Nov 79	0	NA	NA	NA	NA
9 Jan 80	50	NA	NA	NA	NA
7 Mar	108	5.7	82	5.7	0.0
1 Apr	133	8.1	92	8.4	- 0.3
22 Apr	154	9.8	97	9.7	+ 0.1
4 Jun	197	11.8	105	11.9	- 0.1
16 Jun	209	9.5	97	9.7	- 0.2
16 Jun	209	17.7	*	*	*
9 Jul	232	14.0	112	13.8	+ 0.2
29 Jul	252	10.9	101	10.8	+ 0.1
8 Aug	262	12.4	106	12.1	+ 0.3
20 Aug	274	12.4	106	12.1	+ 0.3
26 Aug	280	11.7	104	11.6	+ 0.1
18 Sep	303	11.6	104	11.6	0.0
6 Nov	352	4.0	72	3.0	1.0
11 Nov	357	5.5	73	3.2	2.3
7 Jan 81	414	5.5	56	- 1.3	6.8
12 Feb	450	3.6	50	- 3.0	6.6
12 Mar	478	7.9	63	0.5	7.4

* Unknown

TABLE III.2 - Continued

Date	Time Days	Cell Reading p_j, psi	Tempera-ture, ^{o}F	Preload p_o, psi	Earth Pressure p_e, psi
20 May 81	547	11.9	74	3.5	8.4
2 Jun	560	13.2	82	5.4	7.8
10 Jun	568	14.0	86	6.7	7.3
30 Jun	588	13.6	86	6.7	6.9
9 Jul	597	13.2	83	5.9	7.3
23 Jul	611	14.7	90	7.8	6.9
10 Sep	660	13.0	85	6.5	6.5
1 Oct	681	13.4	85	6.5	6.9
29 Oct	709	9.4	71	2.7	6.7
6 Jan 82	778	8.1	64	0.8	7.3
4 Mar	835	7.5	63	0.5	7.0
15 Apr	877	10.9	73	3.2	7.7
26 May	918	13.4	79	4.9	8.5
10 Jun	933	15.5	86	6.7	8.8
7 Jul	060	15.9	89	7.6	8.3

TABLE III.3 - Cell 927, $p_o = -17.63 + 0.2772T$

($^oC = 0.56(^oF-32)$, 1 psi = 6.89 kPa)

Date	Time Days	Cell Reading p_i, psi	Temperature, ^oF	Preload p_o, psi	Earth Pressure p_e, psi
20 Nov 79	0	NA	NA	NA	NA
9 Jan 80	50	NA	NA	NA	NA
7 Mar	108	5.9	82	5.7	+ 0.2
1 Apr	133	8.7	92	8.5	+ 0.2
22 Apr	154	9.9	97	9.7	+ 0.2
4 Jun	197	12.2	105	12.1	+ 0.1
16 Jun	209	9.7	97	9.7	0.0
16 Jun	209	15.8	*	*	*
9 Jul	232	13.7	112	14.0	- 0.3
29 Jul	252	11.0	101	11.0	0.0
8 Aug	262	12.3	106	12.4	- 0.1
20 Aug	274	12.5	106	12.4	+ 0.1
26 Aug	280	12.0	104	11.8	+ 0.2
18 Sep	303	11.8	104	11.8	0.0
6 Nov	352	5.1	72	2.9	+ 2.2
11 Nov	357	6.4	73	3.2	+ 3.2
7 Jan 81	414	1.5	56	- 1.5	+ 3.0
12 Feb	450	6.4	50	- 3.2	+ 9.6
12 Mar	478	10.0	63	0.4	9.6

* Unknown

TABLE III.3 - Continued

Date	Time Days	Cell Reading p_j, psi	Temperature, ^{o}F	Preload p_o, psi	Earth Pressure p_e, psi
20 May 81	547	14.6	74	3.5	11.1
2 Jun	560	15.7	81	5.4	10.3
10 Jun	568	16.6	86	6.8	9.8
30 Jun	588	16.4	86	6.8	9.6
9 Jul	597	15.9	83	6.0	9.0
23 Jul	611	17.3	90	7.9	9.4
10 Sep	660	16.0	85	6.5	9.7
1 Oct	681	16.5	85	6.5	10.0
20 Oct	709	12.6	71	2.7	9.9
6 Jan 82	778	11.0	64	0.7	10.3
4 Mar	835	10.5	63	0.4	10.1
15 Apr	877	13.5	73	3.2	10.3
26 May	918	15.7	79	4.9	10.8
10 Jun	933	17.4	86	6.8	10.6
7 Jul	960	17.7	89	7.6	10.1

TABLE III.4 - Cell 921, p_o = -28.56 + 0.3540T

($^oC = 0.56(^oF - 32)$, 1 psi = 6.89 kPa)

Date	Time Days	Cell Reading p_i, psi	Temperature, ^oF	Preload p_o, psi	Earth Pressure p, psi
20 Nov 79	0	NA	NA	NA	NA
9 Jan 80	50	NA	NA	NA	NA
7 Mar	108	5.4	82	0.5	4.9**
1 Apr	133	7.1	92	4.1	3.0**
22 Apr	154	10.0	97	5.8	4.2**
4 Jun	197	12.5	105	8.6	3.9**
16 Jun	209	8.5	97	5.8	2.7**
16 Jun	209	12.6	*	*	*
9 Jul	232	11.3	112	11.9	- 0.6
29 Jul	252	8.1	101	7.2	+ 0.9
8 Aug	262	8.4	106	9.0	- 0.6
20 Aug	274	9.5	106	9.0	+ 0.5
26 Aug	280	8.6	104	8.3	+ 0.3
18 Sep	303	4.5	85	1.5	+ 3.0
6 Nov	352	2.3	73	- 2.7	+ 5.0
11 Nov	357	3.6	73	- 2.7	+ 6.3
7 Jan 81	414	1.6	64	- 5.9	+ 7.5
12 Feb	450	1.4	60	- 7.3	+ 8.7

* Unknown
** Response before concrete was placed

TABLE III.4 - Continued

Date	Time Days	Cell Reading p_i, psi	Temperature, ^{o}F	Preload p_o, psi	Earth Pressure p_e, psi
12 Mar 81	478	2.2	64	- 5.9	+ 8.1
20 May	547	6.5	70	- 3.8	+ 10.3
2 Jun	560	7.6	78	- o.9	+ 8.5
10 Jun	568	8.7	78	- 0.9	+ 9.6
30 Jun	588	9.0	79	- 0.6	+ 9.6
9 Jul	597	8.2	78	- 0.9	+ 9.1
23 Jul	611	9.6	82	0.5	+ 9.1
10 Sep	660	8.9	82	0.5	+ 8.4
1 Oct	681	8.6	82	0.5	+ 8.1
29 Oct	709	4.5	73	- 2.7	+ 7.2
6 Jan 82	778	1.7	64	- 5.9	+ 7.6
4 Mar	835	2.5	63	- 6.3	+ 8.8
15 Apr	877	4.5	69	- 4.1	+ 8.6
26 May	918	7.6	75	- 2.0	+ 9.6
10 Jun	933	10.0	79	- 0.6	+ 10.7
7 Jul	960	11.6	82	+ 0.5	+ 11.1

TABLE III.5 - Cell 924, $p_o = -24.85 + 0.3319T$

($^oC = 0.56(^oF - 32)$, 1 psi = 6.89 kPa)

Date	Time Days	Cell Reading p_i, psi	Temperature, ^oF	Preload p_o, psi	Earth Pressure p_e, psi
20 Nov 79	0	5.8	930	6.02	- 0.2
9 Jan 80	50	0.0	74	- 0.3	+ 0.3
7 Mar	108	3.6	82	2.4	+ 1.2
1 Apr	133	4.2	92	5.7	- 1.5
22 Apr	154	7.6	97	7.3	+ 0.3
4 Jun	197	11.0	105	10.0	+ 1.0
16 Jun	209	11.9	97	7.3	+ 4.6**
16 Jun	209	10.9	*	*	*
9 Jul	232	11.9	112	12.3	- 0.4
29 Jul	252	9.0	101	8.7	+ 0.3
8 Aug	262	8.3	106	9.0	- 0.7
20 Aug	274	9.5	106	9.0	+ 0.5
26 Aug	280	10.6	104	9.7	+ 0.8
18 Sep	303	9.7	84	3.0	+ 6.7
6 Nov	352	6.1	74	- 0.3	+ 6.4
11 Nov	357	5.8	73	- 0.6	+ 6.4
7 Jan 81	414	3.8	65	- 3.3	+ 7.1
12 Feb	450	3.6	63	- 3.9	+ 7.5

* Unknown
** Due to construction activity

TABLE III.5 - Continued

Date	Time Days	Cell Reading p_i, psi	Temperature, ^{o}F	Preload p_o, psi	Earth Pressure p_e, psi
12 Mar 81	478	4.1	64	- 3.6	+ 7.7
20 May	547	6.4	69	- 1.0	+ 8.3
2 Jun	560	6.9	73	- 0.6	+ 7.5
10 Jun	568	7.3	75	0.0	+ 7.3
30 Jun	588	8.0	75	0.0	+ 8.0
9 Jul	597	8.4	77	0.7	+ 7.7
23 Jul	611	8.5	78	1.0	+ 7.5
10 Sep	660	9.7	80	1.7	+ 8.0
1 Oct	681	9.5	80	1.7	+ 7.8
29 Oct	709	8.9	78	1.0	+ 7.9
6 Jan 82	778	5.8	69	- 1.9	+ 7.7
4 Mar	835	4.5	64	- 3.6	+ 8.1
15 Apr	877	5.5	69	- 1.9	+ 7.4
26 May	918	6.7	72	- 1.0	+ 7.7
10 Jun	933	7.4	74	- 0.3	+ 7.7
7 Jul	960	8.8	78	1.0	+ 7.8

TABLE III.6 - Cell 935, $p_o = -22.55 + 0.3418T$

($^oC = 0.56(^oF - 32)$, 1 psi = 6.89 kPa)

Date	Time Days	Cell Reading p_i, psi	Temperature, ^oF	Preload p_o, psi	Earth Pressure p_e, psi
20 Nov 79	0	9.8	93	9.2	+ 0.6
9 Jan 80	50	2.4	74	2.7	- 0.3
7 Mar	108	7.8	82	5.5	+ 2.3
1 Apr	133	7.7	92	8.9	- 1.2
22 Apr	154	9.8	97	10.6	- 0.8
4 Jun	197	12.3	105	13.3	- 1.0
16 Jun	209	11.0	*	*	*
16 Jun	209	13.9	*	*	*
9 Jul	232	10.9	112	15.7	- 4.8
29 Jul	252	13.4	*	*	*
8 Aug	262	11.2	*	*	*
20 Aug	274	11.0	*	*	*
26 Aug	280	11.8	*	*	*
18 Sep	303	11.5	84	6.2	5.3
6 Nov	352	8.5	73	2.4	6.1
11 Nov	357	8.8	73	2.4	6.4
7 Jan 81	414	6.2	63	- 1.0	7.2
12 Feb	450	5.9	58	- 2.7	8.6

* Unknown

TABLE III.6 - Continued

Date	Time Days	Cell Reading p_i, psi	Temperature, ^{o}F	Preload p_o, psi	Earth Pressure p_e, psi
12 Mar 81	478	7.3	62	- 1.4	8.7
20 May	547	10.8	69	1.0	9.8
2 Jun	560	12.3	77	3.8	8.5
10 Jun	568	11.5	78	4.1	7.4**
30 Jun	588	12.2	77	3.8	8.4
9 Jul	597	12.3	77	3.8	8.5
23 Jul	611	12.9	78	4.1	8.8
10 Sep	660	14.1	80	4.8	9.6
1 Oct	681	13.5	79	4.5	9.0
29 Oct	709	12.0	74	2.7	9.3
6 Jan 82	778	7.5	61	- 1.7	9.2
4 Mar	835	7.0	61	- 1.7	8.7
15 Apr	877	9.9	67	0.4	9.5
26 May	918	12.0	73	2.4	9.6
10 Jun	933	14.0	77	3.8	10.2
7 Jul	960	15.0	80	4.8	10.2

** Due to thermocouple installation

TABLE III.7 - Cell 926, $p_o = -16.04 + 0.2549T$

($^oC = 0.56(^oF - 32)$, 1 psi = 6.89 kPa)

Date	Time Days	Cell Reading p_i, psi	Temperature, ^oF	Preload p_o, psi	Earth Pressure p_e, psi
20 Nov 79	0	6.1	93	7.7	- 1.6
9 Jan 80	50	7.0	74	2.8	4.2
7 Mar	108	9.5	*	*	*
1 Apr	133	9.0	*	*	*
22 Apr	154	11.0	*	*	*
4 Jun	197	15.8	*	*	*
16 Jun	209	15.7	*	*	*
16 Jun	209	23.1	*	*	*
9 Jul	232	18.7	*	*	*
29 Jul	252	14.8	*	*	*
8 Aug	262	14.5	*	*	*
20 Aug	274	14.4	*	*	*
26 Aug	280	16.0	*	*	*
18 Sep	303	14.4	84	5.4	9.1
6 Nov	352	11.4	73	2.6	8.8
11 Nov	357	11.3	73	2.6	8.7
7 Jan 81	414	9.3	63	0.0	9.3
12 Feb	450	9.0	59	- 1.0	10.0

* Unknown

TABLE III.7 - Continued

Date	Time Days	Cell Reading p_i, psi	Temperature, ^{o}F	Preload p_o, psi	Earth Pressure p_e, psi
12 Mar 81	478	9.7	62	- 0.2	9.9
20 May	547	12.0	69	1.5	10.5
2 Jun	560	13.0	77	3.6	9.4
10 Jun	568	13.2	78	3.8	9.4
30 Jun	588	13.8	77	3.6	10.2
9 Jul	597	14.0	77	3.6	10.4
23 Jul	611	14.5	78	3.8	10.7
10 Sep	660	14.7	80	4.4	10.3
1 Oct	681	13.9	79	4.1	9.8
29 Oct	709	12.5	74	2.8	9.7
6 Jan 82	778	9.9	61	- 0.5	10.4
4 Mar	835	9.2	62	- 0.2	9.4
15 Apr	877	10.5	67	1.0	9.5
26 May	918	12.1	73	2.4	9.5
10 Jun	933	12.3	77	3.6	9.6
7 Jul	960	14.5	80	4.4	10.1

TABLE III.8 - Cell 936, $p_o = -18.47 + 0.2809T$

($^oC = 0.56(^oF - 32)$, 1 psi = 6.89 kPa)

Date	Time Days	Cell Reading p_i, psi	Temperature, ^oF	Preload p_o, psi	Earth Pressure p_e, psi
20 Nov 79	0	7.8	93	7.7	+ 0.0
9 Jan 80	50	3.1	74	2.3	+ 0.8
7 Mar	108	13.0	*	*	*
1 Apr	133	11.5	*	*	*
22 Apr	154	13.9	*	*	*
4 Jun	197	16.2	*	*	*
16 Jun	209	12.6	*	*	*
16 Jun	209	16.5	*	*	*
9 Jul	232	21.4	*	*	*
29 Jul	252	10.8	*	*	*
8 Aug	262	11.4	*	*	*
20 Aug	274	12.7	*	*	*
26 Aug	280	15.8	*	*	*
18 Sep	303	13.0	84	5.1	7.9
6 Nov	352	9.4	73	2.0	7.4
11 Nov	357	9.5	73	2.0	7.5
7 Jan 81	414	7.8	64	- 9.5	8.3
12 Feb	450	7.5	60	- 1.6	9.1

* Unknown

TABLE III.8 - Continued

Date	Time Days	Cell Reading p_i, psi	Temperature, ^{o}F	Preload p_o, psi	Earth Pressure p_e, psi
12 Mar 81	478	8.1	63	- 0.8	8.9
20 May	547	10.4	69	0.9	9.5
2 Jun	560	11.5	77	3.2	8.3
10 Jun	568	11.8	78	3.4	8.4
30 Jun	588	12.4	77	3.2	9.2
9 Jul	597	12.4	77	3.2	9.2
23 Jul	611	13.0	78	3.4	9.6
10 Sep	660	13.5	80	4.0	9.5
1 Oct	681	12.8	79	3.7	9.1
29 Oct	709	11.0	74	2.3	8.7
6 Jan 82	778	8.6	63	- 0.8	9.4
4 Mar	835	8.0	62	- 1.1	9.1
15 Apr	877	9.4	68	0.6	8.8
26 May	918	11.1	74	2.3	8.8
10 Jun	933	12.5	77	3.2	9.3
7 Jul	960	14.2	80	4.0	10.2

TABLE III.9 - Cell 938, $p_o = -15.60 + 0.2435T$

($^oC = 0.56(^oF - 32)$, 1 psi = 6.89 kPa)

Date	Time Days	Cell Reading p_i, psi	Temperature, ^oF	Preload p_o, psi	Earth Pressure p_e, psi
20 Nov 79	0	6.8	93	7.0	- 0.2
9 Jan 80	50	2.8	74	2.4	0.4
7 Mar	108	5.4	*	*	*
1 Apr	133	5.8	*	*	*
22 Apr	154	10.0	*	*	*
4 Jun	197	15.1	*	*	*
16 Jun	209	11.8	*	*	*
16 Jun	209	11.8	*	*	*
9 Jul	232	13.6	*	*	*
29 Jul	252	11.2	*	*	*
8 Aug	262	11.4	*	*	*
20 Aug	274	11.7	*	*	*
26 Aug	280	12.6	*	*	*
18 Sep	303	11.6	84	4.9	6.7
6 Nov	352	8.6	73	2.2	6.4
11 Nov	357	8.5	73	2.2	6.3
7 Jan 81	414	6.4	64	0.0	6.4
12 Feb	450	6.0	60	- 1.0	7.0

* Unknown

TABLE III.9 - Continued

Date	Time Days	Cell Reading p_i, psi	Temperature, ^{o}F	Preload p_o, psi	Earth Pressure p_e, psi
12 Mar 81	478	6.6	63	- 0.3	7.0
20 May	547	8.8	69	1.2	7.6
2 Jun	560	9.5	77	3.1	6.4
10 Jun	568	9.8	77	3.1	6.7
30 Jun	588	10.2	77	3.1	7.1
9 Jul	597	10.4	77	3.1	7.3
23 Jul	611	10.6	78	3.4	7.2
10 Sep	660	11.2	80	3.9	7.3
1 Oct	681	10.9	80	3.9	7.0
29 Oct	709	10.0	74	2.4	7.6
6 Jan 82	778	7.4	64	0.0	7.4
4 Mar	835	6.7	63	- 0.3	7.0
15 Apr	877	7.9	68	1.0	6.9
26 May	918	9.4	74	2.4	7.0
10 Jun	933	10.2	77	3.1	7.1
7 Jul	960	11.0	81	4.1	6.9

TABLE III.10 - CELL 922, $p_o = -24.37 + 0.3445T$

($^oC = 0.56(^oF - 32)$, 1 psi = 6.89 kPa)

Date	Time Days	Cell Reading p_i, psi	Temperature, ^oF	Preload p_o, psi	Earth Pressure p_e, psi
20 Nov 79	0	7.8	93	7.7	+ 0.1
9 Jan 80	50	1.0	74	1.2	- 0.2
7 Mar	108	3.3	*	*	*
1 Apr	133	4.0	*	*	*
22 Apr	154	7.3	*	*	*
4 Jun	197	11.0	*	*	*
16 Jun	209	11.3	*	*	*
16 Jun	209	16.1	*	*	*
9 Jul	232	16.6	*	*	*
29 Jul	252	10.4	*	*	*
8 Aug	262	10.6	*	*	*
20 Aug	274	11.5	*	*	*
26 Aug	280	13.5	*	*	*
18 Sep	303	11.0	84	4.6	6.4
6 Nov	352	8.0	74	1.1	6.9
11 Nov	357	7.8	73	0.8	7.0
7 Jan 81	414	5.5	64	- 2.3	7.8
12 Feb	450	5.0	62	- 3.0	8.0

* Unknown

TABLE III.10 - Continued

Date	Time Days	Cell Reading p_i, psi	Temperature, ^{o}F	Preload p_o, psi	Earth Pressure p_e, psi
12 Mar 81	478	5.5	64	- 2.3	7.8
20 May	547	7.9	69	- 0.6	8.5
2 Jun	560	8.7	75	1.5	7.2
10 Jun	568	9.0	76	1.8	7.2
30 Jun	588	9.7	75	1.5	8.2
9 Jul	597	10.0	77	2.2	7.8
23 Jul	611	10.5	78	2.5	8.0
10 Sep	660	11.8	80	3.2	8.6
1 Oct	681	11.2	80	3.2	8.0
29 Oct	709	10.0	76	1.8	8.2
6 Jan 82	778	6.9	67	- 1.3	8.2
4 Mar	835	5.7	63	- 2.7	8.4
15 Apr	877	6.8	69	- 0.6	7.4
26 May	918	8.5	73	0.8	7.7
10 Jun	933	9.5	75	1.5	8.0
7 Jul	960	11.0	79	2.8	8.2

TABLE III.11 - Cell 937, p_o = -20.70 + 0.3000T

($^oC = 0.56(^oF - 32)$, 1 psi = 6.89 kPa)

Date	Time Days	Cell Reading p_i, psi	Temperature, ^oF	Preload p_o, psi	Earth Pressure p_e, psi
20 Nov 79	0	7.3	93	7.2	+ 0.1
9 Jan 80	50	3.1	74	1.5	1.6
7 Mar	108	5.2	*	*	*
1 Apr	133	5.4	*	*	*
22 Apr	154	9.5	*	*	*
4 Jun	197	14.2	*	*	*
16 Jun	209	14.0	*	*	*
16 Jun	209	19.8	*	*	*
9 Jul	232	17.7	*	*	*
29 Jul	252	9.9	*	*	*
8 Aug	262	10.4	*	*	*
20 Aug	274	11.3	*	*	*
26 Aug	280	14.2	*	*	*
18 Sep	303	12.2	84	4.5	7.7
6 Nov	352	8.2	74	1.4	6.7
11 Nov	357	8.0	73	1.2	6.8
7 Jan 81	414	5.7	65	- 1.2	6.9
12 Feb	450	5.5	63	- 1.8	7.3

* Unknown

TABLE III.11 - Continued

Date	Time Days	Cell Reading p_i, psi	Temperature, ^{o}F	Preload p_o, psi	Earth Pressure p_e, psi
12 Mar 81	478	5.9	64	- 1.5	7.4
20 May	547	7.8	69	0.0	7.9
2 Jun	560	8.5	73	1.2	7.3
10 Jun	568	8.8	75	1.8	7.0
30 Jun	588	9.5	75	1.8	7.7
9 Jul	597	9.9	77	2.4	7.5
23 Jul	611	10.0	78	2.7	7.3
10 Sep	660	11.0	80	3.3	7.7
1 Oct	681	10.7	80	3.3	7.4
29 Oct	709	10.0	78	2.7	7.3
6 Jan 82	778	7.1	69	0.0	7.1
4 Mar	835	6.0	64	- 1.5	7.5
15 Apr	877	6.9	69	0.0	6.9
26 May	918	8.0	72	0.9	7.1
10 Jun	933	8.8	74	1.5	7.3
7 Jul	960	10.3	78	2.7	7.6